Title

Measurements of W+W−+ ≥ 1 jet production cross-sections in pp collisions at s = 13 TeV with the ATLAS detector

Journal

Journal of High Energy Physics, 2021(6)

ISSN

1126-6708

Authors

Aad, G
Abbott, B
Abbott, DC
et al.

Publication Date

2021-06-01

DOI

10.1007/jhep06(2021)003

Peer reviewed

EUROPEAN ORGANISATION FOR NUCLEAR RESEARCH (CERN)

JHEP 06 (2021) 003
DOI: 10.1007/JHEP06(2021)003

CERN-EP-2021-030
1st September 2021

Measurements of $W^+W^-+ \geq 1$ jet production cross-sections in pp collisions at $\sqrt{s} = 13$ TeV with the ATLAS detector

The ATLAS Collaboration

Fiducial and differential cross-section measurements of W^+W^- production in association with at least one hadronic jet are presented. These measurements are sensitive to the properties of electroweak-boson self-interactions and provide a test of perturbative quantum chromodynamics and the electroweak theory. The analysis is performed using proton–proton collision data collected at $\sqrt{s} = 13$ TeV with the ATLAS experiment, corresponding to an integrated luminosity of 139 fb^{-1}. Events are selected with exactly one oppositely charged electron–muon pair and at least one hadronic jet with a transverse momentum of $p_{\mathrm{T}} > 30$ GeV and a pseudorapidity of $|\eta| < 4.5$. After subtracting the background contributions and correcting for detector effects, the jet-inclusive $W^+W^-+ \geq 1$ jet fiducial cross-section and W^+W^-+ jets differential cross-sections with respect to several kinematic variables are measured. These measurements include leptonic quantities, such as the lepton transverse momenta and the transverse mass of the W^+W^- system, as well as jet-related observables such as the leading jet transverse momentum and the jet multiplicity. Limits on anomalous triple-gauge-boson couplings are obtained in a phase space where interference between the Standard Model amplitude and the anomalous amplitude is enhanced.

Contents

1 Introduction

The measurement of W-boson pair (WW) production cross-sections is an important test of the Standard Model (SM). WW production at hadron colliders is sensitive to the properties of electroweak-boson self-interactions and provides a test of perturbative quantum chromodynamics (QCD) and the electroweak (EW) theory. It also constitutes a large background in the measurement of Higgs boson production as well as in searches for physics beyond the SM. Inclusive and fiducial WW production cross-sections have been measured in proton–proton (pp) collisions at $\sqrt{s} = 7$ TeV [1, 2], 8 TeV [3–5] and 13 TeV [6–8], as well as in e^+e^- collisions at LEP [9] and in $p\bar{p}$ collisions at Tevatron [10–12]. However, to reduce backgrounds, the measurements of inclusive cross-sections typically require that the WW pair is produced without additional jet activity, or at most with one additional jet. The production of WW+jets has therefore not been studied in detail.

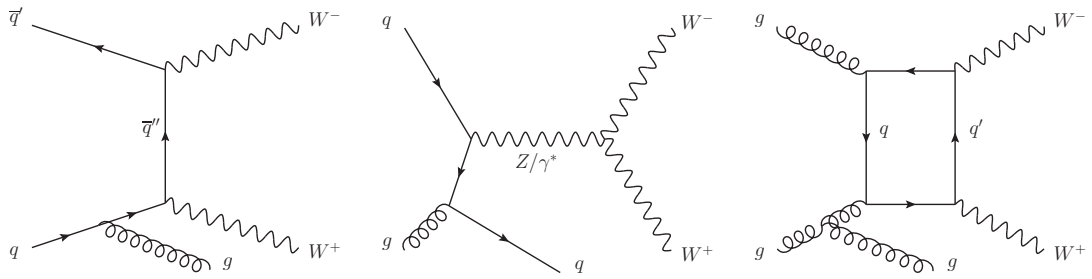

Figure 1: Feynman diagrams for the production of a W^+W^- boson pair in association with a jet.

This article presents results of measurements of fiducial and differential cross-sections for a WW pair produced in association with one or more jets. For the first time at the LHC, differential measurements are performed in a jet-inclusive phase space. This measurement complements previous results as the combination of measurements with and without jets improves the precision of the inclusive WW cross-section due to an anti-correlation of important systematic uncertainties, for example the jet energy scale uncertainty, as demonstrated in previous measurements from ATLAS [5] and CMS [8].

The analysis of one-jet topologies can also improve searches for anomalous triple-gauge-boson couplings (aTGCs), due to the increased interference between the SM amplitude and the anomalous amplitude [13]. The impact of the Q_W aTGC operator, as defined in Ref. [14], increases rapidly with energy, making a measurement at the energies probed by the LHC important. However, at high centre-of-mass energy, the SM amplitude and the anomalous amplitude are dominated by different helicity configurations, so their interference is suppressed, which reduces the impact of the operator. The reduced sensitivity to the interference also poses a problem for the validity of the effective field theory interpretation, as contributions that are quadratic in the dimension-six amplitude, which are expected to be subdominant in the EFT expansion, become large. Requiring hard jets in addition to the diboson pair allows different helicity configurations and, thus, reduces the interference-suppression [13].

In pp collisions, two leading processes contribute to WW production: $q\bar{q} \to WW$ in the t- and s-channel, and loop-induced gluon–gluon fusion processes $gg \to WW$. Beyond leading order in perturbation theory and in particular for WW+jets production, additional partonic initial states can contribute to both processes.[1] Representative diagrams for WW+jet production are shown in Figure 1. In this analysis, the resonant $gg \to H \to WW$ production is included in the signal definition and simulation, although the process is strongly suppressed via kinematic selection requirements.

The measurement of $WW \to e^{\pm}\nu\mu^{\mp}\nu$ production cross-sections at $\sqrt{s} = 13$ TeV is performed, using pp collision data recorded by the ATLAS experiment in 2015–2018, corresponding to an integrated luminosity of 139 fb^{-1}. The number of events due to top-quark pair production ($t\bar{t}$), the largest background for this measurement, is reduced by rejecting events containing jets from b-hadron decays (b-jets). However, the $t\bar{t}$ background is still sizeable due to the requirement that events contain at least one jet, and a data-driven method is required to reduce its contribution to systematic uncertainties in the measurement. This is achieved by simultaneously measuring the number of $t\bar{t}$ events and the efficiency of identifying b-jets in these events. The procedure reduces the impact of systematic uncertainties associated with the modelling of $t\bar{t}$ events and the b-tagging efficiency calibration, and provides a precise and accurate estimate of the background up to partonic centre-of-mass energies of the order of 1 TeV and for up to five jets.

[1] Even though different partonic initial states contribute to both processes, the notation $gg \to WW$ is used to identify the loop-induced gluon–gluon fusion channel while $q\bar{q} \to WW$ describes the dominant production mode.

The measurement is performed in a fiducial phase space close to the geometric and kinematic acceptance of the experimental analysis. The cross-section of WW production is measured differentially as a function of:

- the transverse momentum[2] of the leading lepton, $p_{\mathrm{T}}^{\text{lead. lep.}}$,
- the transverse momentum of the sub-leading lepton, $p_{\mathrm{T}}^{\text{sub-lead. lep.}}$,
- the transverse momentum of the leading jet, $p_{\mathrm{T}}^{\text{lead. jet}}$,
- the jet multiplicity,
- the invariant mass of the lepton pair, $m_{e\mu}$,
- the transverse momentum of the lepton pair, $p_{\mathrm{T},e\mu}$,
- the scalar sum of all jet transverse momenta, H_{T},
- the scalar sum of all jet and lepton transverse momenta, S_{T},
- the transverse mass of the dilepton system and the missing transverse momentum[3], $m_{\mathrm{T},e\mu}$,
- the rapidity of the dilepton system, $y_{e\mu}$,
- the azimuthal separation of the two leptons, $\Delta\phi(e,\mu)$, and
- $\cos\theta^* = |\tanh(\Delta\eta(e,\mu)/2)|$, which is sensitive to the spin structure of the W-boson pair [15].

These observables comprehensively characterize W-boson kinematics and jet production in WW events. To facilitate an anomalous coupling interpretation that is less plagued by the aforementioned interference suppression, the differential cross sections as a function of $m_{e\mu}$ and $\Delta\phi(e,\mu)$ are also measured for $p_{\mathrm{T}}^{\text{lead. jet}} > 200\,\text{GeV}$, where the jet p_{T} threshold is chosen as a compromise between increased interference and good measurement precision. Additional measurements with $p_{\mathrm{T}}^{\text{lead. lep.}} > 200\,\text{GeV}$ are presented in Appendix A.

2 The ATLAS detector

The ATLAS experiment [16] at the LHC [17] is a multipurpose particle detector with a forward–backward symmetric cylindrical geometry and a near 4π coverage in solid angle. It consists of an inner tracking detector surrounded by a thin superconducting solenoid providing a 2 T axial magnetic field, electromagnetic and hadron calorimeters, and a muon spectrometer with three large superconducting toroidal magnets with eight coils each.

[2] ATLAS uses a right-handed coordinate system with its origin at the nominal interaction point (IP) in the centre of the detector and the z-axis along the beam pipe. The x-axis points from the IP to the centre of the LHC ring, and the y-axis points upwards. Cylindrical coordinates (r,ϕ) are used in the transverse plane, ϕ being the azimuthal angle around the z-axis. The rapidity is defined as $y = \frac{1}{2}\ln\frac{E+p_z}{E-p_z}$ while the pseudorapidity is defined in terms of the polar angle θ as $\eta = -\ln\tan(\theta/2)$. Angular distance is measured in units of $\Delta R \equiv \sqrt{(\Delta\eta)^2+(\Delta\phi)^2}$.

[3] The transverse mass is defined as $m_{\mathrm{T},e\mu} = \sqrt{(E_{\mathrm{T},e\mu}+E_{\mathrm{T}}^{\text{miss}})^2 - (\vec{p}_{\mathrm{T},e\mu}+\vec{p}_{\mathrm{T}}^{\text{miss}})^2}$, where $E_{\mathrm{T},e\mu} = \sqrt{|\vec{p}_{\mathrm{T},e\mu}|^2 + m_{e\mu}^2}$ and $E_{\mathrm{T}}^{\text{miss}}$ is the magnitude of the missing transverse momentum.

The inner tracking detector covers the pseudorapidity range $|\eta| < 2.5$. It consists of a high-granularity silicon pixel detector, including the insertable B-layer installed before Run 2 [18, 19], followed by the silicon microstrip tracker. The silicon detectors are complemented by a transition radiation tracking detector, enabling extended track reconstruction within $|\eta| < 2.0$.

Lead/liquid-argon (LAr) sampling calorimeters provide electromagnetic (EM) energy measurements with high granularity. A steel/scintillator-tile hadron calorimeter covers the central pseudorapidity range ($|\eta| < 1.7$). The endcap and forward regions are instrumented with copper/LAr and tungsten/LAr calorimeters for EM and hadronic energy measurements up to $|\eta| = 4.9$.

The muon spectrometer surrounds the calorimeters and is based on three large air-core toroidal superconducting magnets with eight coils each. The field integral of the toroids ranges between 2.0 and 6.0 Tm. across most of the detector. The muon spectrometer includes a system of precision tracking chambers and fast detectors for triggering.

Events are selected using a two-level trigger system. The first-level trigger is implemented in hardware and uses a subset of the detector information to accept events at a rate of about 100 kHz. The level-1 trigger is followed by a software-based trigger that reduces the accepted event rate to 1 kHz on average depending on the data-taking conditions.

3 Data and Monte Carlo samples

The analysis uses data collected in proton–proton collisions at a centre-of-mass energy of 13 TeV from 2015 to 2018. After applying data quality criteria [20], the dataset corresponds to 139 fb^{-1}, with an uncertainty of 1.7% [21], obtained using the LUCID-2 detector [22] for the primary luminosity measurements.

Monte Carlo (MC) simulated event samples are used to correct the signal yield for detector effects and to estimate background contributions. All samples were passed through a full simulation of the ATLAS detector [23], based on GEANT4 [24]. Table 1 lists the configuration for the nominal MC simulation used in the analysis.

Signal events were modelled using the SHERPA 2.2.2 [25] generator at next-to-leading order (NLO) accuracy in QCD for up to one additional parton, and leading-order (LO) accuracy for two to three additional parton emissions for $q\bar{q}$ initial states. The matrix element calculation of $gg \to WW$ production, which includes off-shell effects and Higgs boson contributions, incorporates up to one additional parton emission at LO. It was matched and merged with the SHERPA parton shower based on Catani–Seymour dipole [26, 27] using the MEPS@NLO prescription [28–31]. The virtual QCD corrections were provided by the OPENLOOPS library [32, 33]. The NNPDF3.0NNLO set of parton distribution functions (PDF) was used [34], along with the dedicated set of tuned parton-shower parameters developed by the SHERPA authors.

To assess the uncertainty in the matrix element calculation and the parton shower modelling, alternative events for $q\bar{q} \to WW$ production were generated using the POWHEG-BOX v2 [35–38] generator at NLO accuracy in QCD. Events were interfaced to PYTHIA 8.186 [39] for the modelling of the parton shower, hadronization, and underlying event, with parameter values set according to the AZNLO set of tuned parameters [40]. The CT10nlo set PDF [41] was used for the hard-scattering processes, whereas the CTEQ6L1 PDF set [42] was used for the parton shower. The events were normalized to the next-to-next-to-leading order (NNLO) cross-section [43]. For the $gg \to WW$ initial state, which makes up only 5% of the signal, no alternative simulation is used.

The production of $t\bar{t}$ and single-top Wt events was modelled using the Powheg-Box v2 [35–37, 44] generator at NLO with the NNPDF3.0NLO [34] PDF. The events were interfaced to Pythia 8.230 [45] to model the parton shower, hadronization, and underlying event, with the A14 set of tuned parameters [46] and using the NNPDF2.3LO set of PDFs [47]. For $t\bar{t}$ event generation, the h_{damp} parameter[4] was set to $1.5m_{\text{top}}$ [48]. The diagram-removal scheme [49] was employed to handle the interference between the Wt and $t\bar{t}$ production processes [48]. Alternative samples were generated to assess the uncertainties in the top-background modelling. The uncertainty due to initial-state radiation and higher-order QCD effects was estimated by simultaneous variations of the h_{damp} parameter and the renormalization and factorization scales, and by choosing the Var3c up/down variants of the A14 set of tuned parameters as described in Ref. [50]. The impact of final-state radiation was evaluated with weights that account for the effect of varying the renormalisation scale for final-state parton-shower emissions up or down by a factor two. To assess the dependence on the $t\bar{t}$–Wt overlap removal scheme, the diagram-subtraction scheme [49] was employed as an alternative to the diagram-removal scheme. The uncertainty due to the parton shower and hadronization model was evaluated by comparing the nominal sample of events with an event sample generated by Powheg-Box v2 and interfaced to Herwig 7.04 [51, 52], using the H7UE set of tuned parameters [52] and the MMHT2014LO PDF set [53]. To assess the uncertainty in the matching of NLO matrix elements to the parton shower, the nominal sample was compared with a sample generated by MadGraph5_aMC@NLO 2.6.2 [54] at NLO in QCD using the five-flavour scheme and the NNPDF2.3NLO PDF set. The events were interfaced with Pythia 8, as for the nominal sample. The $t\bar{t}$ sample was normalized to the cross-section prediction at NNLO QCD. in QCD including the resummation of next-to-next-to-leading logarithmic (NNLL) soft-gluon terms calculated using Top++2.0 [55–61]. The inclusive cross-section for single-top Wt was corrected to the theory prediction calculated at NLO in QCD with NNLL soft-gluon corrections [62, 63].

The background due to Z/γ^*+jets production was simulated with the Sherpa 2.2.1 generator using NLO-accurate matrix elements for up to two jets, and LO-accurate matrix elements for three and four jets calculated with the Comix [26] and OpenLoops libraries. They were matched with the Sherpa parton shower [27] using the MEPS@NLO prescription [28–31] and the set of tuned parameters developed by the Sherpa authors. The NNPDF3.0NNLO set of PDFs was used, and the samples were normalised to a NNLO prediction [64]. To assess the uncertainties in modelling the Z+jets process, an alternative sample was simulated using LO-accurate matrix elements with up to four final-state partons with MadGraph5_aMC@NLO 2.2.2, with the NNPDF2.3LO set of PDFs. Events were interfaced to Pythia 8.186 using the A14 set of tuned parameters. The overlap between matrix-element and parton-shower emissions was removed using the CKKW-L merging procedure [65, 66]. The inclusive cross-section of both the nominal simulation and the alternative simulation was corrected to the theory prediction calculated at NNLO in QCD.

The production of WZ, ZZ, $V\gamma$ (with $V = W, Z$) and triboson (VVV, on-shell) final states was simulated with the Sherpa 2.2.2 and Sherpa 2.2.8 generators using OpenLoops at NLO QCD accuracy for up to one additional parton and LO accuracy for two to three additional parton emissions, matched and merged with the Sherpa parton shower. The VZ simulation includes $V\gamma^*$ contributions for $m(\ell\ell) > 4\,\text{GeV}$. Samples were generated using the NNPDF3.0NNLO PDF set and normalized to the cross-section calculated by the event generator. Alternative samples for diboson backgrounds with WZ or ZZ production were generated in the same way as the nominal signal sample: the default Sherpa simulation was exchanged for Powheg + Pythia 8, using NLO-accurate matrix elements. The Powheg diboson cross-section was scaled to NNLO [67–70], while the cross-section calculated by Sherpa was found to be in good agreement with the

[4] The h_{damp} parameter is a resummation damping factor and one of the parameters that control the matching of Powheg matrix elements to the parton shower and thus effectively regulates the high-p_{T} radiation against which the $t\bar{t}$ system recoils.

Table 1: Summary of the nominal Monte Carlo simulated samples used in the analysis. The $gg \to WW$ simulation includes Higgs boson contributions. The last two columns give the order in α_S of the matrix element calculation and the overall cross-section normalization. All nominal MC samples use the NNPDF3.0 PDF set. The samples generated with SHERPA use the default set of tuned parton-shower parameters, while for the POWHEG-BOX samples the A14 set of tuned parameters and the NNPDF2.3LO PDF set are used for the parton shower.

Process	Generator	Parton shower	Matrix element $O(\alpha_S)$	Normalization
$q\bar{q} \to WW$	SHERPA 2.2.2	SHERPA	NLO (0–1 jet), LO (2–3 jets)	Generator†
$gg \to WW$	SHERPA 2.2.2	SHERPA	LO (0–1 jet)	Generator
$t\bar{t}$	POWHEG-BOX v2	PYTHIA 8	NLO	NNLO+NNLL
Wt	POWHEG-BOX v2	PYTHIA 8	NLO	NLO+NNLL
Z+jets	SHERPA 2.2.1	SHERPA	NLO (0–2 jets), LO (3–4 jets)	NNLO
WZ, ZZ	SHERPA 2.2.2	SHERPA	NLO (0–1 jet), LO (2–3 jets)	Generator†
$W\gamma, Z\gamma$	SHERPA 2.2.8	SHERPA	NLO (0–1 jet), LO (2–3 jets)	Generator†
VVV	SHERPA 2.2.2	SHERPA	NLO (0–1 jet), LO (2–3 jets)	Generator†

†: The cross-section calculated by SHERPA is found to be in good agreement with the NNLO result [67–70, 73].

NNLO value.

Samples generated with POWHEG-BOX or MADGRAPH5_aMC@NLO used the EVTGEN 1.2.0 or 1.6.0 program [71] to model the decay of bottom and charm hadrons. The effect of multiple interactions in the same and neighbouring bunch crossings (pile-up) was modelled by overlaying the hard-scattering event with simulated inelastic pp events generated with PYTHIA 8.186 using the NNPDF2.3LO set of PDFs and the A3 set of tuned parameters [72].

4 Event reconstruction and selection

Candidate WW events are selected by requiring exactly one isolated electron and one isolated muon with opposite charges. Events with two isolated leptons of the same flavour are not considered in the analysis due to the higher background from Drell–Yan events.

Events were recorded by either single-electron or single-muon triggers [74, 75]. The minimum p_T threshold varied during data-taking between 24 GeV and 26 GeV for electrons, and between 20 GeV and 26 GeV for muons, both requiring 'loose' to 'medium' isolation criteria. Triggers with higher p_T thresholds and looser isolation requirements are also used to increase the efficiency. The trigger selection efficiency is more than 99% for signal events fulfilling all other selection requirements, which are detailed below.

Candidate events are required to have at least one vertex having at least two associated tracks with $p_T > 400$ MeV. The vertex with the highest $\sum p_T^2$ of the associated tracks is taken as the primary vertex.

Electrons are reconstructed from energy deposits in the calorimeter that are matched to tracks [76]. Electron candidates are required to fulfil the 'tight' likelihood-based identification criteria as defined in Ref. [76]. Furthermore, they are required to have $E_T > 27$ GeV and $|\eta| < 2.47$, excluding the transition region between barrel and endcap regions, $1.37 < |\eta| < 1.52$.

Muon candidates are reconstructed by combining a track in the inner detector (ID) with a track in the muon spectrometer [77]. Muons are required to have $p_{\mathrm{T}} > 27\,\mathrm{GeV}$ and $|\eta| < 2.5$ and to satisfy the `Medium` identification selection, as defined in Ref. [77].

Leptons are required to be compatible with the primary vertex by imposing requirements on the impact parameters of associated tracks. The transverse impact parameter significance, d_0/σ_{d_0} is required to satisfy $|d_0/\sigma_{d_0}| < 5\,(3)$ for electrons (muons). The longitudinal impact parameter z_0 must satisfy $|z_0 \cdot \sin\theta| < 0.5\,\mathrm{mm}$, where θ is the polar angle of the track. Additionally, leptons are required to be isolated using information from the ID tracks and energy clusters in the calorimeters in a cone around the lepton. The `Gradient` working point is used for electrons [76], while for muons the `Tight_FixedRad` working point is used, which is similar to the `Tight` selection defined in Ref. [78] but with altered criteria at muon $p_{\mathrm{T}} > 50\,\mathrm{GeV}$ in order to increase the background rejection. The electron or muon trigger object is required to match the respective reconstructed lepton.

Jets are reconstructed using the anti-k_t algorithm [79] with a radius parameter of $R = 0.4$ using particle-flow objects [80]. They are required to have $p_{\mathrm{T}} > 30\,\mathrm{GeV}$ and $|\eta| < 4.5$. To suppress jets that originate from pile-up, a jet-vertex tagger [81] is applied to jets with $p_{\mathrm{T}} < 60\,\mathrm{GeV}$ and $|\eta| < 2.4$. Jet energy scale and resolution are corrected with η- and p_{T} dependent scale factors [82]. Jets with $p_{\mathrm{T}} > 20\,\mathrm{GeV}$ and $|\eta| < 2.5$ containing decay products of a b-hadron are identified using the DL1r b-tagging algorithm [83, 84] at the 85% efficiency working point.

The missing transverse momentum, with magnitude $E_{\mathrm{T}}^{\mathrm{miss}}$, is computed as the negative of the vectorial sum of the transverse momenta of tracks associated with jets and muons, as well as tracks in the ID that are not associated with any other component. The p_{T} of the electron track is replaced by the calibrated transverse momentum of the reconstructed electron [85].

In order to resolve the overlap between particles reconstructed as multiple physics objects in the detector, non-b-tagged jets are removed if they overlap, within $\Delta R < 0.2$, with an electron, or with a muon if the jet has less than three associated tracks with $p_{\mathrm{T}} > 500\,\mathrm{MeV}$ and satisfies $p_{\mathrm{T}}^{\mu}/p_{\mathrm{T}}^{\mathrm{jet}} > 0.5$, and the ratio of the muon p_{T} to the sum of the track p_{T} associated with the jet is greater than 0.7. Electrons or muons overlapping within $\Delta R < 0.4$ with any jet, including b-tagged jets, after the former selection are removed.

Events having at least one jet, but no b-tagged jets, are selected for the analysis. To reduce the Drell–Yan backgrounds, dominated by Z+jets events with $Z \to \tau^+\tau^-$ decays, the invariant mass of the electron–muon pair is required to be $m_{e\mu} > 85\,\mathrm{GeV}$. This requirement also reduces the contribution of resonant $gg \to H \to WW$ production. Events with additional leptons with $p_{\mathrm{T}} > 10\,\mathrm{GeV}$ and satisfying `Loose` isolation and `LooseLH` (`Loose`) identification requirements for electrons (muons), are vetoed to reduce backgrounds due to WZ and ZZ production. Additionally, the subsets of events with high leading-jet transverse momentum, $p_{\mathrm{T}}^{\text{lead. jet}} > 200\,\mathrm{GeV}$, are analysed in detail, to investigate the reduced interference-suppression in the aTGC interpretation. Table 2 gives a summary of the lepton, jet and event selection requirements used to define the signal region.

5 Background estimate

The top-quark background, from either $t\bar{t}$ or single-top Wt production, comprises about 60% of the events passing the event selection and about 90% of the total background. Additional backgrounds considered are Z+jets production, events with non-prompt or misidentified leptons, diboson production (WZ, $W\gamma$, ZZ, and $Z\gamma$), and triboson production.

Table 2: Summary of the object and event selection criteria.

Selection	Criteria
Lepton p_{T}	$> 27\,\mathrm{GeV}$
Lepton η	$\lvert\eta\rvert < 2.47$ and not $1.37 < \lvert\eta\rvert < 1.52$ (electron)
	$\lvert\eta\rvert < 2.5$ (muon)
Lepton identification	`TightLH` (electron), `Medium` (muon)
Lepton isolation	`Gradient` (electron), `Tight_FixedRad` (muon)
Lepton impact parameter	$\lvert d_0/\sigma_{d_0}\rvert < 5, 3$ (electron, muon)
	$\lvert z_0 \cdot \sin\theta\rvert < 0.5\,\mathrm{mm}$
Jet selection	$p_{\mathrm{T}} > 30\,\mathrm{GeV}$, $\lvert\eta\rvert < 4.5$
b-jet selection	$p_{\mathrm{T}} > 20\,\mathrm{GeV}$, $\lvert\eta\rvert < 2.5$, DL1r (85% eff. WP)
Lepton selection	1 electron and 1 muon of opposite charge, no additional lepton with $p_{\mathrm{T}} > 10\,\mathrm{GeV}$, `Loose` isolation, and `LooseLH` (electron) / `Loose` (muon) identification
Number of jets	≥ 1
Number of b-jets	0
$m_{e\mu}$	$> 85\,\mathrm{GeV}$
High $p_{\mathrm{T}}^{\text{lead. jet}}$ selection	$p_{\mathrm{T}}^{\text{lead. jet}} > 200\,\mathrm{GeV}$

5.1 Top-quark background

An estimate of the $t\bar{t}$ background is obtained using a data-driven technique, while the single-top Wt background is estimated using simulation and is found to contribute about 16% of the top-quark background. Following the procedure used in a measurement of the $t\bar{t}$ cross-section [86], two control regions requiring exactly one and exactly two b-tagged jets are defined. All other selection criteria are the same as in the signal region. These regions are dominated by $t\bar{t}$ events and can be used to infer the number of $t\bar{t}$ events in the signal region with minimal dependence on the selection and b-tagging efficiencies. The contribution of non-$t\bar{t}$ events in the 1-b-jet and 2-b-jet control regions is 13% and 4% of the expected events, respectively, of which 90% can be attributed to single-top Wt production.

The numbers of $t\bar{t}$ events in the two control regions, as well as in the signal region, are given by

$$N_{1b}^{t\bar{t}} = N_{1b} - N_{1b}^{\text{others}} = \mathcal{L}\sigma_{t\bar{t}}\varepsilon_{e\mu} \cdot 2\varepsilon_b\,(1 - C_b\varepsilon_b)\ , \tag{1}$$

$$N_{2b}^{t\bar{t}} = N_{2b} - N_{2b}^{\text{others}} = \mathcal{L}\sigma_{t\bar{t}}\varepsilon_{e\mu} \cdot C_b\varepsilon_b^2\ , \tag{2}$$

$$N_{0b}^{t\bar{t}} = \mathcal{L}\sigma_{t\bar{t}}\varepsilon_{e\mu} \cdot \left(1 - 2\varepsilon_b + C_b\varepsilon_b^2\right)\ , \tag{3}$$

where N_{ib} and N_{ib}^{others} are, respectively, the number of selected events in data and the number of non-$t\bar{t}$ events, estimated using simulation, with exactly i b-tagged jets. The term $\mathcal{L}\sigma_{t\bar{t}}\varepsilon_{e\mu}$ is the product of the integrated luminosity, the $t\bar{t}$ cross-section, and the general selection efficiency, and ε_b is the efficiency of selecting a b-jet in a $t\bar{t}$ event. The correction factor $C_b = \varepsilon_{bb}/\varepsilon_b^2$ accounts for correlation effects between selecting one and two b-jets. It is determined from $t\bar{t}$ simulation as $C_b = 4 \cdot N_{\text{MC}}^{t\bar{t}} N_{2b,\text{MC}}^{t\bar{t}} / \left(N_{1b,\text{MC}}^{t\bar{t}} + 2 \cdot N_{2b,\text{MC}}^{t\bar{t}}\right)^2$, and typically has values close to unity. The b-jet selection efficiency, ε_b, accounts for the efficiency of the

b-tagging algorithm and also for the acceptance of b-jets. Using Eqs. (1)–(3), the number of $t\bar{t}$ events in the signal region can be expressed as

$$N_{0b}^{t\bar{t}} = \frac{C_b}{4} \frac{\left(N_{1b}^{t\bar{t}} + 2N_{2b}^{t\bar{t}}\right)^2}{N_{2b}^{t\bar{t}}} - N_{1b}^{t\bar{t}} - N_{2b}^{t\bar{t}} \,,$$

which depends only on N_{ib} and N_{ib}^{others} ($i = 1, 2$), as well as C_b. The $t\bar{t}$ background estimate is performed in each analysis bin, i.e. for the fiducial selection as well as in each individual bin for the differential measurements. Because b-tagged jets are selected with a lower p_{T} threshold than regular jets, this method also works for events with exactly one regular jet.

As the $t\bar{t}$ background estimate is largely based on observed yields in data control regions and the only input from $t\bar{t}$ simulation is the correlation factor C_b, this method strongly reduces experimental and theoretical uncertainties in the $t\bar{t}$ background, and, thus, lowers the total uncertainty in the background by a factor of approximately five. In regions of phase space where, for a large fraction of events, one or both b-jets are outside the detector acceptance, the reliance on $t\bar{t}$ simulation for the extrapolation into the signal region increases. In such cases, the $t\bar{t}$ estimate remains valid because modelling uncertainties cover rate and shape differences between data and simulation for b-jet kinematic distributions in the control region. Uncertainties in the single-top Wt production rate that are independent of the b-jet multiplicity, such as the cross-section uncertainty, partially cancel out because single-top Wt is the dominant background to $t\bar{t}$ in the $t\bar{t}$ control regions. A variation leading to a larger Wt prediction in the control regions reduces the $t\bar{t}$ estimate, so if the same variation also leads to a larger Wt prediction in the signal region, the overall effect on the combined top background is reduced. The total uncertainty in the top background in the signal region is 2.8%.

The top background estimate is validated in a top-enriched subset of the signal region which requires $m_{\ell j} < 140\,\text{GeV}$ and $\Delta\phi(e, \mu) < \pi/2$ in addition to the normal event selection. Here $m_{\ell j}$ is the invariant mass of the leading jet and the closest lepton. This region is approximately 70% pure in top events and shows good agreement between the data and the combined signal and background prediction, which uses the data-driven top background estimate. The level of agreement of the prediction with the observed events in the control regions and the top-enriched selection is summarized in Table 3. Figure 2 shows the distributions of the $p_{\text{T}}^{\text{lead. lep.}}$ and the jet multiplicity, confirming the accurate modelling of lepton and jet-related properties in events without b-jets.

5.2 Drell–Yan background

The Drell–Yan Z+jets background is estimated using MC simulation. The $m_{e\mu} > 85$ GeV requirement strongly suppresses this background by a factor of about nine. The contribution of this background to the selected events in the signal region is about 3%, almost entirely due to $Z/\gamma^* \to \tau^+\tau^-$+jets events.

The Z+jets estimate is checked in a validation region requiring a dilepton invariant mass between 45 GeV and 80 GeV and either $p_{\text{T},e\mu} < 30\,\text{GeV}$ or $E_{\text{T}}^{\text{miss}} < 20\,\text{GeV}$, in addition to the b-jet veto and the requirement of at least one jet with $p_{\text{T}} > 30\,\text{GeV}$ and $|\eta| < 4.5$. The Z+jets purity of this region is 75% and good modelling of the data is observed, as shown in Table 3. Figure 2 shows the distribution of the dilepton invariant mass $m_{e\mu}$ in the validation region, which features the resonant $Z \to \tau\tau$ distribution over a rising background of top events.

In addition to the theoretical uncertainty in the Z+jets cross-section of 5% [87], uncertainties are estimated by comparing the nominal MC simulation with events simulated by MadGraph5_aMC@NLO. This uncertainty estimate was found to bracket the effect of scale uncertainties. In the signal region, the total uncertainty in the Z+jets background is about 30%.

5.3 Backgrounds with non-prompt or misidentified leptons

Reducible backgrounds from events with non-prompt or misidentified leptons are called fake-lepton backgrounds or 'fakes'. Fake leptons correspond to leptons from heavy-flavour hadron decays and jets misidentified as electrons. Fake-lepton events stem mainly from W+jets production and contribute about 3% of the selected events. Top backgrounds with one prompt lepton contribute about 10% of the fake-lepton backgrounds.

Fake-lepton backgrounds are estimated using a data-driven technique. A control region is defined, where one of the two lepton candidates fails the nominal selection with respect to the impact parameters and isolation criteria, but instead fulfils a looser set of requirements designed to increase the contribution of fake leptons. The fake-lepton background in the signal region is, then, obtained by scaling the number of data events in this control region by an extrapolation factor, after subtracting processes with two prompt leptons using simulation. The extrapolation factor is determined in a data sample that is dominated by fake leptons, and it depends on the p_{T}, $|\eta|$, and flavour of the lepton. The data sample is selected by requiring events with a dijet-like topology with one lepton candidate recoiling against a jet, with $|\Delta\phi(\ell, j)| > 2.8$. To suppress contamination from W+jets events in this sample, the sum of $E_{\mathrm{T}}^{\mathrm{miss}}$ and the transverse mass of the lepton and $E_{\mathrm{T}}^{\mathrm{miss}}$ system is required to be smaller than 50 GeV. The approach used closely follows the one applied in Ref. [88].

Systematic uncertainties in the composition of the different sources of fake leptons are estimated by varying the selection of the data sample in which the extrapolation factors are determined. The variations include selecting events with a b-jet recoiling against the lepton candidate, as well as changing the $E_{\mathrm{T}}^{\mathrm{miss}}$ requirements to increase the fake-lepton contributions. The normalization of the prompt-lepton background in the control region used for the extrapolation factor determination is varied by 10%, which covers the largest discrepancies between simulation and data observed in a dedicated validation region. An additional 25% uncertainty in the fake-lepton background normalization covers a potential mismodelling of the identification efficiency of prompt leptons that fail the tight, but fulfil the looser, lepton identification requirements. The uncertainty in the signal contamination in the control region, which is subtracted using simulation, is determined from the typical size of the largest deviations between the measured and predicted differential cross-sections, which is 20%. The total relative uncertainty in the fake-lepton background is about 40%.

In order to validate the estimate of the fake-lepton backgrounds, the opposite-charge requirement of the signal region selection is inverted, and events with an electron–muon pair of the same charge are selected. As many processes leading to fake leptons are charge symmetric, while most Standard Model processes are not, this selection increases the contribution of W+jets events to about 25%. The modelling of the fake-lepton backgrounds can be validated despite the relatively low purity since the dominant diboson background in this region is known with a precision of about 10%. Reasonable agreement of the prediction with the data is observed, as is shown in Figure 2 in the $p_{\mathrm{T}}^{\text{sub-lead. lep.}}$ distribution, and in Table 3 comparing the numbers of observed and predicted events.

Table 3: Summary of the observed and predicted events in the background control regions (CR) and validation regions (VR), and in the top-background enriched selection. The uncertainty in the prediction includes statistical and systematic effects, excluding theory uncertainties on the signal. The purity column gives the purity of the target process, relative to the total prediction. The $t\bar{t}$ prediction in the two $t\bar{t}$ control regions is from simulation, while in the top-enriched region the data-driven estimate is used.

Region	Observed	Predicted ± Error	Purity
$t\bar{t}$ CR 1b	260 971	268 000 ± 19 000	87%
$t\bar{t}$ CR 2b	257 777	267 000 ± 21 000	96%
Top enriched	7167	7000 ± 1000	72%
Same-sign VR	5095	5000 ± 600	25%
Drell–Yan VR	11 824	13 000 ± 1600	74%
VZ VR	14 770	14 000 ± 1900	94%
$V\gamma$ VR (OS)	2720	2670 ± 240	63%
$V\gamma$ VR (SS)	2401	2250 ± 240	76%

5.4 Other backgrounds

Backgrounds from WZ, ZZ, $W\gamma$ and $Z\gamma$ production are estimated from simulation, and are found to contribute about 3% of the total selected events, dominated by WZ events, which are observed to be well described by the nominal Sherpa simulation in Ref. [89]. Uncertainties are derived by comparing the nominal simulation with events simulated by Powheg + Pythia 8. The difference in generator predictions was found to be larger than the impact of scale uncertainties in the Sherpa simulation, and thus the assigned uncertainty is the conservative option. Additionally, the uncertainty in the diboson cross-section of 10% [90, 91] is included.

The VZ (WZ and ZZ) prediction is validated in events containing a third lepton having $p_{\mathrm{T}} \geq 10\,\mathrm{GeV}$ that must satisfy loosened identification criteria. The invariant mass of the resulting same-flavour opposite-charge pair of leptons is required to be between 80 GeV and 100 GeV, close to the Z boson mass. These selections gives a very pure sample of diboson events, and the prediction is in good agreement with the data, as seen in Figure 2 and Table 3. In Figure 2 the $E_{\mathrm{T}}^{\mathrm{miss}}$ distribution in the VZ validation region shows separation between ZZ and WZ events.

$V\gamma$ ($W\gamma$ and $Z\gamma$) events enter the signal region as backgrounds when the photon is reconstructed and selected as an electron candidate. To validate estimates of these backgrounds, the electron identification requirements are changed such that contributions from photon conversions increase. As the electron candidates reconstructed from photon conversion are charge symmetric, both opposite-charge and same-charge candidates are selected with respect to the selected muon. For the $V\gamma$ validation region the p_{T} distribution of the electron candidates is shown in Figure 2. It is dominated by electrons from photon conversion. Good agreement with the observed data in the validation regions is found.

Based on MC simulations, it is estimated that the triboson background contributes less than 0.1% of the inclusive selected events and at most 0.5% of the selected events in a single bin and is thus neglected in the analysis.

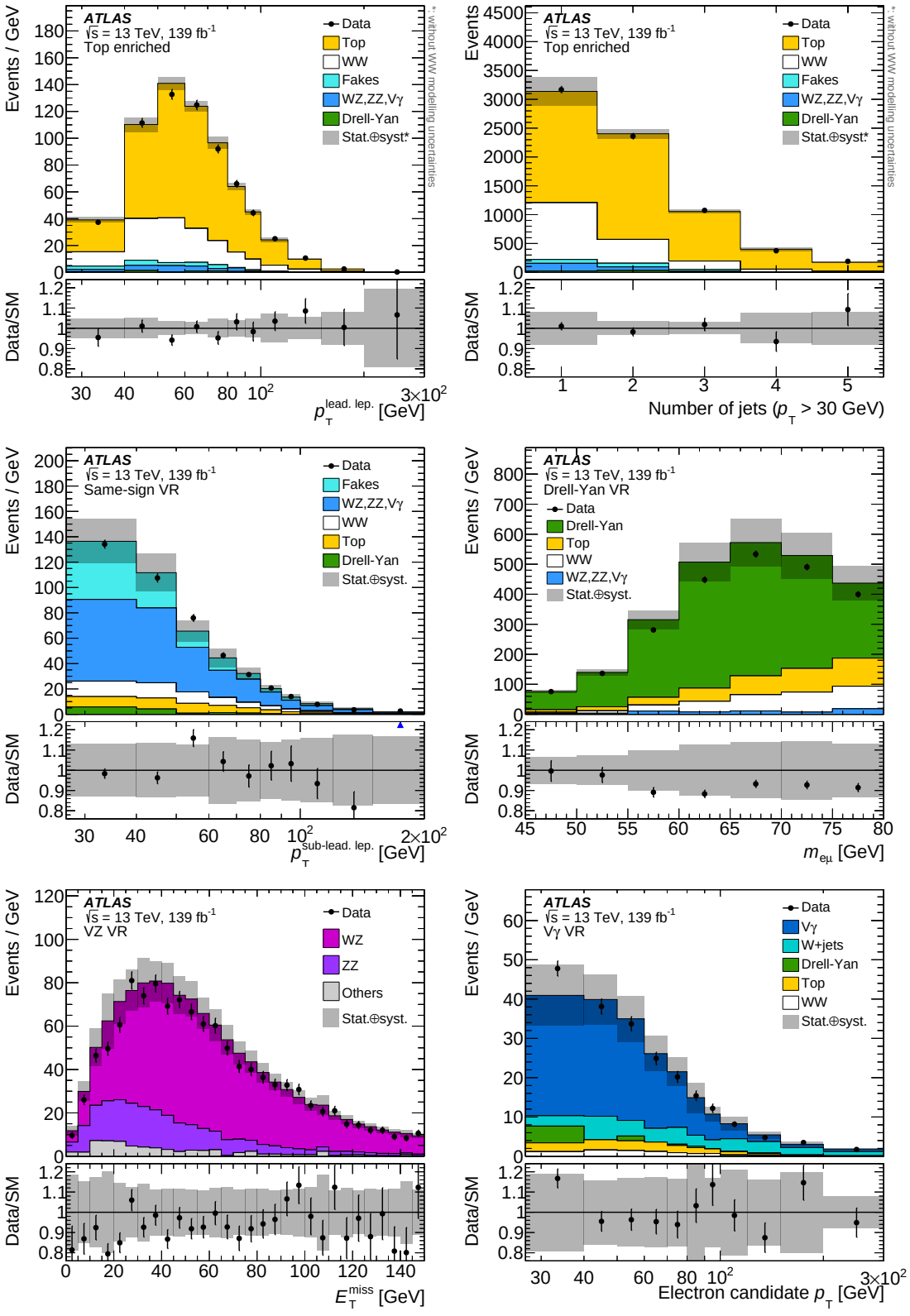

Figure 2: Detector-level distributions of the $p_{\mathrm{T}}^{\text{lead. lep.}}$ (top left) and the jet multiplicity (top right) in the top-enriched region, the $p_{\mathrm{T}}^{\text{sub-lead. lep.}}$ in the same-sign validation region (VR) (middle left), the $m_{e\mu}$ in the Drell–Yan VR (middle right), the $E_{\mathrm{T}}^{\text{miss}}$ in the VZ VR (bottom left), and the electron candidate p_{T} in the $V\gamma$ VR with opposite-sign leptons (bottom right). The last bin contains overflow events. Data are shown as black markers, together with the predictions for the signal and background production processes. The top background in the top-enriched region is estimated using the data-driven method explained in the text; in all other regions the nominal MC prediction is used. The lower panels show the ratio of the data to the total prediction. The uncertainty bands shown include statistical and systematic uncertainties, excluding theory uncertainties on the signal.

Table 4: Selected WW candidate events, together with the signal prediction and the background estimates. The uncertainties include statistical and systematic contributions, excluding theory uncertainties on the signal. The fractions in percent give the relative contribution to the total SM prediction. The individual uncertainties are correlated, and do not add up in quadrature to the total uncertainty.

	Signal region		$p_{\mathrm{T}}^{\text{lead. jet}} > 200\,\text{GeV}$	
Data	89 239		5825	
Total SM	91 600 ± 2500		5980 ± 150	
WW	28 100 ± 1200	31%	2480 ± 60	42%
Total bkg.	63 500 ± 1800	69%	3500 ± 140	58%
Top	55 800 ± 1500	61%	3030 ± 110	51%
Drell–Yan	2200 ± 700	2%	66 ± 9	1%
Fake leptons	2700 ± 1100	3%	140 ± 70	2%
$WZ, ZZ, V\gamma$	2800 ± 500	3%	270 ± 70	4%

5.5 Selected WW candidate events

Table 4 lists the number of selected WW candidate events, as well as the breakdown of the background predictions. Details of the systematic uncertainties are given in Section 7. Figure 3 shows selected distributions at detector level in the final analysis binning and compares the observed data with the signal prediction and the background estimate. Reasonable agreement between data and expectations is observed for both the event yields and the shapes of the distributions. For the nominal signal model, small excesses are seen in the predictions at low $p_{\mathrm{T}}^{\text{lead. lep.}}$, as well as at low $m_{e\mu}$ in the high-$p_{\mathrm{T}}^{\text{lead. jet}}$ selection (both in Figure 3). These are, however, covered by the theory uncertainties of the signal, which are not included in the error bands in this figure.

6 Fiducial and differential cross-section determination

The WW+jets cross-section is evaluated in the fiducial phase space of the $WW \to e^{\pm}\nu\mu^{\mp}\nu$ decay channel as defined in Table 5. In simulated events, electrons and muons are required to originate directly from the hard interaction and not from τ-lepton or hadron decays. The momenta of photons emitted in a cone of size $\Delta R = 0.1$ around the lepton direction that do not originate from hadron decays are added to the lepton momentum to form 'dressed' leptons. Stable final-state particles,[5] excluding prompt leptons and the associated photons, are clustered into particle-level jets using the anti-k_t algorithm with radius parameter $R = 0.4$. The missing transverse momentum is defined at particle level as the transverse component of the vectorial sum of the neutrino momenta. The nominal definition of the particle-level fiducial phase space does not include a veto on b-jets. Alternative results that include a veto on particle-level b-jets[6] with $p_{\mathrm{T}} > 20$ GeV are provided in HEPData[7].

[5] Particles are considered stable if their decay length $c\tau$ is greater than 1 cm.

[6] At particle level, b-jets are defined by ghost-association [92], wherein b-hadrons are included in the jet clustering as infinitely soft particles (ghosts). Jets with b-hadron ghosts among their constituents are b-jets.

[7] https://www.hepdata.net/record/100511

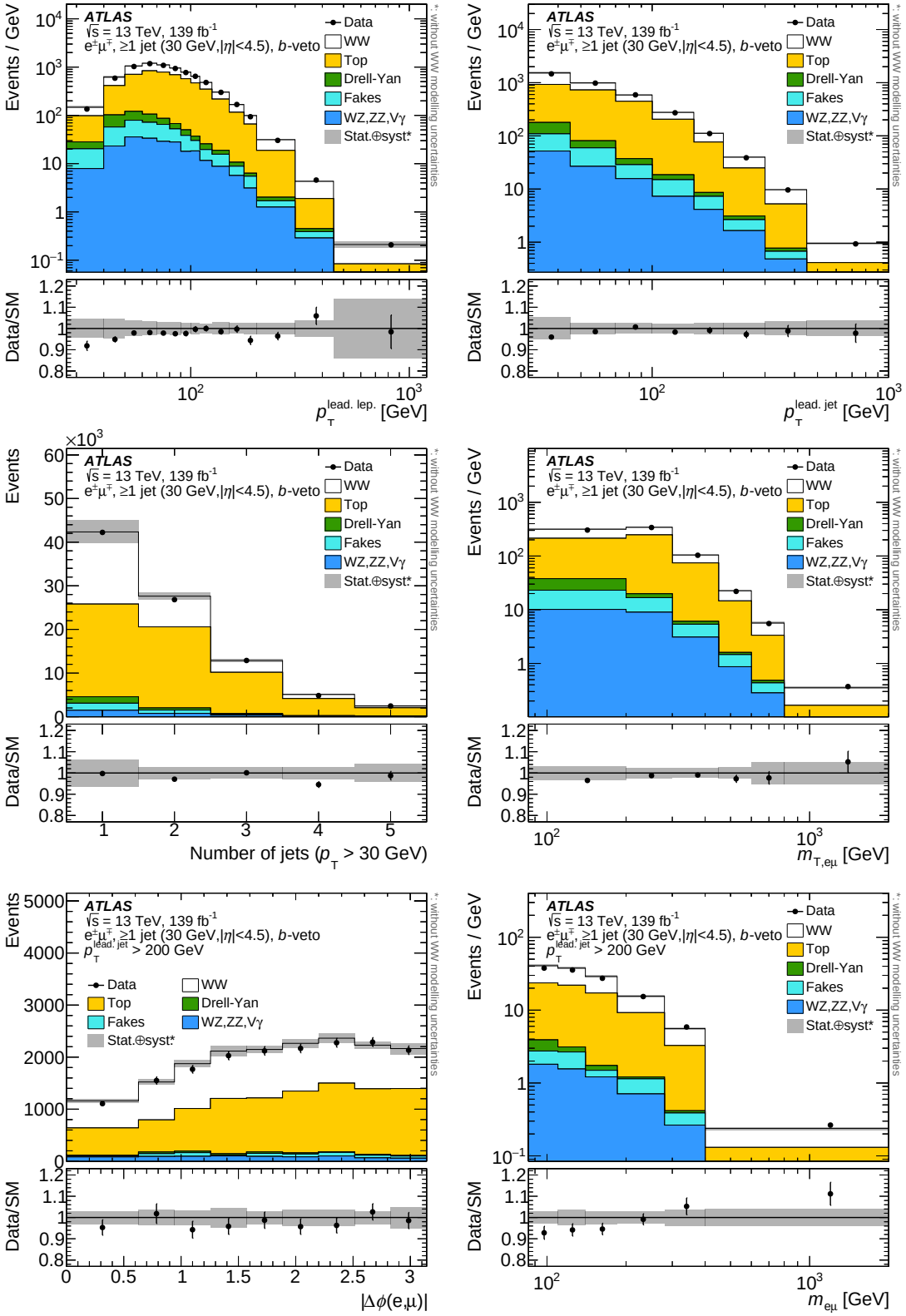

Figure 3: Signal region detector-level distributions of the $p_{\mathrm{T}}^{\text{lead. lep.}}$ (top left), the $p_{\mathrm{T}}^{\text{lead. jet}}$ (top right), the jet multiplicity (middle left), the $m_{\mathrm{T},e\mu}$ (middle right), and, for events with $p_{\mathrm{T}}^{\text{lead. jet}} > 200\,\text{GeV}$, the $\Delta\phi(e,\mu)$ (bottom left) and $m_{e\mu}$ (bottom right). Data are shown as black markers together with the predictions for the signal and background production processes. The last bin contains overflow events. The lower panels show the ratio of the data to the total prediction. The uncertainty bands shown include statistical and systematic uncertainties, excluding theory uncertainties on the signal.

Table 5: Definition of the $WW \to e\mu$+jets fiducial phase space, where p_{T}^{ℓ} (η^{ℓ}) refers to the transverse momentum (pseudorapidity) of charged leptons and p_{T}^{j} (y^{j}) to the transverse momentum (rapidity) of jets.

Fiducial selection requirements		
p_{T}^{ℓ}	>	27 GeV
$\lvert\eta^{\ell}\rvert$	<	2.5
$m_{e\mu}$	>	85 GeV
p_{T}^{j}	>	30 GeV
$\lvert y^{j}\rvert$	<	4.5

The fiducial cross-section is obtained as follows:

$$\sigma^{\mathrm{fid}} = \frac{N_{\mathrm{obs}} - N_{\mathrm{bkg}}}{C \times \mathcal{L}},$$

where $\mathcal{L}$ is the integrated luminosity, N_{obs} is the observed number of events, N_{bkg} is the estimated number of background events and C accounts for detector inefficiencies, resolution effects, and contributions from τ-lepton decays. C is calculated as the number of simulated signal events passing the reconstruction-level event selection divided by the events in the fiducial phase space. Its numerical value is $C = 0.747 \pm 0.061$ and its uncertainty is dominated by uncertainties in jet energy scale, jet energy resolution, and pile-up modelling. The fraction of WW events passing the event selection but containing at least one lepton from τ-lepton decays is 9%.

The differential cross-sections are determined using an iterative Bayesian unfolding method [93, 94]. The unfolding procedure corrects for migrations between bins in the distributions during the reconstruction of the events, and applies fiducial as well as reconstruction efficiency corrections. The fiducial corrections take into account events that are reconstructed in the signal region, but originate from outside the fiducial region; the reconstruction efficiency corrects for events inside the fiducial region that are not reconstructed in the signal region due to detector inefficiencies. Tests with MC simulation demonstrate that the method is successful in retrieving the true distribution in the fiducial region from the reconstructed distribution in the signal region. To reduce bias due to the assumed true distribution, the method can be applied iteratively, at the cost of an increased statistical uncertainty. Two iterations are used to unfold the H_{T}, S_{T}, and $p_{\mathrm{T}}^{\text{lead. jet}}$ distributions and the exclusive jet multiplicity, which are subject to large modelling uncertainties. For the remaining distributions, either the result is independent of the number of iterations, or the modelling uncertainty is not reduced and the statistical uncertainties increase. For these cases, only one unfolding iteration is performed.

7 Uncertainties

Systematic uncertainties in the WW+jets cross-section measurements arise from experimental sources, the background determination, the procedures used to correct for detector effects, and theoretical uncertainties in the signal modelling.

The dominant experimental systematic uncertainties arise in the calibration of the jet energy scale and resolution and the calibration of the b-tagging efficiency and mis-tag rates. Experimental uncertainties

also encompass uncertainties in the calibration of lepton trigger, reconstruction, identification and isolation efficiencies, the calibration of the lepton momentum or energy scale and resolution, and the modelling of pile-up. All experimental uncertainties are evaluated by varying the respective calibrations, and propagating their effects through the analysis, affecting both the background estimates and the unfolding of detector effects.

Systematic uncertainties in the estimate of fake leptons are derived by changing the selection used to estimate the weights, in order to change the composition of the sources of fake leptons. Additionally, the subtraction of the prompt-lepton sources in the control region is varied, and the statistical uncertainties of the weights are propagated. More details on the uncertainties affecting the fake-lepton estimate can be found in Section 5.

The estimate of the top background is affected by the statistical uncertainty of the number of events in the control region, and by uncertainties in the modelling of $t\bar{t}$ and single-top Wt events, such as the uncertainty in the matrix element calculation, the parton shower modelling, the QCD scale choices, the initial- and final-state radiation and the interference between $t\bar{t}$ and single-top Wt events. These are evaluated by using the alternative simulations described in Section 3 and propagating the results through the top background estimate. The effect of the PDF uncertainty on the top background was evaluated, but found to be negligible.

The uncertainty in minor backgrounds is estimated by varying their total cross-section within its uncertainty and by using alternative simulations, as described in Section 5. The difference between nominal and alternative simulations covers PDF uncertainties, missing higher-order QCD corrections, and the parton shower model.

The bias introduced by using distributions generated by the nominal signal simulation as a prior in the unfolding is estimated by reweighting these distributions at generator level with a smooth function such that, after including simulated detector effects, they closely resemble the background-subtracted data. This reweighted detector-level prediction is unfolded using the nominal unfolding set-up. The unfolding procedure is able to very accurately recover the generator-level distribution, so this uncertainty source is negligible. Uncertainties in the unfolding procedure due to the theoretical modelling of the signal are evaluated by repeating the unfolding procedure with alternative signal simulations. The uncertainty due to missing higher-order QCD corrections is evaluated by varying the renormalization and factorization scales. The uncertainty due to the choice of generator for the hard interaction, the parton shower model and the underlying-event modelling is estimated using the alternative simulation of $q\bar{q} \rightarrow WW$ production, from Powheg-Box v2, interfaced to Pythia 8.186. For the uncertainty estimation, the alternative model is first reweighted to the nominal model, so that uncertainties due to disagreement in the predicted shape of distributions can be ignored, and only the difference in the prediction of the migration matrix and fiducial and efficiency corrections are taken into account. Statistical uncertainties are evaluated by creating pseudo data samples that are obtained by varying the data within their Poisson uncertainties in each bin and then propagating these varied samples through the unfolding. The statistical uncertainties of the background estimates, which include statistical uncertainties in MC predictions and due to the control regions used in estimating the top and fake-lepton backgrounds, are evaluated using the same method. If not stated otherwise, 'statistical uncertainties' refers to the combined statistical uncertainties from signal and control regions.

Table 6 gives a breakdown of the uncertainties in the fiducial cross-section measurements, and Figure 4 displays the uncertainties as a function of the unfolded $p_{\mathrm{T}}^{\text{lead. lep.}}$ and $p_{\mathrm{T}}^{\text{lead. jet}}$ distributions. Jet-related uncertainties generally decrease with $p_{\mathrm{T}}^{\text{lead. jet}}$ and with correlated quantities such as $p_{\mathrm{T}}^{\text{lead. lep.}}$, while

Table 6: Breakdown of the uncertainties in the measured fiducial cross-section. "Jet calibration" uncertainties encompass jet energy scale and resolution uncertainties, "Top modelling" and "Signal modelling" are uncertainties in the theoretical modelling of the respective processes, "Fake-lepton background" is the uncertainty in the fake-lepton estimate while "Other background" is the uncertainty due to minor prompt-lepton backgrounds, "Flavour tagging" is all uncertainties in flavour tagging efficiency and mis-tag rate, and "Luminosity" is the uncertainty in the measurement of the integrated luminosity. All systematic uncertainties belonging to none of the above categories are included in "Other systematic uncertainties". Statistical uncertainties arise in both the signal region and control region used for the data-driven top and fake-lepton estimates and also from backgrounds that are estimated using MC simulations.

Uncertainty source	Relative effect
Total uncertainty	10%
Signal region statistical uncertainty	1.1%
Data-driven background and MC statistics	1.2%
Jet calibration	6.3%
Top modelling	4.5%
Fake-lepton background	4.3%
Signal modelling	2.7%
Other background	2.3%
Flavour tagging	2.3%
Luminosity	1.9%
Other systematic uncertainties	0.6%

statistical uncertainties increase at high energy. This leads to a minimum of the total uncertainty for intermediate values of $p_{\mathrm{T}}^{\text{lead. jet}}$ and $p_{\mathrm{T}}^{\text{lead. lep.}}$.

8 Results

The measured fiducial cross-section for WW+jets production, with $WW \to e^{\pm}\nu\mu^{\mp}\nu$, at $\sqrt{s} = 13\,\text{TeV}$, for the phase space defined in Table 5 is

$$\sigma_{\text{fid}} = 258 \pm 4\ (\text{stat.}) \pm 25\ (\text{syst.})\ \text{fb},$$

with a total uncertainty of 10%. In Figure 5, the measured result is compared with various predictions for WW+jets production, and good agreement is found. Differential fiducial cross-sections are presented in Figures 6 to 8. Figure 9 displays distributions in a phase space that additionally requires a jet with a transverse momentum of at least 200 GeV.

8.1 Comparison with theoretical predictions

The measurement is compared to the theory predictions listed in Table 7. The measured fiducial cross-section is compatible with the prediction of $279 \pm 2\ (\text{pdf})\ ^{+20}_{-16}\ (\text{scale})$ fb from MATRIX [32, 33, 43, 73, 95–99], which is accurate to NNLO (NLO) for $q\bar{q} \to WW$ ($gg \to WW$) production, denoted nNNLO, but only NLO (LO) accurate for $q\bar{q} \to WW$ ($gg \to WW$) production in association with a jet. For

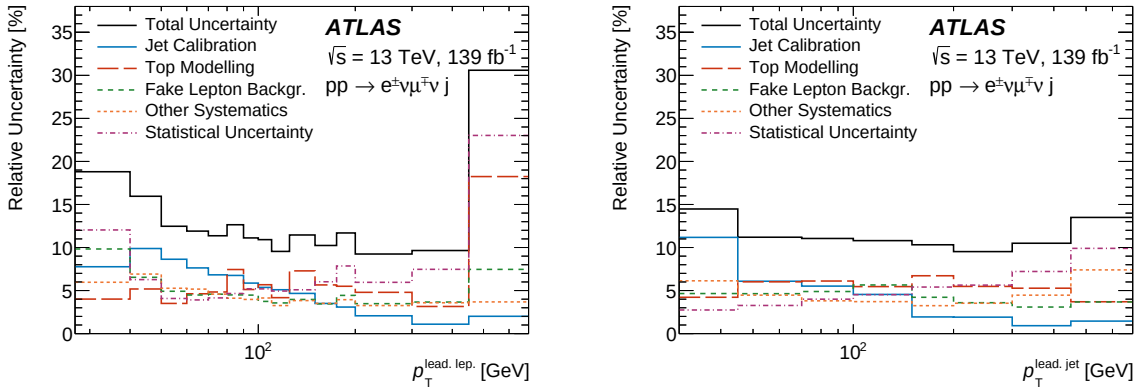

Figure 4: Relative size of uncertainties for the unfolded $p_{\mathrm{T}}^{\text{lead. lep.}}$ and $p_{\mathrm{T}}^{\text{lead. jet}}$ distributions. "Jet Calibration" uncertainties encompass jet energy scale and resolution uncertainties while "Top Modelling" encompasses all $t\bar{t}$ and single-top modelling uncertainties. "Fake Lepton Backgr." is the uncertainty in the non-prompt-lepton estimate from the fake-factor method. "Other Systematics" includes modelling and total cross-section uncertainties in the remaining backgrounds, lepton-related uncertainties as well as uncertainties due to pile-up reweighting and the signal modelling in the unfolding, while "Statistical Uncertainty" is the combined statistical uncertainty in the signal region, from control regions, and from MC simulations.

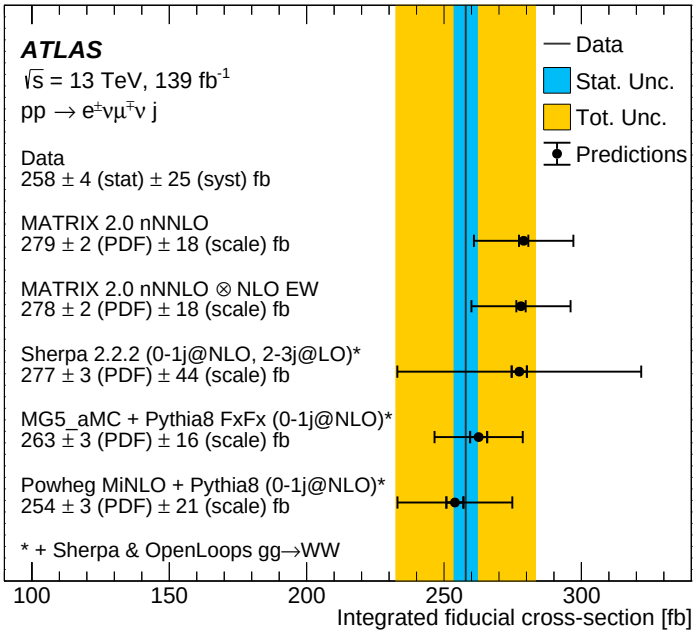

Figure 5: Comparison of the measured fiducial WW+jets cross-section with various theoretical predictions. Theoretical predictions are indicated as points with inner (outer) error bars denoting PDF (PDF+scale) uncertainties. The central value of the measured cross-section is indicated by a vertical line with the narrow band showing the statistical uncertainty and the wider band the total uncertainty including statistical and systematic uncertainties. The result is compared with a fixed-order parton-level prediction from MATRIX 2.0 that is accurate to NNLO (NLO) for $q\bar{q} \to WW$ ($gg \to WW$) production, and a prediction that additionally accounts for EW corrections to WW + jet production, which have been calculated with Sherpa 2.2.2 + OpenLoops. It is also compared with predictions from Sherpa 2.2.2, MadGraph5_aMC@NLO + Pythia 8 with FxFx merging, and Powheg MiNLO + Pythia 8, which are all supplemented by a Sherpa 2.2.2 + OpenLoops $gg \to WW$ LO+PS prediction.

Table 7: Summary of the theoretical predictions that are compared with the measured cross-sections. The samples generated with SHERPA use the default parton-shower tune, while for those using PYTHIA 8 the A14 tune and the NNPDF2.3LO PDF set are used for the parton shower.

Process	Generator	Parton shower	PDF	Matrix element $O(\alpha_S)$
$q\bar{q} \to WW$	MATRIX 2.0	–	NNPDF3.1	NNLO
$gg \to WW$	MATRIX 2.0	–	NNPDF3.1	NLO
$q\bar{q} \to WW$	SHERPA 2.2.2	SHERPA	NNPDF3.0	NLO (0–1 jet), LO (2–3 jets)
$q\bar{q} \to WW$	POWHEG MINLO	PYTHIA 8	NNPDF3.0	NLO (0–1 jet)
$q\bar{q} \to WW$	MADGRAPH 2.3.3	PYTHIA 8	NNPDF3.0	NLO (0–1 jet)
$gg \to WW$	SHERPA 2.2.2 + OPENLOOPS	SHERPA	NNPDF3.0	LO (0–1 jet)

this prediction, the NNPDF3.1NNLO parton distribution function is used, while renormalization and factorization scales are set to m_W. In Figure 5, the measured integrated fiducial cross-section is also compared with a prediction that combines the QCD corrections from MATRIX with NLO EW corrections to WW+jets production that were generated with SHERPA 2.2.2 + OPENLOOPS [25, 100–102]. Photon-induced contributions are included as an additive correction, while the EW correction to $q\bar{q} \to WW$ is taken into account multiplicatively. The latter correction decreases the cross-section by 4%, while the former leads to an increase of 4%. The importance of both corrections increases with energy. The difference between an additive and multiplicative combination scheme for QCD and EW corrections is typically of the order 1% but can be as large as 10% in the highest H_T and S_T bins.

Also displayed in Figure 5 are the nominal $q\bar{q} \to WW$ SHERPA 2.2.2 prediction, a prediction from MADGRAPH 2.3.3 using FXFX merging [103] and interfaced to PYTHIA 8.212, and a POWHEG MINLO [104] prediction interfaced to PYTHIA 8.244. All three calculations are NLO-accurate for WW production with one jet and use the NNPDF3.0 PDF set. The effects of scale uncertainties for all predictions are estimated by varying the factorization and renormalization scales of the hard process. The effects of scale uncertainties on the SHERPA 2.2.2 prediction are large in comparison with the other generators as this calculation includes leading-order matrix elements with up to three jets, which are strongly affected by scale variations. Both predictions are supplemented by the SHERPA 2.2.2 + OPENLOOPS simulation of $gg \to WW$, which is normalized to the total NLO QCD cross-section [99].

The measured distributions in Figures 6–9 are also compared with the predictions described above. Within uncertainties, all predictions give an excellent description of the observed data. For the nominal SHERPA 2.2.2 prediction, values of χ^2 divided by the number of degrees of freedom are below one, except for the $m_{e\mu}$ distribution measured for $p_T^{\text{lead. jet}} > 200$ GeV, for which the value is 1.4. Comparisons of the remaining predictions with the data yield similar χ^2 values, except for the jet multiplicity, H_T, and S_T distributions, where, for the highest multiplicities and energies, small discrepancies exist between data and predictions.

8.2 Effective field theory interpretation

Many new-physics models that introduce new states at a high energy scale (Λ) can be described, at lower energy scales, by operators with mass dimensions larger than four in an effective field theory (EFT) framework. The higher-dimensional operators of the lowest order that can generate anomalous triple-gauge-boson couplings (aTGC) are of dimension six. The Q_W dimension-six operator, as defined in

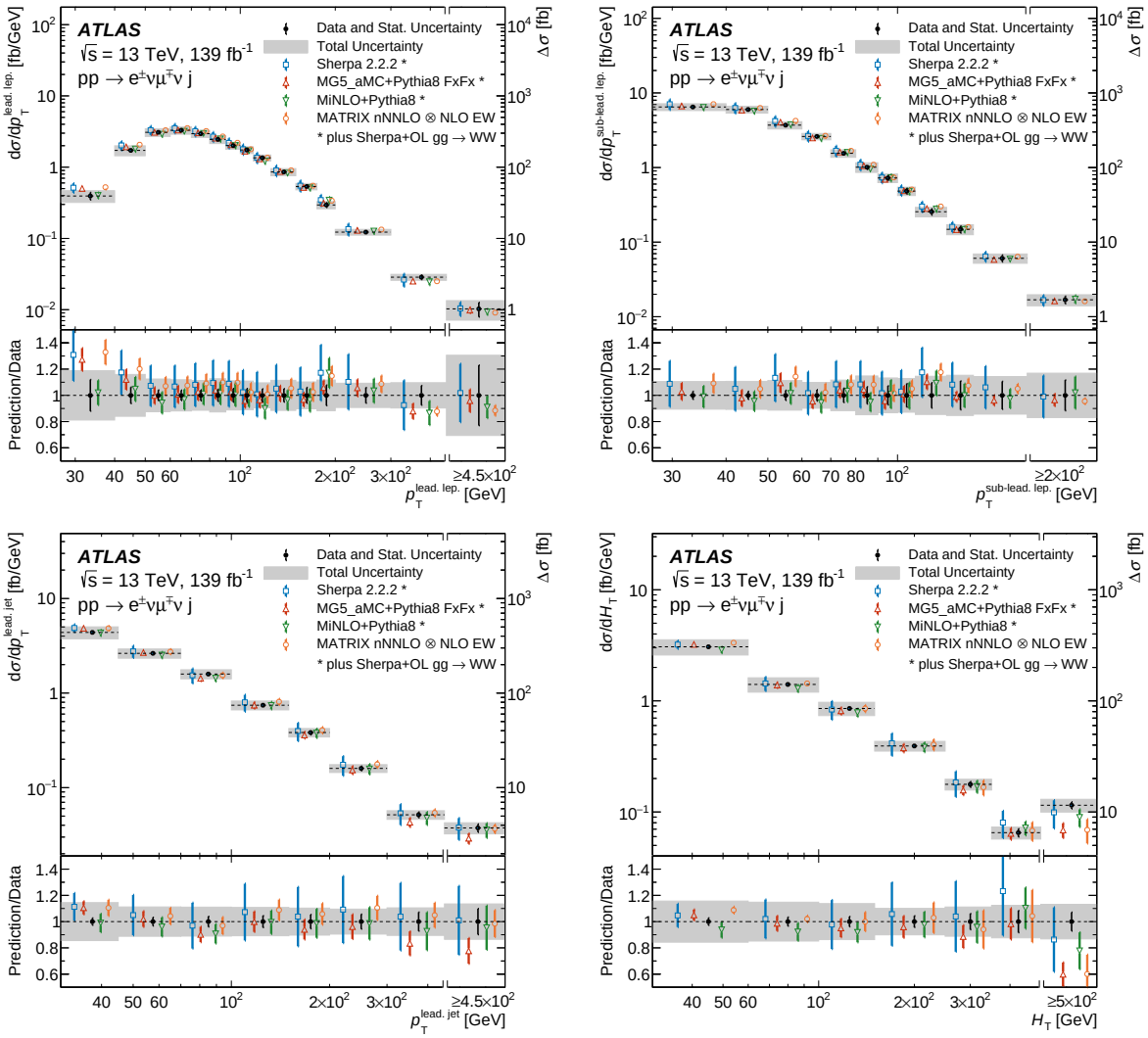

Figure 6: Measured fiducial cross-sections of WW+jets production for (from left to right and top to bottom): $p_{\mathrm{T}}^{\text{lead. lep.}}$, $p_{\mathrm{T}}^{\text{sub-lead. lep.}}$, $p_{\mathrm{T}}^{\text{lead. jet}}$, and H_{T}. The last bin of each distribution is inclusive in the measured observable and the corresponding integrated cross-section is indicated by the right-hand-side axis. The measured cross-section values are shown as points with error bars giving the statistical uncertainty and solid bands indicating the size of the total uncertainty. The results are compared with the NNLO prediction with extra NLO EW corrections and NLO corrections for $gg \to WW$ production (denoted MATRIX ⊗ NLO EW) as well as NLO+PS predictions from Sherpa 2.2.2, MadGraph5_aMC@NLO + Pythia 8 with FxFx merging, and Powheg MiNLO + Pythia 8 for $q\bar{q}$ initial states, combined with Sherpa + OpenLoops (LO+PS) for the gg initial state. The Sherpa 2.2.2 + OpenLoops prediction is normalized to the total cross-section calculated at NLO in QCD. Theoretical predictions are indicated as markers with vertical lines denoting PDF and scale uncertainties.

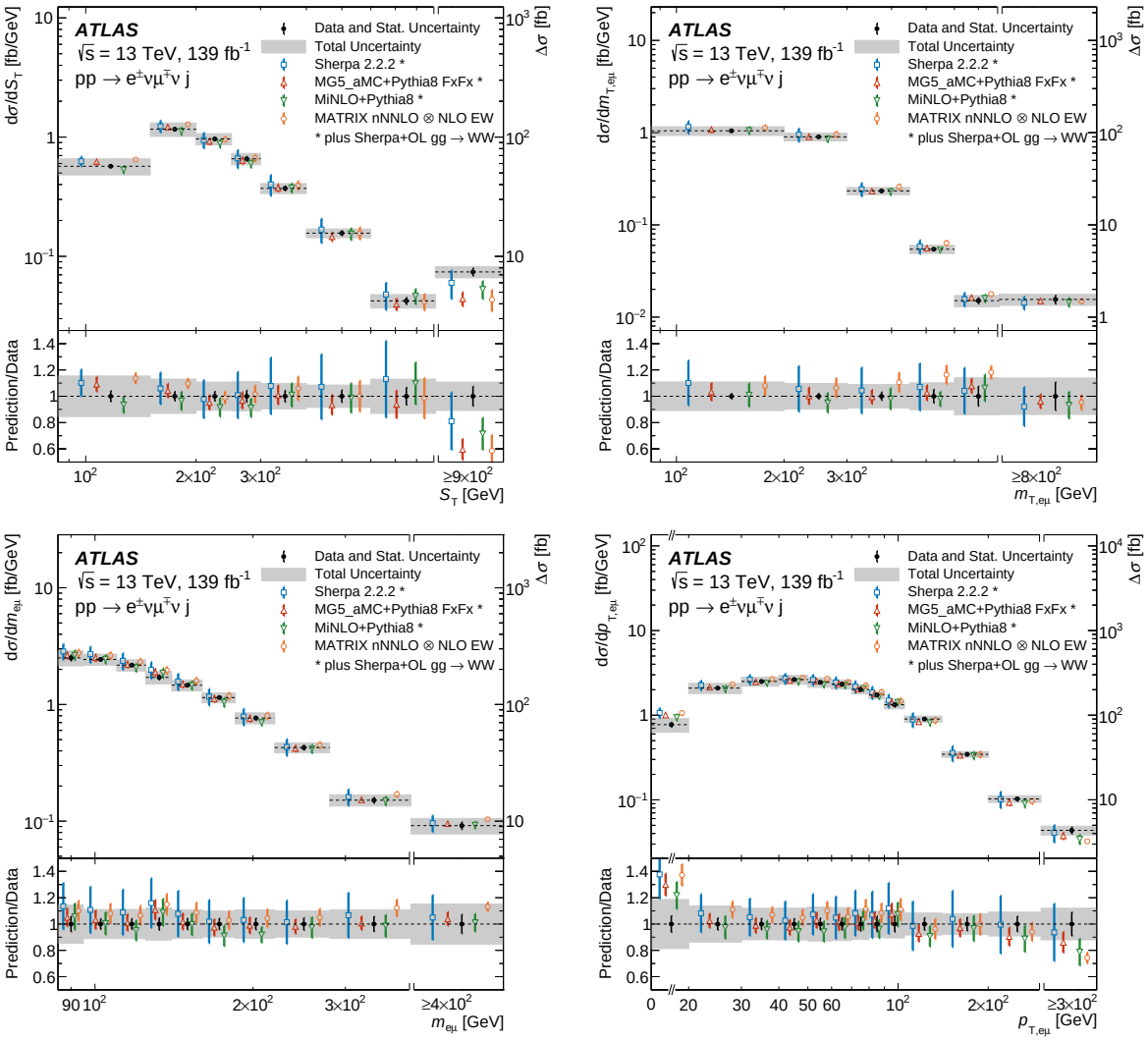

Figure 7: Measured fiducial cross-sections of WW+jets production for (from left to right and top to bottom): S_{T}, $m_{\mathrm{T},e\mu}$, $m_{e\mu}$, and $p_{\mathrm{T},e\mu}$. The last bin of each distribution is inclusive in the measured observable and the corresponding integrated cross-section is indicated by the right-hand-side axis. The measured cross-section values are shown as points with error bars giving the statistical uncertainty and solid bands indicating the size of the total uncertainty. The results are compared with the NNLO prediction with extra NLO EW corrections and NLO corrections for $gg \to WW$ production (denoted MATRIX ⊗ NLO EW) as well as NLO+PS predictions from Sherpa 2.2.2, MadGraph5_aMC@NLO + Pythia 8 with FxFx merging, and Powheg MiNLO + Pythia 8 for $q\bar{q}$ initial states, combined with Sherpa + OpenLoops (LO+PS) for the gg initial state. The Sherpa 2.2.2 + OpenLoops prediction is normalized to the total cross-section calculated at NLO in QCD. Theoretical predictions are indicated as markers with vertical lines denoting PDF and scale uncertainties.

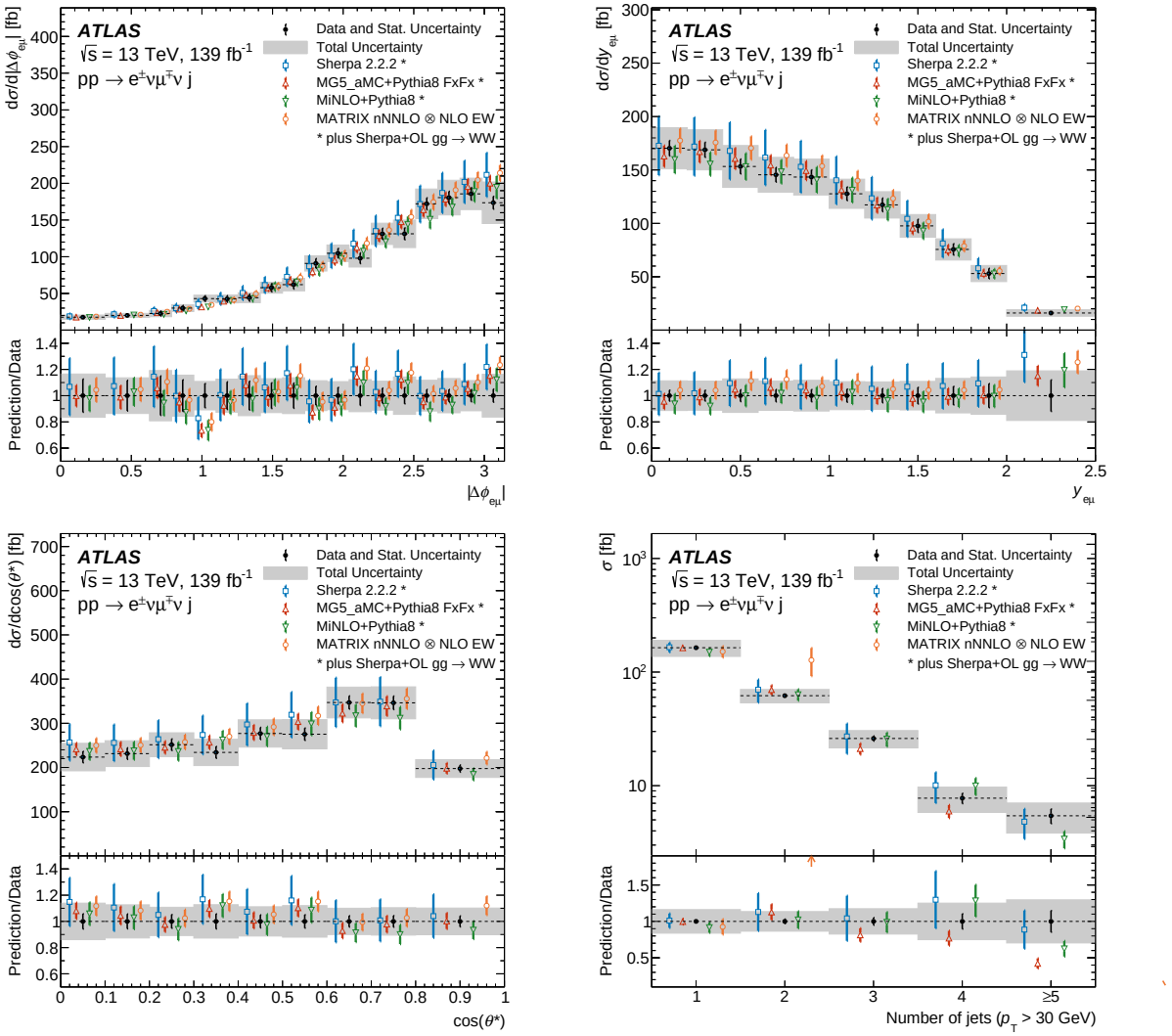

Figure 8: Measured fiducial cross-sections of WW+jets production for (from left to right and top to bottom): $\Delta\phi(e,\mu)$, $y_{e\mu}$, $\cos\theta^*$, and the exclusive jet multiplicity. The measured cross-section values are shown as points with error bars giving the statistical uncertainty and solid bands indicating the size of the total uncertainty. The results are compared with the NNLO prediction with extra NLO EW corrections and NLO corrections for $gg \to WW$ production (denoted MATRIX ⊗ NLO EW) as well as NLO+PS predictions from Sherpa 2.2.2, MadGraph5_aMC@NLO + Pythia 8 with FxFx merging, and Powheg MiNLO + Pythia 8 for $q\bar{q}$ initial states, combined with Sherpa + OpenLoops (LO+PS) for the gg initial state. The Sherpa 2.2.2 + OpenLoops prediction is normalized to the total cross-section calculated at NLO in QCD. Theoretical predictions are indicated as markers with vertical lines denoting PDF and scale uncertainties.The MATRIX prediction is not defined for more than two jet emissions.

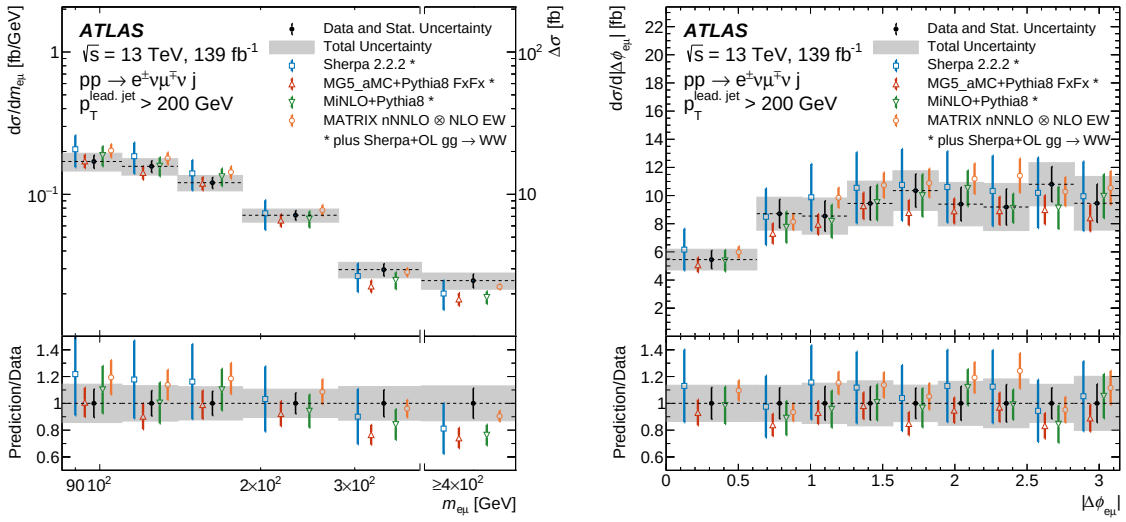

Figure 9: Measured fiducial cross-sections of WW+jets production for $m_{e\mu}$ (left) and $\Delta\phi(e,\mu)$ (right) in the fiducial phase space requiring $p_{\mathrm{T}}^{\text{lead. jet}} > 200\,\text{GeV}$. The last bin of the $m_{e\mu}$ distribution is inclusive and the corresponding integrated cross-section is indicated by the right-hand-side axis. The measured cross-section values are shown as points with error bars giving the statistical uncertainty and solid bands indicating the size of the total uncertainty. The results are compared with the NNLO prediction with extra NLO EW corrections and NLO corrections for $gg \to WW$ production (denoted MATRIX ⊗ NLO EW) as well as NLO+PS predictions from Sherpa 2.2.2, MadGraph5_aMC@NLO + Pythia 8 with FxFx merging, and Powheg MiNLO + Pythia 8 for $q\bar{q}$ initial states, combined with Sherpa + OpenLoops (LO+PS) for the gg initial state. The Sherpa 2.2.2 + OpenLoops prediction is normalized to the total cross-section calculated at NLO in QCD. Theoretical predictions are indicated as markers with vertical lines denoting PDF and scale uncertainties.

Ref. [14], is of particular interest for an analysis of diboson production because it can only be measured in processes affected by modifications of the gauge-boson self-couplings. Its effect increases rapidly with the centre-of-mass energy, making a measurement at the energies probed by the LHC important. However, the interference of the SM and anomalous amplitudes, and, thus, the observable consequences of the operator, decrease with increasing energy due to the different helicities of the dominant contributions to the two amplitudes [105, 106]. As a consequence, the square of the anomalous dimension-six amplitude, which is quadratic in the ratio of the Wilson coefficient, c_W, to Λ^2, dominates, while, in general, the interference of dimension-six operators with the SM is expected to be larger, as it is linear in c_W/Λ^2 and, thus, less suppressed by Λ. The interference-suppression weakens the limits on c_W that can be achieved by a measurement of diboson production and also poses a problem for the validity of an interpretation in a dimension-six model, since other terms of order Λ^{-4}, for example those due to dimension-eight operators, are neglected. Requiring a hard jet in addition to the diboson pair alters the relative contributions of different helicity configurations and reduces the suppression of the interference of SM and anomalous amplitudes [13].

Constraints on the Wilson coefficient, c_W, are determined using the unfolded $m_{e\mu}$ cross-section, which is the measured distribution most sensitive to the interference of the Q_W operator with the SM. The fit is performed both for jet $p_{\mathrm{T}} > 30\,\text{GeV}$ and for jet $p_{\mathrm{T}} > 200\,\text{GeV}$. The latter selection is used to enhance the effect of the interference term per the above discussion.

Templates of the distributions representing the pure SM contribution, the new-physics contribution, and the interference between the SM and the new-physics contributions at LO are prepared using

Table 8: Observed and expected confidence intervals (CI) for c_W for a linearized and a quadratic EFT fit of $m_{e\mu}$, when requiring either jet $p_T > 30$ GeV or jet $p_T > 200$ GeV. The new-physics scale Λ is set to 1 TeV.

Jet p_T	Linear only	68% CI obs.	95% CI obs.	68% CI exp.	95% CI exp.
> 30 GeV	yes	[–1.64, 2.86]	[–3.85, 4.97]	[–2.30, 2.27]	[–4.53, 4.41]
> 30 GeV	no	[–0.20, 0.20]	[–0.33, 0.33]	[–0.28, 0.27]	[–0.39, 0.38]
> 200 GeV	yes	[–0.29, 1.84]	[–1.37, 2.81]	[–1.12, 1.09]	[–2.24, 2.10]
> 200 GeV	no	[–0.43, 0.46]	[–0.60, 0.58]	[–0.38, 0.33]	[–0.53, 0.48]

MadGraph5_aMC@NLO 2.7.2 [107], interfaced to Pythia 8.244 [45], with the A14 tune [46], for parton showering, and hadronization. Events with zero or one jet are simulated in MadGraph5_aMC@NLO and the overlap between matrix-element and parton-shower emissions is removed using the CKKW-L merging procedure [65, 66]. Agreement of the MadGraph5_aMC@NLO prediction with the baseline Sherpa 2.2.2 generator is ensured by applying a bin-wise correction, determined as the ratio of the SM predictions from Sherpa and MadGraph5_aMC@NLO. It is assumed that the relative scale-induced uncertainties of the Sherpa prediction are also applicable, differentially in $m_{e\mu}$, to the prediction that includes the effect of dimension-six operators. The prediction and the measured cross-section are, then, used to construct a likelihood function. Measurement uncertainties are modelled using a multivariate Gaussian distribution, while QCD scale and PDF uncertainties affecting the theory prediction are considered as nuisance parameters, constrained with a Gaussian distribution. Two nuisance parameters are introduced to model the scale uncertainty affecting the predicted $m_{e\mu}$ distribution so that its effect is not fully correlated between bins. The first (second) parameter models the full effect of the scale uncertainty in the first (last) bin of the distribution. The effect decreases linearly with $\log(m_{e\mu})$ such that the parameter has no effect in the last (first) bin. The decorrelation of scale-uncertainty effects increases the width of confidence intervals by up to 40% relative to a model in which the scale-uncertainty effects are assumed to be fully correlated between bins of $m_{e\mu}$. Confidence intervals for c_W are derived using Wilk's theorem [108], assuming that the profile likelihood test statistic is χ^2 distributed [109].

Observed and expected 95% confidence intervals for the EFT coefficients are summarized in Table 8. They are presented both for a fit that takes into account only linear terms in the cross-section parameterization and for a fit that also takes into account quadratic terms due to the square of the dimension-six amplitude. For jet $p_T > 200$ GeV, limits in the linearized EFT expansion are improved relative to a $p_T > 30$ GeV requirement, and the impact of the quadratic term is reduced. As expected, the analysis of the phase space characterized by a high-p_T jet increases the experimental sensitivity to effects proportional to c_W/Λ^2 due to the reduced suppression of the interference between the SM amplitude and the dimension-six amplitude. However, pure dimension-six contributions, which are $O(\Lambda^{-4})$, are still dominant in this phase space, and the EFT expansion in Λ^{-1} does not converge quickly. The limits are, thus, not valid in a general SM EFT scenario that includes additional Λ^{-4} contributions due to dimension-eight operators.

The presented constraints on c_W, obtained accounting for quadratic terms, are weaker than those obtained by the ATLAS measurement of WW events with no associated jets [7]. There, a dataset corresponding to only 36 fb^{-1} was analysed and the results constrain c_W/Λ^2 to a 95% confidence interval with a width of $0.5/\text{TeV}^2$. Limits obtained from this measurement when only including linear terms are improved relative to the previous measurement, for which the corresponding confidence interval has a width of $11/\text{TeV}^2$. The limits from such a linear fit are, however, an order of magnitude weaker than those obtained by the ATLAS analysis of electroweak production of dijets in association with a Z boson [110].

9 Conclusion

The cross-section for the production of W-boson pairs decaying into $e^{\pm}\nu_e\mu^{\mp}\nu_\mu$ final states in pp collisions at $\sqrt{s} = 13\,\text{TeV}$ is measured in a fiducial phase space that requires the presence of at least one hadronic jet with transverse momentum of at least 30 GeV, providing jet-inclusive measurements in WW events. The measurement is performed with data recorded by the ATLAS experiment at the LHC between 2015 and 2018 that correspond to an integrated luminosity of $139\,\text{fb}^{-1}$. The measured fiducial cross-section, $\sigma_{\text{fid}} = 258 \pm 4\,(\text{stat}) \pm 25\,(\text{syst})$ fb, is found to be consistent with theoretical predictions. With a total uncertainty of 10%, this result represents a precise measurement of WW production in association with jets at the LHC that probes a previously unexplored event topology. Differential cross-sections for WW+jets production are measured as a function of the kinematics of the final-state charged leptons, jets, and missing transverse momentum, and are compared with predictions from perturbative QCD calculations. The data agree well with predictions in all differential distributions, up to the highest measured transverse momenta and for up to five jets. Dimension six operators that produce anomalous triple-gauge-boson interactions are studied in a phase space that benefits from enhanced interference between the Standard Model amplitude and the anomalous amplitude.

Appendix

A Measurement at high $p_{\mathrm{T}}^{\text{lead. lep.}}$

At high vector-boson p_{T}, predictions for inclusive WW events suffer from so-called 'giant K-factors', which correspond to large higher-order corrections for QCD and electroweak effects [111]. These come in part from event topologies similar to those in W+jets production with the additional emission of a real W boson from a hard jet.

In order to study kinematic configurations that are expected to be strongly affected by higher-order EW and QCD corrections, a sample of events is selected with the requirement that $p_{\mathrm{T}}^{\text{lead. lep.}} > 200\,\text{GeV}$. This selects event topologies that generally have a high-p_{T} W boson accompanied by a lower-p_{T} W boson. Here the cross-section is measured differentially in the azimuthal separation between the sub-leading lepton and the leading jet, $\Delta\phi(\text{sub-lead. lep.}, \text{jet})$, and their η–ϕ separation $\Delta R(\text{sub-lead. lep.}, \text{jet})$, as well as in the ratio of the lepton transverse momenta, $p_{\mathrm{T}}^{\text{sub-lead. lep.}}/p_{\mathrm{T}}^{\text{lead. lep.}}$, and the ratio of the sub-leading lepton and leading jet transverse momenta, $p_{\mathrm{T}}^{\text{sub-lead. lep.}}/p_{\mathrm{T}}^{\text{lead. jet}}$.

Table 9 lists the selected WW candidate events in this region, as well as the breakdown of the background estimates. Figure 10 shows the measured distributions at detector level in the final analysis binning, comparing the observed data with the signal prediction and the background estimate.

The unfolded distributions are shown in Figure 11. In general, the predictions are in good agreement with the measurement.

Table 9: Selected WW candidate events, together with the signal prediction and the background estimates for $p_{\mathrm{T}}^{\text{lead. lep.}} > 200\,\text{GeV}$. The uncertainties include statistical and systematic contributions. The fractions in percent give the relative contribution to the total SM prediction.

	$p_{\mathrm{T}}^{\text{lead. lep.}} > 200\,\text{GeV}$	
Data	3873	
Total SM	3960 ± 120	
WW	1740 ± 50	44%
Total bkg.	2210 ± 110	56%
Top	1920 ± 90	49%
Drell–Yan	42 ± 6	1%
Fake leptons	70 ± 40	2%
$WZ, ZZ, V\gamma$	180 ± 40	4%

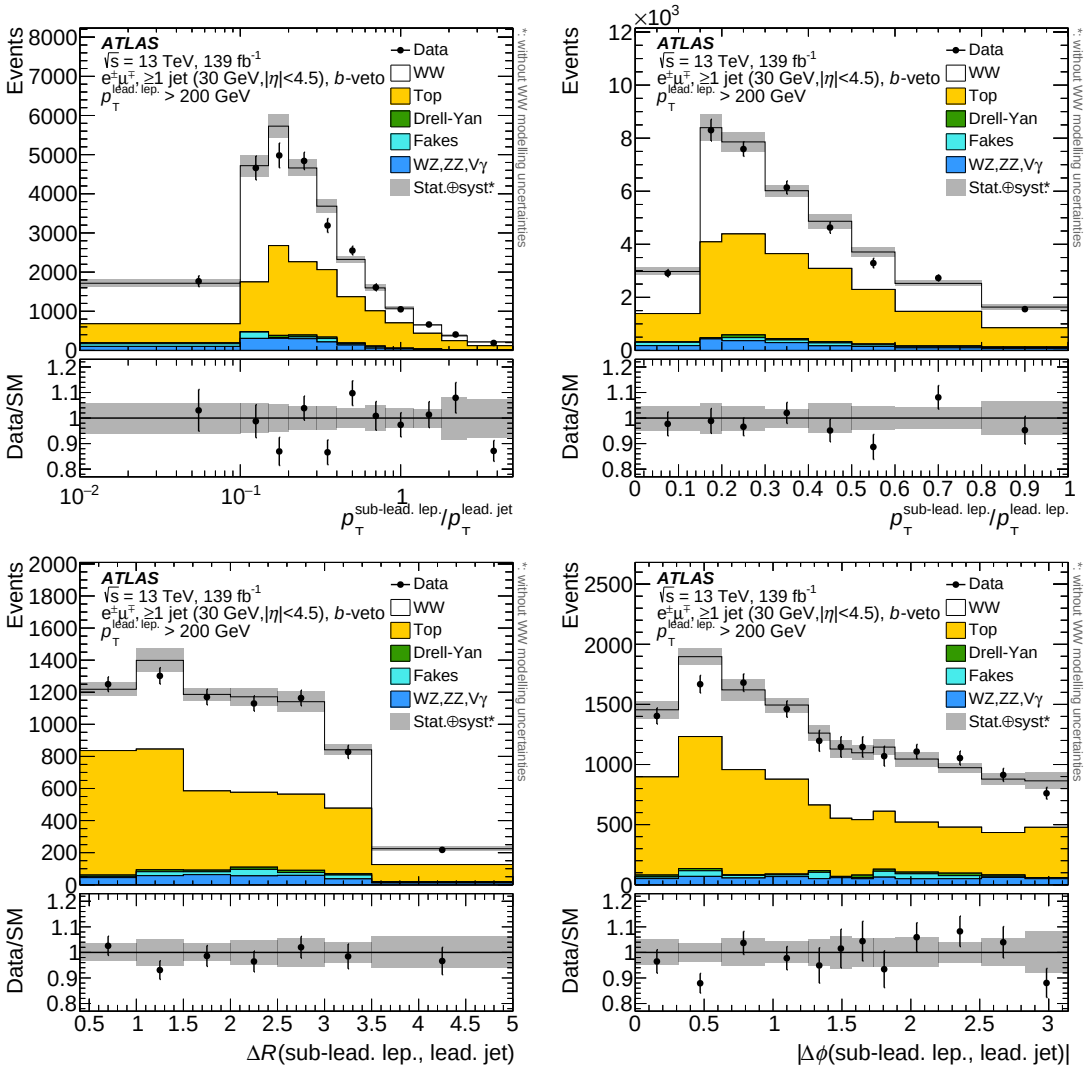

Figure 10: Signal region detector-level distributions, requiring $p_{\mathrm{T}}^{\text{lead. lep.}} > 200\,\text{GeV}$, of $p_{\mathrm{T}}^{\text{sub-lead. lep.}}/p_{\mathrm{T}}^{\text{lead. jet}}$ (top left), $p_{\mathrm{T}}^{\text{sub-lead. lep.}}/p_{\mathrm{T}}^{\text{lead. lep.}}$ (top right), $\Delta R(\text{sub-lead. lep., jet})$ (bottom left) and $\Delta\phi(\text{sub-lead. lep., jet})$ (bottom right). Data are shown as black markers together with the predictions for the signal and background production processes. The last bin contains overflow events. The lower panels show the ratio of the data to the total prediction. The uncertainty bands shown include statistical and systematic uncertainties, excluding theory uncertainties on the signal.

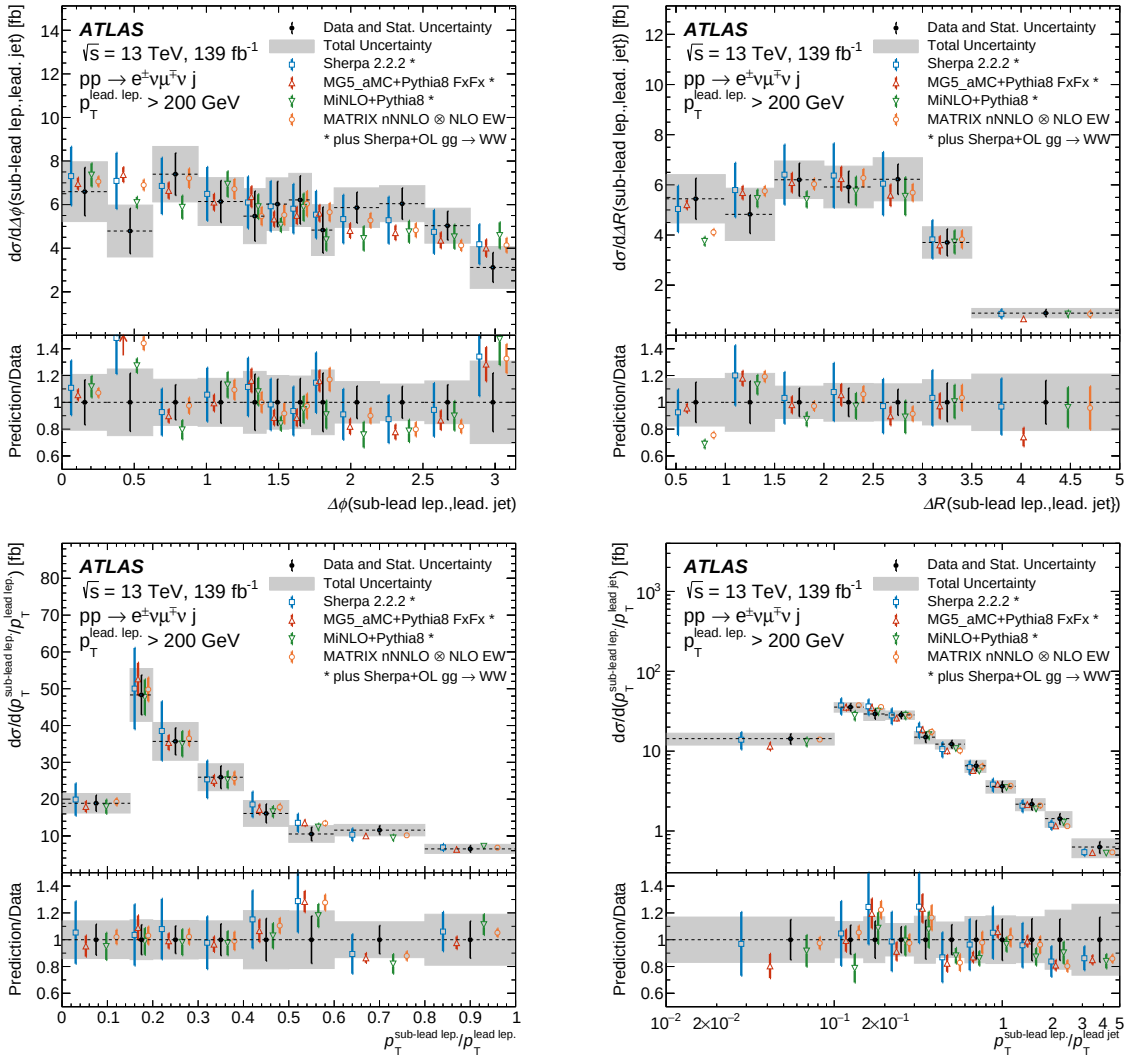

Figure 11: Measured fiducial cross-sections of WW+jets production for (from left to right and top to bottom): $\Delta\phi$(sub-lead. lep., jet), ΔR(sub-lead. lep., jet), $p_{\mathrm{T}}^{\text{sub-lead. lep.}}/p_{\mathrm{T}}^{\text{lead. lep.}}$, and $p_{\mathrm{T}}^{\text{sub-lead. lep.}}/p_{\mathrm{T}}^{\text{lead. jet}}$ in the fiducial phase space requiring $p_{\mathrm{T}}^{\text{lead. lep.}} > 200\,\mathrm{GeV}$. The measured cross-section values are shown as points with error bars giving the statistical uncertainty and solid bands indicating the size of the total uncertainty. The results are compared with the NNLO prediction with extra NLO EW corrections and NLO corrections for $gg \to WW$ production (denoted MATRIX ⊗ NLO EW) as well as NLO+PS predictions from Sherpa 2.2.2, MadGraph5_aMC@NLO + Pythia 8 with FxFx merging, and Powheg MiNLO + Pythia 8 for $q\bar{q}$ initial states, combined with Sherpa + OpenLoops (LO+PS) for the gg initial state. The Sherpa 2.2.2 + OpenLoops prediction is normalized to the total cross-section calculated at NLO in QCD. Theoretical predictions are indicated as markers with vertical lines denoting PDF and scale uncertainties.

B $t\bar{t}$ background estimate

Figure 12 shows the $p_{\mathrm{T}}^{\text{lead. lep.}}$ and jet multiplicity distributions in the two $t\bar{t}$ control regions, which require exactly one and exactly two b-jets, respectively. The b-jet correlation factor C_b for the two distributions is shown in Figure 13. Figure 14 shows the $m_{e\mu}$ distribution for $p_{\mathrm{T}}^{\text{lead. jet}} > 200\,\mathrm{GeV}$ in the two control regions and for the top-enriched selection, together with the b-jet correlation factor C_b. The excess of events predicted at high $p_{\mathrm{T}}^{\text{lead. lep.}}$, in comparison with data, is corrected for by the data-driven estimate, and no discrepancy is seen in the top-enriched selection, as shown in Figure 2 in the main body. The jet multiplicity is well modelled up to five selected jets.

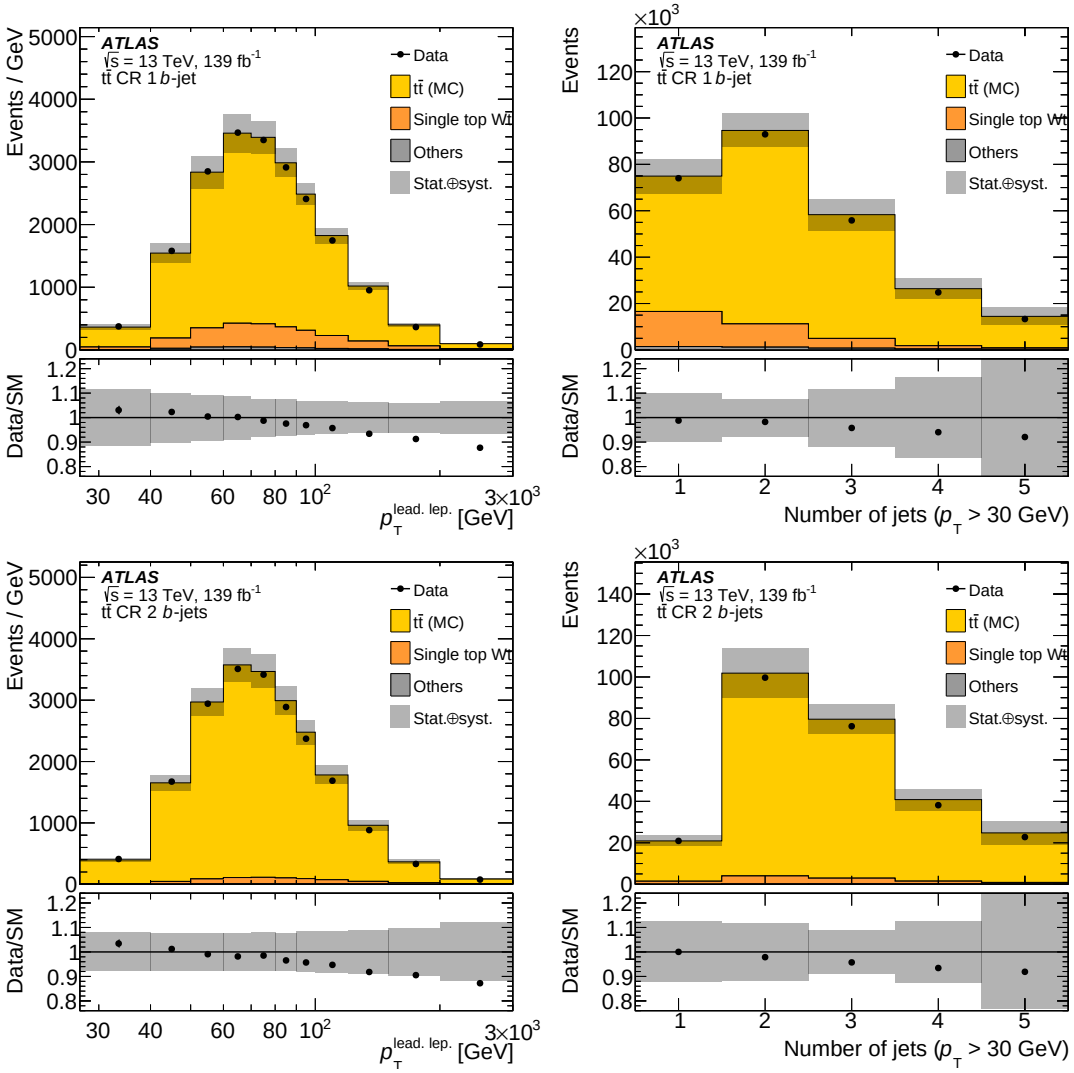

Figure 12: Detector-level distributions of the $p_{\mathrm{T}}^{\text{lead. lep.}}$ (left) and the jet multiplicity (right) in the $t\bar{t}$ control regions with one b-jet (left) and two b-jets (right). Data are shown together with the predictions for $t\bar{t}$, single-top Wt and other production processes from simulation. The last bin contains overflow events. The lower panels show the ratio of the data to the total prediction. The uncertainties shown include statistical and systematic uncertainties.

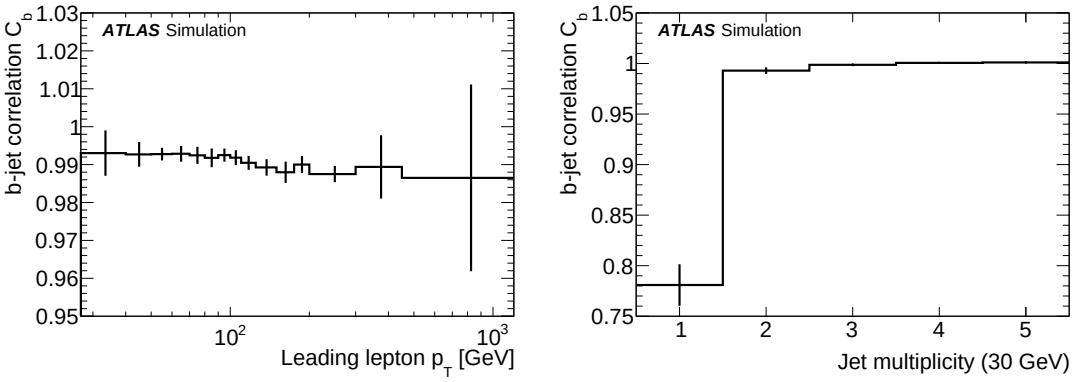

Figure 13: Distribution of the b-jet correlation factor C_b as a function of the $p_{\mathrm{T}}^{\text{lead. lep.}}$ (left) and the jet multiplicity (right), as determined from the nominal $t\bar{t}$ simulation. The uncertainties shown include MC statistical and systematic uncertainties.

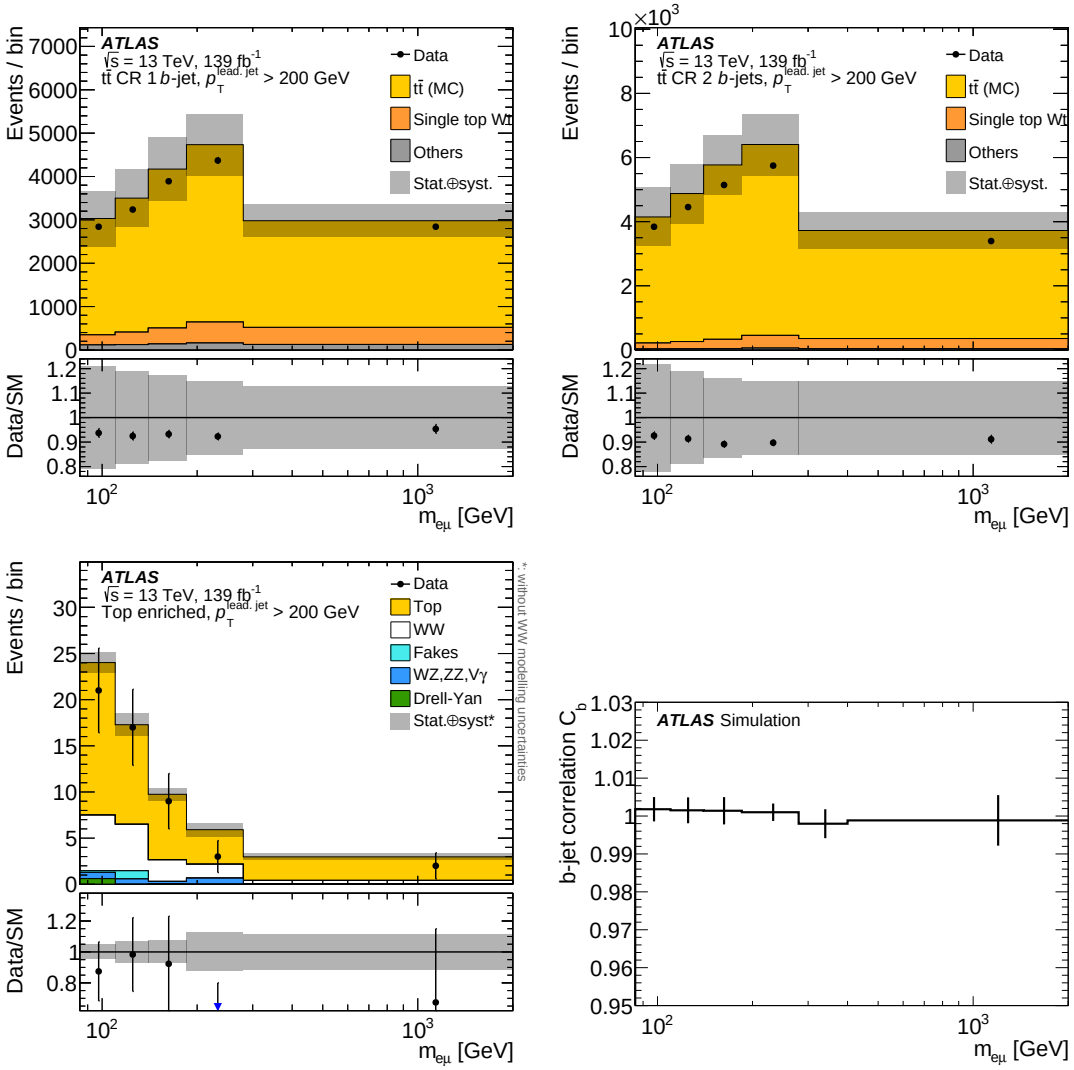

Figure 14: Detector-level distributions of the dilepton invariant mass $m_{e\mu}$ for $p_{\mathrm{T}}^{\text{lead. jet}} > 200\,\text{GeV}$ in the one b-tag and two b-tag control regions as well as the top-enriched region, together with the b-jet correlation factor C_b. The lower panels in the plots of detector-level distributions show the ratio of the data to the total prediction. The uncertainties shown include statistical and systematic uncertainties, for both the distributions and the correlation factor.

Acknowledgements

We thank CERN for the very successful operation of the LHC, as well as the support staff from our institutions without whom ATLAS could not be operated efficiently.

We acknowledge the support of ANPCyT, Argentina; YerPhI, Armenia; ARC, Australia; BMWFW and FWF, Austria; ANAS, Azerbaijan; SSTC, Belarus; CNPq and FAPESP, Brazil; NSERC, NRC and CFI, Canada; CERN; ANID, Chile; CAS, MOST and NSFC, China; COLCIENCIAS, Colombia; MSMT CR, MPO CR and VSC CR, Czech Republic; DNRF and DNSRC, Denmark; IN2P3-CNRS and CEA-DRF/IRFU, France; SRNSFG, Georgia; BMBF, HGF and MPG, Germany; GSRT, Greece; RGC and Hong Kong SAR, China; ISF and Benoziyo Center, Israel; INFN, Italy; MEXT and JSPS, Japan; CNRST, Morocco; NWO, Netherlands; RCN, Norway; MNiSW and NCN, Poland; FCT, Portugal; MNE/IFA, Romania; JINR; MES of Russia and NRC KI, Russian Federation; MESTD, Serbia; MSSR, Slovakia; ARRS and MIZŠ, Slovenia; DST/NRF, South Africa; MICINN, Spain; SRC and Wallenberg Foundation, Sweden; SERI, SNSF and Cantons of Bern and Geneva, Switzerland; MOST, Taiwan; TAEK, Turkey; STFC, United Kingdom; DOE and NSF, United States of America. In addition, individual groups and members have received support from BCKDF, CANARIE, Compute Canada, CRC and IVADO, Canada; Beijing Municipal Science & Technology Commission, China; COST, ERC, ERDF, Horizon 2020 and Marie Skłodowska-Curie Actions, European Union; Investissements d'Avenir Labex, Investissements d'Avenir Idex and ANR, France; DFG and AvH Foundation, Germany; Herakleitos, Thales and Aristeia programmes co-financed by EU-ESF and the Greek NSRF, Greece; BSF-NSF and GIF, Israel; La Caixa Banking Foundation, CERCA Programme Generalitat de Catalunya and PROMETEO and GenT Programmes Generalitat Valenciana, Spain; Göran Gustafssons Stiftelse, Sweden; The Royal Society and Leverhulme Trust, United Kingdom.

The crucial computing support from all WLCG partners is acknowledged gratefully, in particular from CERN, the ATLAS Tier-1 facilities at TRIUMF (Canada), NDGF (Denmark, Norway, Sweden), CC-IN2P3 (France), KIT/GridKA (Germany), INFN-CNAF (Italy), NL-T1 (Netherlands), PIC (Spain), ASGC (Taiwan), RAL (UK) and BNL (USA), the Tier-2 facilities worldwide and large non-WLCG resource providers. Major contributors of computing resources are listed in Ref. [112].

References

[1] ATLAS Collaboration, *Measurement of W^+W^- production in pp collisions at $\sqrt{s} = 7$ TeV with the ATLAS detector and limits on anomalous WWZ and $WW\gamma$ couplings*, Phys. Rev. D **87** (2013) 112001, arXiv: 1210.2979 [hep-ex], Erratum: Phys. Rev. D **88** (2013) 079906.

[2] CMS Collaboration, *Measurement of the W^+W^- cross section in pp collisions at $\sqrt{s} = 7$ TeV and limits on anomalous $WW\gamma$ and WWZ couplings*, Eur. Phys. J. C **73** (2013) 2610, arXiv: 1306.1126 [hep-ex].

[3] ATLAS Collaboration, *Measurement of total and differential W^+W^- production cross sections in proton–proton collisions at $\sqrt{s} = 8$ TeV with the ATLAS detector and limits on anomalous triple-gauge-boson couplings*, JHEP **09** (2016) 029, arXiv: 1603.01702 [hep-ex].

[4] CMS Collaboration, *Measurement of the W^+W^- cross section in pp collisions at $\sqrt{s} = 8$ TeV and limits on anomalous gauge couplings*, Eur. Phys. J. C **76** (2016) 401, arXiv: 1507.03268 [hep-ex].

[5] ATLAS Collaboration, *Measurement of W^+W^- production in association with one jet in proton–proton collisions at $\sqrt{s}$ = 8 TeV with the ATLAS detector*, Phys. Lett. B **763** (2016) 114, arXiv: 1608.03086 [hep-ex].

[6] ATLAS Collaboration, *Measurement of the W^+W^- production cross section in pp collisions at a centre-of-mass energy of $\sqrt{s}$ = 13 TeV with the ATLAS experiment*, Phys. Lett. B **773** (2017) 354, arXiv: 1702.04519 [hep-ex].

[7] ATLAS Collaboration, *Measurement of fiducial and differential W^+W^- production cross-sections at $\sqrt{s}$ = 13 TeV with the ATLAS detector*, Eur. Phys. J. C **79** (2019) 884, arXiv: 1905.04242 [hep-ex].

[8] CMS Collaboration, *W^+W^- boson pair production in proton–proton collisions at $\sqrt{s}$ = 13 TeV*, Phys. Rev. D **102** (2020) 092001, arXiv: 2009.00119 [hep-ex].

[9] ALEPH, DELPHI, L3 and OPAL Collaborations and the LEP Electroweak Working Group, *Electroweak measurements in electron–positron collisions at W-boson-pair energies at LEP*, Phys. Rept. **532** (2013) 119, arXiv: 1302.3415 [hep-ex].

[10] CDF Collaboration, *Observation of W^+W^- Production in $p\bar{p}$ collisions at $\sqrt{s}$ = 1.8 TeV*, Phys. Rev. Lett. **78** (1997) 4536.

[11] CDF Collaboration, *Measurement of the W^+W^- Production Cross Section and Search for Anomalous $WW\gamma$ and WWZ Couplings in $p\bar{p}$ Collisions at $\sqrt{s}$ = 1.96 TeV*, Phys. Rev. Lett. **104** (2010) 201801, [Erratum: Phys. Rev. Lett. 105 (2010) 019905], arXiv: 0912.4500 [hep-ex].

[12] DØ Collaboration, *Measurement of the WW Production Cross Section with Dilepton Final States in $p\bar{p}$ Collisions at $\sqrt{s}$ = 1.96 TeV and Limits on Anomalous Trilinear Gauge Couplings*, Phys. Rev. Lett. **103** (2009) 191801, arXiv: 0904.0673 [hep-ex].

[13] A. Azatov, J. Elias-Miro, Y. Reyimuaji and E. Venturini, *Novel measurements of anomalous triple gauge couplings for the LHC*, JHEP **10** (2017) 027, arXiv: 1707.08060 [hep-ph].

[14] B. Grzadkowski, M. Iskrzynski, M. Misiak and J. Rosiek, *Dimension-Six Terms in the Standard Model Lagrangian*, JHEP **10** (2010) 085, arXiv: 1008.4884 [hep-ph].

[15] A. Barr, *Measuring slepton spin at the LHC*, JHEP **02** (2006) 042, arXiv: hep-ph/0511115.

[16] ATLAS Collaboration, *The ATLAS Experiment at the CERN Large Hadron Collider*, JINST **3** (2008) S08003.

[17] L. Evans and P. Bryant, *LHC Machine*, JINST **3** (2008) S08001.

[18] ATLAS Collaboration, *ATLAS Insertable B-Layer Technical Design Report*, ATLAS-TDR-19; CERN-LHCC-2010-013, 2010, URL: https://cds.cern.ch/record/1291633.

[19] B. Abbott et al., *Production and integration of the ATLAS Insertable B-Layer*, JINST **13** (2018) T05008, arXiv: 1803.00844 [physics.ins-det].

[20] ATLAS Collaboration, *ATLAS data quality operations and performance for 2015–2018 data-taking*, JINST **15** (2020) P04003, arXiv: 1911.04632 [physics.ins-det].

[21] ATLAS Collaboration,
Luminosity determination in pp collisions at $\sqrt{s} = 13$ TeV using the ATLAS detector at the LHC,
ATLAS-CONF-2019-021, 2019, URL: https://cds.cern.ch/record/2677054.

[22] G. Avoni et al., *The new LUCID-2 detector for luminosity measurement and monitoring in ATLAS*,
JINST **13** (2018) P07017.

[23] ATLAS Collaboration, *The ATLAS Simulation Infrastructure*, Eur. Phys. J. C **70** (2010) 823,
arXiv: 1005.4568 [physics.ins-det].

[24] S. Agostinelli et al., *GEANT4 – a simulation toolkit*, Nucl. Instrum. Meth. A **506** (2003) 250.

[25] E. Bothmann et al., *Event generation with Sherpa 2.2*, SciPost Phys. **7** (2019) 034,
arXiv: 1905.09127 [hep-ph].

[26] T. Gleisberg and S. Höche, *Comix, a new matrix element generator*, JHEP **12** (2008) 039,
arXiv: 0808.3674 [hep-ph].

[27] S. Schumann and F. Krauss,
A parton shower algorithm based on Catani–Seymour dipole factorisation, JHEP **03** (2008) 038,
arXiv: 0709.1027 [hep-ph].

[28] S. Höche, F. Krauss, M. Schönherr and F. Siegert,
A critical appraisal of NLO+PS matching methods, JHEP **09** (2012) 049,
arXiv: 1111.1220 [hep-ph].

[29] S. Höche, F. Krauss, M. Schönherr and F. Siegert,
QCD matrix elements + parton showers. The NLO case, JHEP **04** (2013) 027,
arXiv: 1207.5030 [hep-ph].

[30] S. Catani, F. Krauss, R. Kuhn and B. R. Webber, *QCD Matrix Elements + Parton Showers*,
JHEP **11** (2001) 063, arXiv: hep-ph/0109231.

[31] S. Höche, F. Krauss, S. Schumann and F. Siegert, *QCD matrix elements and truncated showers*,
JHEP **05** (2009) 053, arXiv: 0903.1219 [hep-ph].

[32] F. Cascioli, P. Maierhöfer and S. Pozzorini, *Scattering Amplitudes with Open Loops*,
Phys. Rev. Lett. **108** (2012) 111601, arXiv: 1111.5206 [hep-ph].

[33] A. Denner, S. Dittmaier and L. Hofer,
COLLIER: A fortran-based complex one-loop library in extended regularizations,
Comput. Phys. Commun. **212** (2017) 220, arXiv: 1604.06792 [hep-ph].

[34] R. D. Ball et al., *Parton distributions for the LHC run II*, JHEP **04** (2015) 040,
arXiv: 1410.8849 [hep-ph].

[35] P. Nason, *A new method for combining NLO QCD with shower Monte Carlo algorithms*,
JHEP **11** (2004) 040, arXiv: hep-ph/0409146.

[36] S. Frixione, P. Nason and C. Oleari,
Matching NLO QCD computations with parton shower simulations: the POWHEG method,
JHEP **11** (2007) 070, arXiv: 0709.2092 [hep-ph].

[37] S. Alioli, P. Nason, C. Oleari and E. Re, *A general framework for implementing NLO calculations in shower Monte Carlo programs: the POWHEG BOX*, JHEP **06** (2010) 043,
arXiv: 1002.2581 [hep-ph].

[38] P. Nason and G. Zanderighi, *W^+W^-, WZ and ZZ production in the POWHEG-BOX-V2*,
Eur. Phys. J. C **74** (2014) 2702, arXiv: 1311.1365 [hep-ph].

[39] T. Sjöstrand, S. Mrenna and P. Skands, *A brief introduction to PYTHIA 8.1*, Comput. Phys. Commun. **178** (2008) 852, arXiv: 0710.3820 [hep-ph].

[40] ATLAS Collaboration, *Measurement of the Z/γ^* boson transverse momentum distribution in pp collisions at $\sqrt{s} = 7$ TeV with the ATLAS detector*, JHEP **09** (2014) 145, arXiv: 1406.3660 [hep-ex].

[41] H.-L. Lai et al., *New parton distributions for collider physics*, Phys. Rev. D **82** (2010) 074024, arXiv: 1007.2241 [hep-ph].

[42] J. Pumplin et al., *New Generation of Parton Distributions with Uncertainties from Global QCD Analysis*, JHEP **07** (2002) 012, arXiv: hep-ph/0201195.

[43] T. Gehrmann et al., *W^+W^- Production at Hadron Colliders in Next to Next to Leading Order QCD*, Phys. Rev. Lett. **113** (2014) 212001, arXiv: 1408.5243 [hep-ph].

[44] S. Frixione, P. Nason and G. Ridolfi, *A positive-weight next-to-leading-order Monte Carlo for heavy flavour hadroproduction*, JHEP **09** (2007) 126, arXiv: 0707.3088 [hep-ph].

[45] T. Sjöstrand et al., *An introduction to PYTHIA 8.2*, Comput. Phys. Commun. **191** (2015) 159, arXiv: 1410.3012 [hep-ph].

[46] ATLAS Collaboration, *ATLAS Pythia 8 tunes to 7 TeV data*, ATL-PHYS-PUB-2014-021, 2014, URL: https://cds.cern.ch/record/1966419.

[47] R. D. Ball et al., *Parton distributions with LHC data*, Nucl. Phys. B **867** (2013) 244, arXiv: 1207.1303 [hep-ph].

[48] ATLAS Collaboration, *Studies on top-quark Monte Carlo modelling for Top2016*, ATL-PHYS-PUB-2016-020, 2016, URL: https://cds.cern.ch/record/2216168.

[49] S. Frixione, E. Laenen, P. Motylinski, C. White and B. R. Webber, *Single-top hadroproduction in association with a W boson*, JHEP **07** (2008) 029, arXiv: 0805.3067 [hep-ph].

[50] ATLAS Collaboration, *Studies on top-quark Monte Carlo modelling with Sherpa and MG5_aMC@NLO*, ATL-PHYS-PUB-2017-007, 2017, URL: https://cds.cern.ch/record/2261938.

[51] M. Bähr et al., *Herwig++ physics and manual*, Eur. Phys. J. C **58** (2008) 639, arXiv: 0803.0883 [hep-ph].

[52] J. Bellm et al., *Herwig 7.0/Herwig++ 3.0 release note*, Eur. Phys. J. C **76** (2016) 196, arXiv: 1512.01178 [hep-ph].

[53] L. Harland-Lang, A. Martin, P. Motylinski and R. Thorne, *Parton distributions in the LHC era: MMHT 2014 PDFs*, Eur. Phys. J. C **75** (2015) 204, arXiv: 1412.3989 [hep-ph].

[54] J. Alwall et al., *The automated computation of tree-level and next-to-leading order differential cross sections, and their matching to parton shower simulations*, JHEP **07** (2014) 079, arXiv: 1405.0301 [hep-ph].

[55] M. Beneke, P. Falgari, S. Klein and C. Schwinn, *Hadronic top-quark pair production with NNLL threshold resummation*, Nucl. Phys. B **855** (2012) 695, arXiv: 1109.1536 [hep-ph].

[56] M. Cacciari, M. Czakon, M. Mangano, A. Mitov and P. Nason, *Top-pair production at hadron colliders with next-to-next-to-leading logarithmic soft-gluon resummation*, Phys. Lett. B **710** (2012) 612, arXiv: 1111.5869 [hep-ph].

[57] P. Bärnreuther, M. Czakon and A. Mitov, *Percent-Level-Precision Physics at the Tevatron: Next-to-Next-to-Leading Order QCD Corrections to $q\bar{q} \to t\bar{t} + X$*, Phys. Rev. Lett. **109** (2012) 132001, arXiv: 1204.5201 [hep-ph].

[58] M. Czakon and A. Mitov, *NNLO corrections to top-pair production at hadron colliders: the all-fermionic scattering channels*, JHEP **12** (2012) 054, arXiv: 1207.0236 [hep-ph].

[59] M. Czakon and A. Mitov, *NNLO corrections to top pair production at hadron colliders: the quark-gluon reaction*, JHEP **01** (2013) 080, arXiv: 1210.6832 [hep-ph].

[60] M. Czakon, P. Fiedler and A. Mitov, *Total Top-Quark Pair-Production Cross Section at Hadron Colliders Through $O(\alpha_S^4)$*, Phys. Rev. Lett. **110** (2013) 252004, arXiv: 1303.6254 [hep-ph].

[61] M. Czakon and A. Mitov, *Top++: A program for the calculation of the top-pair cross-section at hadron colliders*, Comput. Phys. Commun. **185** (2014) 2930, arXiv: 1112.5675 [hep-ph].

[62] N. Kidonakis, *Two-loop soft anomalous dimensions for single top quark associated production with a W^- or H^-*, Phys. Rev. D **82** (2010) 054018, arXiv: 1005.4451 [hep-ph].

[63] N. Kidonakis, 'Top Quark Production', *Proceedings, Helmholtz International Summer School on Physics of Heavy Quarks and Hadrons (HQ 2013)* (JINR, Dubna, Russia, 15th–28th July 2013) 139, arXiv: 1311.0283 [hep-ph].

[64] C. Anastasiou, L. J. Dixon, K. Melnikov and F. Petriello, *High precision QCD at hadron colliders: Electroweak gauge boson rapidity distributions at next-to-next-to leading order*, Phys. Rev. D **69** (2004) 094008, arXiv: hep-ph/0312266.

[65] L. Lönnblad, *Correcting the Colour-Dipole Cascade Model with Fixed Order Matrix Elements*, JHEP **05** (2002) 046, arXiv: hep-ph/0112284.

[66] L. Lönnblad and S. Prestel, *Matching tree-level matrix elements with interleaved showers*, JHEP **03** (2012) 019, arXiv: 1109.4829 [hep-ph].

[67] M. Grazzini, S. Kallweit, D. Rathlev and M. Wiesemann, *$W^\pm Z$ production at hadron colliders in NNLO QCD*, Phys. Lett. B **761** (2016) 179, arXiv: 1604.08576 [hep-ph].

[68] M. Grazzini, S. Kallweit, D. Rathlev and M. Wiesemann, *$W^\pm Z$ production at the LHC: fiducial cross sections and distributions in NNLO QCD*, JHEP **05** (2017) 139, arXiv: 1703.09065 [hep-ph].

[69] M. Grazzini, S. Kallweit and D. Rathlev, *ZZ production at the LHC: fiducial cross sections and distributions in NNLO QCD*, Phys. Lett. B **750** (2015) 407, arXiv: 1507.06257 [hep-ph].

[70] F. Cascioli et al., *ZZ production at hadron colliders in NNLO QCD*, Phys. Lett. B **735** (2014) 311, arXiv: 1405.2219 [hep-ph].

[71] D. J. Lange, *The EvtGen particle decay simulation package*, Nucl. Instrum. Meth. A **462** (2001) 152.

[72] ATLAS Collaboration, *The Pythia 8 A3 tune description of ATLAS minimum bias and inelastic measurements incorporating the Donnachie–Landshoff diffractive model*, ATL-PHYS-PUB-2016-017, 2016, URL: https://cds.cern.ch/record/2206965.

[73] M. Grazzini, S. Kallweit, S. Pozzorini, D. Rathlev and M. Wiesemann, *W^+W^- production at the LHC: fiducial cross sections and distributions in NNLO QCD*, JHEP **08** (2016) 140, arXiv: 1605.02716 [hep-ph].

[74] ATLAS Collaboration, *Performance of electron and photon triggers in ATLAS during LHC Run 2*, Eur. Phys. J. C **80** (2020) 47, arXiv: 1909.00761 [hep-ex].

[75] ATLAS Collaboration, *Performance of the ATLAS muon triggers in Run 2*, JINST **15** (2020) P09015, arXiv: 2004.13447 [hep-ex].

[76] ATLAS Collaboration, *Electron and photon performance measurements with the ATLAS detector using the 2015–2017 LHC proton–proton collision data*, JINST **14** (2019) P12006, arXiv: 1908.00005 [hep-ex].

[77] ATLAS Collaboration, *Muon reconstruction and identification efficiency in ATLAS using the full Run 2 pp collision data set at $\sqrt{s}$ = 13 TeV*, (2020), arXiv: 2012.00578 [hep-ex].

[78] ATLAS Collaboration, *Muon reconstruction performance of the ATLAS detector in proton–proton collision data at $\sqrt{s}$ = 13 TeV*, Eur. Phys. J. C **76** (2016) 292, arXiv: 1603.05598 [hep-ex].

[79] M. Cacciari, G. P. Salam and G. Soyez, *The anti-k_t jet clustering algorithm*, JHEP **04** (2008) 063, arXiv: 0802.1189 [hep-ph].

[80] ATLAS Collaboration, *Jet reconstruction and performance using particle flow with the ATLAS Detector*, Eur. Phys. J. C **77** (2017) 466, arXiv: 1703.10485 [hep-ex].

[81] ATLAS Collaboration, *Performance of pile-up mitigation techniques for jets in pp collisions at $\sqrt{s}$ = 8 TeV using the ATLAS detector*, Eur. Phys. J. C **76** (2016) 581, arXiv: 1510.03823 [hep-ex].

[82] ATLAS Collaboration, *Jet energy scale and resolution measured in proton–proton collisions at $\sqrt{s}$ = 13 TeV with the ATLAS detector*, (2020), arXiv: 2007.02645 [hep-ex].

[83] ATLAS Collaboration, *Optimisation and performance studies of the ATLAS b-tagging algorithms for the 2017-18 LHC run*, ATL-PHYS-PUB-2017-013, 2017, URL: https://cds.cern.ch/record/2273281.

[84] ATLAS Collaboration, *ATLAS b-jet identification performance and efficiency measurement with $t\bar{t}$ events in pp collisions at $\sqrt{s}$ = 13 TeV*, Eur. Phys. J. C **79** (2019) 970, arXiv: 1907.05120 [hep-ex].

[85] ATLAS Collaboration, *Performance of missing transverse momentum reconstruction with the ATLAS detector using proton–proton collisions at $\sqrt{s}$ = 13 TeV*, Eur. Phys. J. C **78** (2018) 903, arXiv: 1802.08168 [hep-ex].

[86] ATLAS Collaboration, *Measurement of the $t\bar{t}$ production cross-section and lepton differential distributions in $e\mu$ dilepton events from pp collisions at $\sqrt{s}$ = 13 TeV with the ATLAS detector*, Eur. Phys. J. C **80** (2020) 528, arXiv: 1910.08819 [hep-ex].

[87] ATLAS Collaboration, *Measurement of $W^{\pm}$ and Z-boson production cross sections in pp collisions at $\sqrt{s} = 13$ TeV with the ATLAS detector*, Phys. Lett. B **759** (2016) 601, arXiv: 1603.09222 [hep-ex].

[88] ATLAS Collaboration, *Observation of Electroweak Production of a Same-Sign W Boson Pair in Association with Two Jets in pp Collisions at $\sqrt{s} = 13$ TeV with the ATLAS Detector*, Phys. Rev. Lett. **123** (2019) 161801, arXiv: 1906.03203 [hep-ex].

[89] ATLAS Collaboration, *Measurement of $W^{\pm}Z$ production cross sections and gauge boson polarisation in pp collisions at $\sqrt{s} = 13$ TeV with the ATLAS detector*, Eur. Phys. J. C **79** (2019) 535, arXiv: 1902.05759 [hep-ex].

[90] ATLAS Collaboration, *Multi-boson simulation for 13 TeV ATLAS analyses*, ATL-PHYS-PUB-2016-002, 2016, URL: https://cds.cern.ch/record/2119986.

[91] M. Grazzini, S. Kallweit and D. Rathlev, *$W\gamma$ and $Z\gamma$ production at the LHC in NNLO QCD*, JHEP **07** (2015) 085, arXiv: 1504.01330 [hep-ph].

[92] M. Cacciari and G. P. Salam, *Pileup subtraction using jet areas*, Phys. Lett. B **659** (2008) 119, arXiv: 0707.1378 [hep-ph].

[93] G. D'Agostini, *A multidimensional unfolding method based on Bayes' theorem*, Nucl. Instr. Meth. A **362** (1995) 487.

[94] G. D'Agostini, *Improved iterative Bayesian unfolding*, (2010), arXiv: 1010.0632 [physics.data-an].

[95] S. Catani and M. Grazzini, *An NNLO subtraction formalism in hadron collisions and its application to Higgs boson production at the LHC*, Phys. Rev. Lett. **98** (2007) 222002, arXiv: hep-ph/0703012 [hep-ph].

[96] S. Catani, L. Cieri, D. de Florian, G. Ferrera and M. Grazzini, *Vector boson production at hadron colliders: hard-collinear coefficients at the NNLO*, Eur. Phys. J. C **72** (2012) 2195, arXiv: 1209.0158 [hep-ph].

[97] T. Gehrmann, A. von Manteuffel and L. Tancredi, *The two-loop helicity amplitudes for $q\overline{q}' \to V_1V_2 \to 4$ leptons*, JHEP **09** (2015) 128, arXiv: 1503.04812 [hep-ph].

[98] M. Grazzini, S. Kallweit and M. Wiesemann, *Fully differential NNLO computations with MATRIX*, Eur. Phys. J. C **78** (2018) 537, arXiv: 1711.06631 [hep-ph].

[99] M. Grazzini, S. Kallweit, M. Wiesemann and J. Y. Yook, *W^+W^- production at the LHC: NLO QCD corrections to the loop-induced gluon fusion channel*, Phys. Lett. B **804** (2020) 135399, arXiv: 2002.01877 [hep-ph].

[100] S. Kallweit, J. M. Lindert, P. Maierhöfer, S. Pozzorini and M. Schönherr, *NLO electroweak automation and precise predictions for W+multijet production at the LHC*, JHEP **04** (2015) 012, arXiv: 1412.5157 [hep-ph].

[101] M. Schönherr, *An automated subtraction of NLO EW infrared divergences*, Eur. Phys. J. C **78** (2018) 119, arXiv: 1712.07975 [hep-ph].

[102] F. Buccioni et al., *OpenLoops 2*, Eur. Phys. J. C **79** (2019) 866, arXiv: 1907.13071 [hep-ph].

[103] R. Frederix and S. Frixione, *Merging meets matching in MC@NLO*, JHEP **12** (2012) 061, arXiv: 1209.6215 [hep-ph].

[104] K. Hamilton, T. Melia, P. F. Monni, E. Re and G. Zanderighi,
Merging WW and WW+jet with MINLO, JHEP **09** (2016) 057, arXiv: 1606.07062 [hep-ph].

[105] A. Azatov, R. Contino, C. S. Machado and F. Riva,
Helicity selection rules and noninterference for BSM amplitudes, Phys. Rev. D **95** (2017) 065014, arXiv: 1607.05236 [hep-ph].

[106] A. Falkowski, M. Gonzalez-Alonso, A. Greljo, D. Marzocca and M. Son,
Anomalous Triple Gauge Couplings in the Effective Field Theory Approach at the LHC, JHEP **02** (2017) 115, arXiv: 1609.06312 [hep-ph].

[107] J. Alwall, M. Herquet, F. Maltoni, O. Mattelaer and T. Stelzer, *MadGraph 5 : Going Beyond*, JHEP **06** (2011) 128, arXiv: 1106.0522 [hep-ph].

[108] S. Wilks,
The Large-Sample Distribution of the Likelihood Ratio for Testing Composite Hypotheses, Annals Math. Statist. **9** (1938) 60.

[109] G. Cowan, K. Cranmer, E. Gross and O. Vitells,
Asymptotic formulae for likelihood-based tests of new physics, Eur. Phys. J. C **71** (2011) 1554, arXiv: 1007.1727 [physics.data-an], Erratum: Eur. Phys. J. C **73** (2013) 2501.

[110] ATLAS Collaboration, *Differential cross-section measurements for the electroweak production of dijets in association with a Z boson in proton–proton collisions at ATLAS*, Eur. Phys. J. C **81** (2020) 163, arXiv: 2006.15458 [hep-ex].

[111] M. Grazzini, S. Kallweit, J. M. Lindert, S. Pozzorini and M. Wiesemann, *NNLO QCD + NLO EW with Matrix+OpenLoops: precise predictions for vector-boson pair production*, JHEP **02** (2020) 087, arXiv: 1912.00068 [hep-ph].

[112] ATLAS Collaboration, *ATLAS Computing Acknowledgements*, ATL-SOFT-PUB-2020-001, URL: https://cds.cern.ch/record/2717821.

The ATLAS Collaboration

G. Aad[101], B. Abbott[127], D.C. Abbott[102], A. Abed Abud[36], K. Abeling[53], D.K. Abhayasinghe[93], S.H. Abidi[29], O.S. AbouZeid[40], N.L. Abraham[155], H. Abramowicz[160], H. Abreu[159], Y. Abulaiti[6], A.C. Abusleme Hoffman[145a], B.S. Acharya[66a,66b,p], B. Achkar[53], L. Adam[99], C. Adam Bourdarios[5], L. Adamczyk[83a], L. Adamek[165], J. Adelman[120], A. Adiguzel[12c,ad], S. Adorni[54], T. Adye[142], A.A. Affolder[144], Y. Afik[159], C. Agapopoulou[64], M.N. Agaras[38], A. Aggarwal[118], C. Agheorghiesei[27c], J.A. Aguilar-Saavedra[138f,138a,ac], A. Ahmad[36], F. Ahmadov[79], W.S. Ahmed[103], X. Ai[46], G. Aielli[73a,73b], S. Akatsuka[85], M. Akbiyik[99], T.P.A. Åkesson[96], E. Akilli[54], A.V. Akimov[110], K. Al Khoury[39], G.L. Alberghi[23b,23a], J. Albert[174], M.J. Alconada Verzini[160], S. Alderweireldt[36], M. Aleksa[36], I.N. Aleksandrov[79], C. Alexa[27b], T. Alexopoulos[10], A. Alfonsi[119], F. Alfonsi[23b,23a], M. Alhroob[127], B. Ali[140], S. Ali[157], M. Aliev[164], G. Alimonti[68a], C. Allaire[36], B.M.M. Allbrooke[155], P.P. Allport[21], A. Aloisio[69a,69b], F. Alonso[88], C. Alpigiani[147], E. Alunno Camelia[73a,73b], M. Alvarez Estevez[98], M.G. Alviggi[69a,69b], Y. Amaral Coutinho[80b], A. Ambler[103], L. Ambroz[133], C. Amelung[36], D. Amidei[105], S.P. Amor Dos Santos[138a], S. Amoroso[46], C.S. Amrouche[54], C. Anastopoulos[148], N. Andari[143], T. Andeen[11], J.K. Anders[20], S.Y. Andrean[45a,45b], A. Andreazza[68a,68b], V. Andrei[61a], S. Angelidakis[9], A. Angerami[39], A.V. Anisenkov[121b,121a], A. Annovi[71a], C. Antel[54], M.T. Anthony[148], E. Antipov[128], M. Antonelli[51], D.J.A. Antrim[18], F. Anulli[72a], M. Aoki[81], J.A. Aparisi Pozo[172], M.A. Aparo[155], L. Aperio Bella[46], N. Aranzabal[36], V. Araujo Ferraz[80a], C. Arcangeletti[51], A.T.H. Arce[49], E. Arena[90], J-F. Arguin[109], S. Argyropoulos[52], J.-H. Arling[46], A.J. Armbruster[36], A. Armstrong[169], O. Arnaez[165], H. Arnold[36], Z.P. Arrubarrena Tame[113], G. Artoni[133], H. Asada[116], K. Asai[125], S. Asai[162], N.A. Asbah[59], E.M. Asimakopoulou[170], L. Asquith[155], J. Assahsah[35e], K. Assamagan[29], R. Astalos[28a], R.J. Atkin[33a], M. Atkinson[171], N.B. Atlay[19], H. Atmani[64], P.A. Atmasiddha[105], K. Augsten[140], V.A. Austrup[180], G. Avolio[36], M.K. Ayoub[15c], G. Azuelos[109,ak], D. Babal[28a], H. Bachacou[143], K. Bachas[161], F. Backman[45a,45b], P. Bagnaia[72a,72b], M. Bahmani[84], H. Bahrasemani[151], A.J. Bailey[172], V.R. Bailey[171], J.T. Baines[142], C. Bakalis[10], O.K. Baker[181], P.J. Bakker[119], E. Bakos[16], D. Bakshi Gupta[8], S. Balaji[156], R. Balasubramanian[119], E.M. Baldin[121b,121a], P. Balek[178], E. Ballabene[68a,68b], F. Balli[143], W.K. Balunas[133], J. Balz[99], E. Banas[84], M. Bandieramonte[137], A. Bandyopadhyay[19], L. Barak[160], W.M. Barbe[38], E.L. Barberio[104], D. Barberis[55b,55a], M. Barbero[101], G. Barbour[94], K.N. Barends[33a], T. Barillari[114], M-S. Barisits[36], J. Barkeloo[130], T. Barklow[152], B.M. Barnett[142], R.M. Barnett[18], Z. Barnovska-Blenessy[60a], A. Baroncelli[60a], G. Barone[29], A.J. Barr[133], L. Barranco Navarro[45a,45b], F. Barreiro[98], J. Barreiro Guimarães da Costa[15a], U. Barron[160], S. Barsov[136], F. Bartels[61a], R. Bartoldus[152], G. Bartolini[101], A.E. Barton[89], P. Bartos[28a], A. Basalaev[46], A. Basan[99], I. Bashta[74a,74b], A. Bassalat[64,ah], M.J. Basso[165], C.R. Basson[100], R.L. Bates[57], S. Batlamous[35f], J.R. Batley[32], B. Batool[150], M. Battaglia[144], M. Bauce[72a,72b], F. Bauer[143,*], P. Bauer[24], H.S. Bawa[31], A. Bayirli[12c], J.B. Beacham[49], T. Beau[134], P.H. Beauchemin[168], F. Becherer[52], P. Bechtle[24], H.P. Beck[20,r], K. Becker[176], C. Becot[46], A.J. Beddall[12a], V.A. Bednyakov[79], C.P. Bee[154], T.A. Beermann[180], M. Begalli[80b], M. Begel[29], A. Behera[154], J.K. Behr[46], J.F. Beirer[53,36], F. Beisiegel[24], M. Belfkir[5], G. Bella[160], L. Bellagamba[23b], A. Bellerive[34], P. Bellos[21], K. Beloborodov[121b,121a], K. Belotskiy[111], N.L. Belyaev[111], D. Benchekroun[35a], Y. Benhammou[160], D.P. Benjamin[6], M. Benoit[29], J.R. Bensinger[26], S. Bentvelsen[119], L. Beresford[133], M. Beretta[51], D. Berge[19], E. Bergeaas Kuutmann[170], N. Berger[5], B. Bergmann[140], L.J. Bergsten[26], J. Beringer[18], S. Berlendis[7], G. Bernardi[134], C. Bernius[152], F.U. Bernlochner[24], T. Berry[93], P. Berta[46], A. Berthold[48], I.A. Bertram[89], O. Bessidskaia Bylund[180], S. Bethke[114], A. Betti[42], A.J. Bevan[92], S. Bhatta[154], D.S. Bhattacharya[175], P. Bhattarai[26], V.S. Bhopatkar[6], R. Bi[137], R.M. Bianchi[137], O. Biebel[113], R. Bielski[36], K. Bierwagen[99], N.V. Biesuz[71a,71b], M. Biglietti[74a], T.R.V. Billoud[140], M. Bindi[53], A. Bingul[12d], C. Bini[72a,72b], S. Biondi[23b,23a], C.J. Birch-sykes[100], G.A. Bird[21,142], M. Birman[178],

T. Bisanz[36], J.P. Biswal[3], D. Biswas[179,k], A. Bitadze[100], C. Bittrich[48], K. Bjørke[132], T. Blazek[28a], I. Bloch[46], C. Blocker[26], A. Blue[57], U. Blumenschein[92], G.J. Bobbink[119], V.S. Bobrovnikov[121b,121a], D. Bogavac[14], A.G. Bogdanchikov[121b,121a], C. Bohm[45a], V. Boisvert[93], P. Bokan[46], T. Bold[83a], M. Bomben[134], M. Bona[92], M. Boonekamp[143], C.D. Booth[93], A.G. Borbély[57], H.M. Borecka-Bielska[109], L.S. Borgna[94], G. Borissov[89], D. Bortoletto[133], D. Boscherini[23b], M. Bosman[14], J.D. Bossio Sola[103], K. Bouaouda[35a], J. Boudreau[137], E.V. Bouhova-Thacker[89], D. Boumediene[38], R. Bouquet[134], A. Boveia[126], J. Boyd[36], D. Boye[29], I.R. Boyko[79], A.J. Bozson[93], J. Bracinik[21], N. Brahimi[60d,60c], G. Brandt[180], O. Brandt[32], F. Braren[46], B. Brau[102], J.E. Brau[130], W.D. Breaden Madden[57], K. Brendlinger[46], R. Brener[159], L. Brenner[36], R. Brenner[170], S. Bressler[178], B. Brickwedde[99], D.L. Briglin[21], D. Britton[57], D. Britzger[114], I. Brock[24], R. Brock[106], G. Brooijmans[39], W.K. Brooks[145d], E. Brost[29], P.A. Bruckman de Renstrom[84], B. Brüers[46], D. Bruncko[28b], A. Bruni[23b], G. Bruni[23b], M. Bruschi[23b], N. Bruscino[72a,72b], L. Bryngemark[152], T. Buanes[17], Q. Buat[154], P. Buchholz[150], A.G. Buckley[57], I.A. Budagov[79], M.K. Bugge[132], O. Bulekov[111], B.A. Bullard[59], T.J. Burch[120], S. Burdin[90], C.D. Burgard[46], A.M. Burger[128], B. Burghgrave[8], J.T.P. Burr[46], C.D. Burton[11], J.C. Burzynski[102], V. Büscher[99], E. Buschmann[53], P.J. Bussey[57], J.M. Butler[25], C.M. Buttar[57], J.M. Butterworth[94], W. Buttinger[142], C.J. Buxo Vazquez[106], A.R. Buzykaev[121b,121a], G. Cabras[23b,23a], S. Cabrera Urbán[172], D. Caforio[56], H. Cai[137], V.M.M. Cairo[152], O. Cakir[4a], N. Calace[36], P. Calafiura[18], G. Calderini[134], P. Calfayan[65], G. Callea[57], L.P. Caloba[80b], A. Caltabiano[73a,73b], S. Calvente Lopez[98], D. Calvet[38], S. Calvet[38], T.P. Calvet[101], M. Calvetti[71a,71b], R. Camacho Toro[134], S. Camarda[36], D. Camarero Munoz[98], P. Camarri[73a,73b], M.T. Camerlingo[74a,74b], D. Cameron[132], C. Camincher[36], M. Campanelli[94], A. Camplani[40], V. Canale[69a,69b], A. Canesse[103], M. Cano Bret[77], J. Cantero[128], Y. Cao[171], M. Capua[41b,41a], R. Cardarelli[73a], F. Cardillo[172], G. Carducci[41b,41a], T. Carli[36], G. Carlino[69a], B.T. Carlson[137], E.M. Carlson[174,166a], L. Carminati[68a,68b], M. Carnesale[72a,72b], R.M.D. Carney[152], S. Caron[118], E. Carquin[145d], S. Carrá[46], G. Carratta[23b,23a], J.W.S. Carter[165], T.M. Carter[50], D. Casadei[33c], M.P. Casado[14,h], A.F. Casha[165], E.G. Castiglia[181], F.L. Castillo[172], L. Castillo Garcia[14], V. Castillo Gimenez[172], N.F. Castro[138a,138e], A. Catinaccio[36], J.R. Catmore[132], A. Cattai[36], V. Cavaliere[29], N. Cavalli[23b,23a], V. Cavasinni[71a,71b], E. Celebi[12b], F. Celli[133], K. Cerny[129], A.S. Cerqueira[80a], A. Cerri[155], L. Cerrito[73a,73b], F. Cerutti[18], A. Cervelli[23b,23a], S.A. Cetin[12b], Z. Chadi[35a], D. Chakraborty[120], M. Chala[138f], J. Chan[179], W.S. Chan[119], W.Y. Chan[90], J.D. Chapman[32], B. Chargeishvili[158b], D.G. Charlton[21], T.P. Charman[92], M. Chatterjee[20], C.C. Chau[34], S. Chekanov[6], S.V. Chekulaev[166a], G.A. Chelkov[79,af], B. Chen[78], C. Chen[60a], C.H. Chen[78], H. Chen[15c], H. Chen[29], J. Chen[60a], J. Chen[39], J. Chen[26], S. Chen[135], S.J. Chen[15c], X. Chen[15b], Y. Chen[60a], Y-H. Chen[46], C.L. Cheng[179], H.C. Cheng[62a], H.J. Cheng[15a], A. Cheplakov[79], E. Cheremushkina[46], R. Cherkaoui El Moursli[35f], E. Cheu[7], K. Cheung[63], L. Chevalier[143], V. Chiarella[51], G. Chiarelli[71a], G. Chiodini[67a], A.S. Chisholm[21], A. Chitan[27b], I. Chiu[162], Y.H. Chiu[174], M.V. Chizhov[79,t], K. Choi[11], A.R. Chomont[72a,72b], Y. Chou[102], Y.S. Chow[119], L.D. Christopher[33f], M.C. Chu[62a], X. Chu[15a,15d], J. Chudoba[139], J.J. Chwastowski[84], D. Cieri[114], K.M. Ciesla[84], V. Cindro[91], I.A. Cioară[27b], A. Ciocio[18], F. Cirotto[69a,69b], Z.H. Citron[178,l], M. Citterio[68a], D.A. Ciubotaru[27b], B.M. Ciungu[165], A. Clark[54], P.J. Clark[50], S.E. Clawson[100], C. Clement[45a,45b], L. Clissa[23b,23a], Y. Coadou[101], M. Cobal[66a,66c], A. Coccaro[55b], J. Cochran[78], R. Coelho Lopes De Sa[102], S. Coelli[68a], H. Cohen[160], A.E.C. Coimbra[36], B. Cole[39], J. Collot[58], P. Conde Muiño[138a,138h], S.H. Connell[33c], I.A. Connelly[57], E.I. Conroy[133], F. Conventi[69a,al], A.M. Cooper-Sarkar[133], F. Cormier[173], L.D. Corpe[94], M. Corradi[72a,72b], E.E. Corrigan[96], F. Corriveau[103,aa], M.J. Costa[172], F. Costanza[5], D. Costanzo[148], B.M. Cote[126], G. Cowan[93], J.W. Cowley[32], J. Crane[100], K. Cranmer[124], R.A. Creager[135], S. Crépé-Renaudin[58], F. Crescioli[134], M. Cristinziani[150], M. Cristoforetti[75a,75b,b], V. Croft[168], G. Crosetti[41b,41a], A. Cueto[5], T. Cuhadar Donszelmann[169], H. Cui[15a,15d], A.R. Cukierman[152], W.R. Cunningham[57], S. Czekierda[84], P. Czodrowski[36], M.M. Czurylo[61b], M.J. Da Cunha Sargedas De Sousa[60b], J.V. Da Fonseca Pinto[80b], C. Da Via[100], W. Dabrowski[83a],

T. Dado[47], S. Dahbi[33f], T. Dai[105], C. Dallapiccola[102], M. Dam[40], G. D'amen[29], V. D'Amico[74a,74b], J. Damp[99], J.R. Dandoy[135], M.F. Daneri[30], M. Danninger[151], V. Dao[36], G. Darbo[55b], A. Dattagupta[130], S. D'Auria[68a,68b], C. David[166b], T. Davidek[141], D.R. Davis[49], B.R. Davis-purcell[34], I. Dawson[92], K. De[8], R. De Asmundis[69a], M. De Beurs[119], S. De Castro[23b,23a], N. De Groot[118], P. de Jong[119], H. De la Torre[106], A. De Maria[15c], D. De Pedis[72a], A. De Salvo[72a], U. De Sanctis[73a,73b], M. De Santis[73a,73b], A. De Santo[155], J.B. De Vivie De Regie[58], D.V. Dedovich[79], J. Degens[119], A.M. Deiana[42], J. Del Peso[98], Y. Delabat Diaz[46], F. Deliot[143], C.M. Delitzsch[7], M. Della Pietra[69a,69b], D. Della Volpe[54], A. Dell'Acqua[36], L. Dell'Asta[73a,73b], M. Delmastro[5], P.A. Delsart[58], S. Demers[181], M. Demichev[79], G. Demontigny[109], S.P. Denisov[122], L. D'Eramo[120], D. Derendarz[84], J.E. Derkaoui[35e], F. Derue[134], P. Dervan[90], K. Desch[24], K. Dette[165], C. Deutsch[24], P.O. Deviveiros[36], F.A. Di Bello[72a,72b], A. Di Ciaccio[73a,73b], L. Di Ciaccio[5], C. Di Donato[69a,69b], A. Di Girolamo[36], G. Di Gregorio[71a,71b], A. Di Luca[75a,75b], B. Di Micco[74a,74b], R. Di Nardo[74a,74b], C. Diaconu[101], F.A. Dias[119], T. Dias Do Vale[138a], M.A. Diaz[145a], F.G. Diaz Capriles[24], J. Dickinson[18], M. Didenko[164], E.B. Diehl[105], J. Dietrich[19], S. Díez Cornell[46], C. Diez Pardos[150], A. Dimitrievska[18], W. Ding[15b], J. Dingfelder[24], S.J. Dittmeier[61b], F. Dittus[36], F. Djama[101], T. Djobava[158b], J.I. Djuvsland[17], M.A.B. Do Vale[146], M. Dobre[27b], D. Dodsworth[26], C. Doglioni[96], J. Dolejsi[141], Z. Dolezal[141], M. Donadelli[80c], B. Dong[60c], J. Donini[38], A. D'onofrio[15c], M. D'Onofrio[90], J. Dopke[142], A. Doria[69a], M.T. Dova[88], A.T. Doyle[57], E. Drechsler[151], E. Dreyer[151], T. Dreyer[53], A.S. Drobac[168], D. Du[60b], T.A. du Pree[119], Y. Duan[60d], F. Dubinin[110], M. Dubovsky[28a], A. Dubreuil[54], E. Duchovni[178], G. Duckeck[113], O.A. Ducu[36,27b], D. Duda[114], A. Dudarev[36], A.C. Dudder[99], M. D'uffizi[100], L. Duflot[64], M. Dührssen[36], C. Dülsen[180], M. Dumancic[178], A.E. Dumitriu[27b], M. Dunford[61a], S. Dungs[47], A. Duperrin[101], H. Duran Yildiz[4a], M. Düren[56], A. Durglishvili[158b], B. Dutta[46], D. Duvnjak[1], G.I. Dyckes[135], M. Dyndal[83a], S. Dysch[100], B.S. Dziedzic[84], B. Eckerova[28a], M.G. Eggleston[49], E. Egidio Purcino De Souza[80b], L.F. Ehrke[54], T. Eifert[8], G. Eigen[17], K. Einsweiler[18], T. Ekelof[170], H. El Jarrari[35f], A. El Moussaouy[35a], V. Ellajosyula[170], M. Ellert[170], F. Ellinghaus[180], A.A. Elliot[92], N. Ellis[36], J. Elmsheuser[29], M. Elsing[36], D. Emeliyanov[142], A. Emerman[39], Y. Enari[162], J. Erdmann[47], A. Ereditato[20], P.A. Erland[84], M. Errenst[180], M. Escalier[64], C. Escobar[172], O. Estrada Pastor[172], E. Etzion[160], G. Evans[138a], H. Evans[65], M.O. Evans[155], A. Ezhilov[136], F. Fabbri[57], L. Fabbri[23b,23a], V. Fabiani[118], G. Facini[176], R.M. Fakhrutdinov[122], S. Falciano[72a], P.J. Falke[24], S. Falke[36], J. Faltova[141], Y. Fan[15a], Y. Fang[15a], Y. Fang[15a], G. Fanourakis[44], M. Fanti[68a,68b], M. Faraj[60c], A. Farbin[8], A. Farilla[74a], E.M. Farina[70a,70b], T. Farooque[106], S.M. Farrington[50], P. Farthouat[36], F. Fassi[35f], D. Fassouliotis[9], M. Faucci Giannelli[73a,73b], W.J. Fawcett[32], L. Fayard[64], O.L. Fedin[136,q], A. Fehr[20], M. Feickert[171], L. Feligioni[101], A. Fell[148], C. Feng[60b], M. Feng[49], M.J. Fenton[169], A.B. Fenyuk[122], S.W. Ferguson[43], J. Ferrando[46], A. Ferrari[170], P. Ferrari[119], R. Ferrari[70a], D. Ferrere[54], C. Ferretti[105], F. Fiedler[99], A. Filipčič[91], F. Filthaut[118], K.D. Finelli[25], M.C.N. Fiolhais[138a,138c,a], L. Fiorini[172], F. Fischer[113], J. Fischer[99], W.C. Fisher[106], T. Fitschen[21], I. Fleck[150], P. Fleischmann[105], T. Flick[180], B.M. Flierl[113], L. Flores[135], L.R. Flores Castillo[62a], F.M. Follega[75a,75b], N. Fomin[17], J.H. Foo[165], G.T. Forcolin[75a,75b], B.C. Forland[65], A. Formica[143], F.A. Förster[14], A.C. Forti[100], E. Fortin[101], M.G. Foti[133], D. Fournier[64], H. Fox[89], P. Francavilla[71a,71b], S. Francescato[72a,72b], M. Franchini[23b,23a], S. Franchino[61a], D. Francis[36], L. Franco[5], L. Franconi[20], M. Franklin[59], G. Frattari[72a,72b], P.M. Freeman[21], B. Freund[109], W.S. Freund[80b], E.M. Freundlich[47], D.C. Frizzell[127], D. Froidevaux[36], J.A. Frost[133], Y. Fu[60a], M. Fujimoto[125], E. Fullana Torregrosa[172], T. Fusayasu[115], J. Fuster[172], A. Gabrielli[23b,23a], A. Gabrielli[36], P. Gadow[46], G. Gagliardi[55b,55a], L.G. Gagnon[18], G.E. Gallardo[133], E.J. Gallas[133], B.J. Gallop[142], R. Gamboa Goni[92], K.K. Gan[126], S. Ganguly[178], J. Gao[60a], Y. Gao[50], Y.S. Gao[31,n], F.M. Garay Walls[145a], C. García[172], J.E. García Navarro[172], J.A. García Pascual[15a], M. Garcia-Sciveres[18], R.W. Gardner[37], D. Garg[77], S. Gargiulo[52], C.A. Garner[165], V. Garonne[132], S.J. Gasiorowski[147], P. Gaspar[80b], G. Gaudio[70a], P. Gauzzi[72a,72b], I.L. Gavrilenko[110], A. Gavrilyuk[123], C. Gay[173], G. Gaycken[46], E.N. Gazis[10], A.A. Geanta[27b], C.M. Gee[144], C.N.P. Gee[142], J. Geisen[96], M. Geisen[99], C. Gemme[55b], M.H. Genest[58],

C. Geng[105], S. Gentile[72a,72b], S. George[93], T. Geralis[44], L.O. Gerlach[53], P. Gessinger-Befurt[99], G. Gessner[47], M. Ghasemi Bostanabad[174], M. Ghneimat[150], A. Ghosh[169], A. Ghosh[77], B. Giacobbe[23b], S. Giagu[72a,72b], N. Giangiacomi[165], P. Giannetti[71a], A. Giannini[69a,69b], S.M. Gibson[93], M. Gignac[144], D.T. Gil[83b], B.J. Gilbert[39], D. Gillberg[34], G. Gilles[180], N.E.K. Gillwald[46], D.M. Gingrich[3,ak], M.P. Giordani[66a,66c], P.F. Giraud[143], G. Giugliarelli[66a,66c], D. Giugni[68a], F. Giuli[73a,73b], S. Gkaitatzis[161], I. Gkialas[9,i], E.L. Gkougkousis[14], P. Gkountoumis[10], L.K. Gladilin[112], C. Glasman[98], G.R. Gledhill[130], M. Glisic[130], I. Gnesi[41b,d], M. Goblirsch-Kolb[26], D. Godin[109], S. Goldfarb[104], T. Golling[54], D. Golubkov[122], A. Gomes[138a,138b], R. Goncalves Gama[53], R. Gonçalo[138a,138c], G. Gonella[130], L. Gonella[21], A. Gongadze[79], F. Gonnella[21], J.L. Gonski[39], S. González de la Hoz[172], S. Gonzalez Fernandez[14], R. Gonzalez Lopez[90], C. Gonzalez Renteria[18], R. Gonzalez Suarez[170], S. Gonzalez-Sevilla[54], G.R. Gonzalvo Rodriguez[172], R.Y. González Andana[145a], L. Goossens[36], N.A. Gorasia[21], P.A. Gorbounov[123], H.A. Gordon[29], B. Gorini[36], E. Gorini[67a,67b], A. Gorišek[91], A.T. Goshaw[49], M.I. Gostkin[79], C.A. Gottardo[118], M. Gouighri[35b], V. Goumarre[46], A.G. Goussiou[147], N. Govender[33c], C. Goy[5], I. Grabowska-Bold[83a], K. Graham[34], E. Gramstad[132], S. Grancagnolo[19], M. Grandi[155], V. Gratchev[136], P.M. Gravila[27f], F.G. Gravili[67a,67b], H.M. Gray[18], C. Grefe[24], I.M. Gregor[46], P. Grenier[152], K. Grevtsov[46], C. Grieco[14], N.A. Grieser[127], A.A. Grillo[144], K. Grimm[31,m], S. Grinstein[14,x], J.-F. Grivaz[64], S. Groh[99], E. Gross[178], J. Grosse-Knetter[53], Z.J. Grout[94], C. Grud[105], A. Grummer[117], J.C. Grundy[133], L. Guan[105], W. Guan[179], C. Gubbels[173], J. Guenther[36], J.G.R. Guerrero Rojas[172], F. Guescini[114], D. Guest[19], R. Gugel[99], A. Guida[46], T. Guillemin[5], S. Guindon[36], J. Guo[60c], L. Guo[64], Y. Guo[105], R. Gupta[46], S. Gurbuz[24], G. Gustavino[127], M. Guth[52], P. Gutierrez[127], L.F. Gutierrez Zagazeta[135], C. Gutschow[94], C. Guyot[143], C. Gwenlan[133], C.B. Gwilliam[90], E.S. Haaland[132], A. Haas[124], M.H. Habedank[19], C. Haber[18], H.K. Hadavand[8], A. Hadef[99], M. Haleem[175], J. Haley[128], J.J. Hall[148], G. Halladjian[106], G.D. Hallewell[101], L. Halser[20], K. Hamano[174], H. Hamdaoui[35f], M. Hamer[24], G.N. Hamity[50], K. Han[60a], L. Han[15c], L. Han[60a], S. Han[18], Y.F. Han[165], K. Hanagaki[81,v], M. Hance[144], M.D. Hank[37], R. Hankache[100], E. Hansen[96], J.B. Hansen[40], J.D. Hansen[40], M.C. Hansen[24], P.H. Hansen[40], E.C. Hanson[100], K. Hara[167], T. Harenberg[180], S. Harkusha[107], Y.T. Harris[133], P.F. Harrison[176], N.M. Hartman[152], N.M. Hartmann[113], Y. Hasegawa[149], A. Hasib[50], S. Hassani[143], S. Haug[20], R. Hauser[106], M. Havranek[140], C.M. Hawkes[21], R.J. Hawkings[36], S. Hayashida[116], D. Hayden[106], C. Hayes[105], R.L. Hayes[173], C.P. Hays[133], J.M. Hays[92], H.S. Hayward[90], S.J. Haywood[142], F. He[60a], Y. He[163], Y. He[134], M.P. Heath[50], V. Hedberg[96], A.L. Heggelund[132], N.D. Hehir[92], C. Heidegger[52], K.K. Heidegger[52], W.D. Heidorn[78], J. Heilman[34], S. Heim[46], T. Heim[18], B. Heinemann[46,ai], J.G. Heinlein[135], J.J. Heinrich[130], L. Heinrich[36], J. Hejbal[139], L. Helary[46], A. Held[124], S. Hellesund[132], C.M. Helling[144], S. Hellman[45a,45b], C. Helsens[36], R.C.W. Henderson[89], L. Henkelmann[32], A.M. Henriques Correia[36], H. Herde[152], Y. Hernández Jiménez[33f], H. Herr[99], M.G. Herrmann[113], T. Herrmann[48], G. Herten[52], R. Hertenberger[113], L. Hervas[36], N.P. Hessey[166a], H. Hibi[82], S. Higashino[81], E. Higón-Rodriguez[172], K. Hildebrand[37], K.K. Hill[29], K.H. Hiller[46], S.J. Hillier[21], M. Hils[48], I. Hinchliffe[18], F. Hinterkeuser[24], M. Hirose[131], S. Hirose[167], D. Hirschbuehl[180], B. Hiti[91], O. Hladik[139], J. Hobbs[154], R. Hobincu[27e], N. Hod[178], M.C. Hodgkinson[148], B.H. Hodkinson[32], A. Hoecker[36], J. Hofer[46], D. Hohn[52], T. Holm[24], T.R. Holmes[37], M. Holzbock[114], L.B.A.H. Hommels[32], B.P. Honan[100], T.M. Hong[137], J.C. Honig[52], A. Hönle[114], B.H. Hooberman[171], W.H. Hopkins[6], Y. Horii[116], P. Horn[48], L.A. Horyn[37], S. Hou[157], J. Howarth[57], J. Hoya[88], M. Hrabovsky[129], A. Hrynevich[108], T. Hryn'ova[5], P.J. Hsu[63], S.-C. Hsu[147], Q. Hu[39], S. Hu[60c], Y.F. Hu[15a,15d,am], D.P. Huang[94], X. Huang[15c], Y. Huang[60a], Y. Huang[15a], Z. Hubacek[140], F. Hubaut[101], M. Huebner[24], F. Huegging[24], T.B. Huffman[133], M. Huhtinen[36], R. Hulsken[58], R.F.H. Hunter[34], N. Huseynov[79,ab], J. Huston[106], J. Huth[59], R. Hyneman[152], S. Hyrych[28a], G. Iacobucci[54], G. Iakovidis[29], I. Ibragimov[150], L. Iconomidou-Fayard[64], P. Iengo[36], R. Ignazzi[40], R. Iguchi[162], T. Iizawa[54], Y. Ikegami[81], N. Ilic[165,165], H. Imam[35a], G. Introzzi[70a,70b], M. Iodice[74a], K. Iordanidou[166a], V. Ippolito[72a,72b], M. Ishino[162], W. Islam[128], C. Issever[19,46], S. Istin[12c],

J.M. Iturbe Ponce[62a], R. Iuppa[75a,75b], A. Ivina[178], J.M. Izen[43], V. Izzo[69a], P. Jacka[139], P. Jackson[1], R.M. Jacobs[46], B.P. Jaeger[151], C.S. Jagfeld[113], G. Jäkel[180], K.B. Jakobi[99], K. Jakobs[52], T. Jakoubek[178], J. Jamieson[57], K.W. Janas[83a], G. Jarlskog[96], A.E. Jaspan[90], N. Javadov[79,ab], T. Javůrek[36], M. Javurkova[102], F. Jeanneau[143], L. Jeanty[130], J. Jejelava[158a], P. Jenni[52,e], S. Jézéquel[5], J. Jia[154], Z. Jia[15c], Y. Jiang[60a], S. Jiggins[52], F.A. Jimenez Morales[38], J. Jimenez Pena[114], S. Jin[15c], A. Jinaru[27b], O. Jinnouchi[163], H. Jivan[33f], P. Johansson[148], K.A. Johns[7], C.A. Johnson[65], E. Jones[176], R.W.L. Jones[89], T.J. Jones[90], J. Jovicevic[36], X. Ju[18], J.J. Junggeburth[114], A. Juste Rozas[14,x], A. Kaczmarska[84], M. Kado[72a,72b], H. Kagan[126], M. Kagan[152], A. Kahn[39], C. Kahra[99], T. Kaji[177], E. Kajomovitz[159], C.W. Kalderon[29], A. Kaluza[99], A. Kamenshchikov[122], M. Kaneda[162], N.J. Kang[144], S. Kang[78], Y. Kano[116], J. Kanzaki[81], D. Kar[33f], K. Karava[133], M.J. Kareem[166b], I. Karkanias[161], S.N. Karpov[79], Z.M. Karpova[79], V. Kartvelishvili[89], A.N. Karyukhin[122], E. Kasimi[161], C. Kato[60d], J. Katzy[46], K. Kawade[149], K. Kawagoe[87], T. Kawaguchi[116], T. Kawamoto[143], G. Kawamura[53], E.F. Kay[174], F.I. Kaya[168], S. Kazakos[14], V.F. Kazanin[121b,121a], Y. Ke[154], J.M. Keaveney[33a], R. Keeler[174], J.S. Keller[34], D. Kelsey[155], J.J. Kempster[21], J. Kendrick[21], K.E. Kennedy[39], O. Kepka[139], S. Kersten[180], B.P. Kerševan[91], S. Ketabchi Haghighat[165], F. Khalil-Zada[13], M. Khandoga[134], A. Khanov[128], A.G. Kharlamov[121b,121a], T. Kharlamova[121b,121a], E.E. Khoda[173], T.J. Khoo[19], G. Khoriauli[175], E. Khramov[79], J. Khubua[158b], S. Kido[82], M. Kiehn[36], A. Kilgallon[130], E. Kim[163], Y.K. Kim[37], N. Kimura[94], A. Kirchhoff[53], D. Kirchmeier[48], J. Kirk[142], A.E. Kiryunin[114], T. Kishimoto[162], D.P. Kisliuk[165], V. Kitali[46], C. Kitsaki[10], O. Kivernyk[24], T. Klapdor-Kleingrothaus[52], M. Klassen[61a], C. Klein[34], L. Klein[175], M.H. Klein[105], M. Klein[90], U. Klein[90], P. Klimek[36], A. Klimentov[29], F. Klimpel[36], T. Klingl[24], T. Klioutchnikova[36], F.F. Klitzner[113], P. Kluit[119], S. Kluth[114], E. Kneringer[76], T.M. Knight[165], A. Knue[52], D. Kobayashi[87], M. Kobel[48], M. Kocian[152], T. Kodama[162], P. Kodys[141], D.M. Koeck[155], P.T. Koenig[24], T. Koffas[34], N.M. Köhler[36], M. Kolb[143], I. Koletsou[5], T. Komarek[129], K. Köneke[52], A.X.Y. Kong[1], T. Kono[125], V. Konstantinides[94], N. Konstantinidis[94], B. Konya[96], R. Kopeliansky[65], S. Koperny[83a], K. Korcyl[84], K. Kordas[161], G. Koren[160], A. Korn[94], S. Korn[53], I. Korolkov[14], E.V. Korolkova[148], N. Korotkova[112], O. Kortner[114], S. Kortner[114], V.V. Kostyukhin[148,164], A. Kotsokechagia[64], A. Kotwal[49], A. Koulouris[9], A. Kourkoumeli-Charalampidi[70a,70b], C. Kourkoumelis[9], E. Kourlitis[6], R. Kowalewski[174], W. Kozanecki[143], A.S. Kozhin[122], V.A. Kramarenko[112], G. Kramberger[91], D. Krasnopevtsev[60a], M.W. Krasny[134], A. Krasznahorkay[36], J.A. Kremer[99], J. Kretzschmar[90], K. Kreul[19], P. Krieger[165], F. Krieter[113], S. Krishnamurthy[102], A. Krishnan[61b], M. Krivos[141], K. Krizka[18], K. Kroeninger[47], H. Kroha[114], J. Kroll[139], J. Kroll[135], K.S. Krowpman[106], U. Kruchonak[79], H. Krüger[24], N. Krumnack[78], M.C. Kruse[49], J.A. Krzysiak[84], A. Kubota[163], O. Kuchinskaia[164], S. Kuday[4b], D. Kuechler[46], J.T. Kuechler[46], S. Kuehn[36], T. Kuhl[46], V. Kukhtin[79], Y. Kulchitsky[107,ae], S. Kuleshov[145b], M. Kumar[33f], N. Kumari[101], M. Kuna[58], A. Kupco[139], T. Kupfer[47], O. Kuprash[52], H. Kurashige[82], L.L. Kurchaninov[166a], Y.A. Kurochkin[107], A. Kurova[111], M.G. Kurth[15a,15d], E.S. Kuwertz[36], M. Kuze[163], A.K. Kvam[147], J. Kvita[129], T. Kwan[103], C. Lacasta[172], F. Lacava[72a,72b], D.P.J. Lack[100], H. Lacker[19], D. Lacour[134], E. Ladygin[79], R. Lafaye[5], B. Laforge[134], T. Lagouri[145c], S. Lai[53], I.K. Lakomiec[83a], N. Lalloue[58], J.E. Lambert[127], S. Lammers[65], W. Lampl[7], C. Lampoudis[161], E. Lançon[29], U. Landgraf[52], M.P.J. Landon[92], V.S. Lang[52], J.C. Lange[53], R.J. Langenberg[102], A.J. Lankford[169], F. Lanni[29], K. Lantzsch[24], A. Lanza[70a], A. Lapertosa[55b,55a], J.F. Laporte[143], T. Lari[68a], F. Lasagni Manghi[23b,23a], M. Lassnig[36], V. Latonova[139], T.S. Lau[62a], A. Laudrain[99], A. Laurier[34], M. Lavorgna[69a,69b], S.D. Lawlor[93], M. Lazzaroni[68a,68b], B. Le[100], A. Lebedev[78], M. LeBlanc[7], T. LeCompte[6], F. Ledroit-Guillon[58], A.C.A. Lee[94], C.A. Lee[29], G.R. Lee[17], L. Lee[59], S.C. Lee[157], S. Lee[78], L.L. Leeuw[33c], B. Lefebvre[166a], H.P. Lefebvre[93], M. Lefebvre[174], C. Leggett[18], K. Lehmann[151], N. Lehmann[20], G. Lehmann Miotto[36], W.A. Leight[46], A. Leisos[161,w], M.A.L. Leite[80c], C.E. Leitgeb[113], R. Leitner[141], K.J.C. Leney[42], T. Lenz[24], S. Leone[71a], C. Leonidopoulos[50], A. Leopold[134], C. Leroy[109], R. Les[106], C.G. Lester[32], M. Levchenko[136], J. Levêque[5], D. Levin[105], L.J. Levinson[178], D.J. Lewis[21], B. Li[15b], B. Li[105], C-Q. Li[60c,60d], F. Li[60c],

H. Li[60a], H. Li[60b], J. Li[60c], K. Li[147], L. Li[60c], M. Li[15a,15d], Q.Y. Li[60a], S. Li[60d,60c,c], X. Li[46], Y. Li[46], Z. Li[60b], Z. Li[133], Z. Li[103], Z. Li[90], Z. Liang[15a], M. Liberatore[46], B. Liberti[73a], K. Lie[62c], C.Y. Lin[32], K. Lin[106], R.A. Linck[65], R.E. Lindley[7], J.H. Lindon[21], A. Linss[46], A.L. Lionti[54], E. Lipeles[135], A. Lipniacka[17], T.M. Liss[171,aj], A. Lister[173], J.D. Little[8], B. Liu[15a], B.X. Liu[151], J.B. Liu[60a], J.K.K. Liu[37], K. Liu[60d,60c], M. Liu[60a], M.Y. Liu[60a], P. Liu[15a], X. Liu[60a], Y. Liu[46], Y. Liu[15a,15d], Y.L. Liu[105], Y.W. Liu[60a], M. Livan[70a,70b], A. Lleres[58], J. Llorente Merino[151], S.L. Lloyd[92], E.M. Lobodzinska[46], P. Loch[7], S. Loffredo[73a,73b], T. Lohse[19], K. Lohwasser[148], M. Lokajicek[139], J.D. Long[171], R.E. Long[89], I. Longarini[72a,72b], L. Longo[36], R. Longo[171], I. Lopez Paz[14], A. Lopez Solis[46], J. Lorenz[113], N. Lorenzo Martinez[5], A.M. Lory[113], A. Lösle[52], X. Lou[45a,45b], X. Lou[15a], A. Lounis[64], J. Love[6], P.A. Love[89], J.J. Lozano Bahilo[172], G. Lu[15a], M. Lu[60a], S. Lu[135], Y.J. Lu[63], H.J. Lubatti[147], C. Luci[72a,72b], F.L. Lucio Alves[15c], A. Lucotte[58], F. Luehring[65], I. Luise[154], L. Luminari[72a], B. Lund-Jensen[153], N.A. Luongo[130], M.S. Lutz[160], D. Lynn[29], H. Lyons[90], R. Lysak[139], E. Lytken[96], F. Lyu[15a], V. Lyubushkin[79], T. Lyubushkina[79], H. Ma[29], L.L. Ma[60b], Y. Ma[94], D.M. Mac Donell[174], G. Maccarrone[51], C.M. Macdonald[148], J.C. MacDonald[148], R. Madar[38], W.F. Mader[48], M. Madugoda Ralalage Don[128], N. Madysa[48], J. Maeda[82], T. Maeno[29], M. Maerker[48], V. Magerl[52], J. Magro[66a,66c], D.J. Mahon[39], C. Maidantchik[80b], A. Maio[138a,138b,138d], K. Maj[83a], O. Majersky[28a], S. Majewski[130], N. Makovec[64], B. Malaescu[134], Pa. Malecki[84], V.P. Maleev[136], F. Malek[58], D. Malito[41b,41a], U. Mallik[77], C. Malone[32], S. Maltezos[10], S. Malyukov[79], J. Mamuzic[172], G. Mancini[51], J.P. Mandalia[92], I. Mandić[91], L. Manhaes de Andrade Filho[80a], I.M. Maniatis[161], M. Manisha[143], J. Manjarres Ramos[48], K.H. Mankinen[96], A. Mann[113], A. Manousos[76], B. Mansoulie[143], I. Manthos[161], S. Manzoni[119], A. Marantis[161], L. Marchese[133], G. Marchiori[134], M. Marcisovsky[139], L. Marcoccia[73a,73b], C. Marcon[96], M. Marjanovic[127], Z. Marshall[18], S. Marti-Garcia[172], T.A. Martin[176], V.J. Martin[50], B. Martin dit Latour[17], L. Martinelli[74a,74b], M. Martinez[14,x], P. Martinez Agullo[172], V.I. Martinez Outschoorn[102], S. Martin-Haugh[142], V.S. Martoiu[27b], A.C. Martyniuk[94], A. Marzin[36], S.R. Maschek[114], L. Masetti[99], T. Mashimo[162], R. Mashinistov[110], J. Masik[100], A.L. Maslennikov[121b,121a], L. Massa[23b,23a], P. Massarotti[69a,69b], P. Mastrandrea[71a,71b], A. Mastroberardino[41b,41a], T. Masubuchi[162], D. Matakias[29], T. Mathisen[170], A. Matic[113], N. Matsuzawa[162], J. Maurer[27b], B. Maček[91], D.A. Maximov[121b,121a], R. Mazini[157], I. Maznas[161], S.M. Mazza[144], C. Mc Ginn[29], J.P. Mc Gowan[103], S.P. Mc Kee[105], T.G. McCarthy[114], W.P. McCormack[18], E.F. McDonald[104], A.E. McDougall[119], J.A. Mcfayden[155], G. Mchedlidze[158b], M.A. McKay[42], K.D. McLean[174], S.J. McMahon[142], P.C. McNamara[104], R.A. McPherson[174,aa], J.E. Mdhluli[33f], Z.A. Meadows[102], S. Meehan[36], T. Megy[38], S. Mehlhase[113], A. Mehta[90], B. Meirose[43], D. Melini[159], B.R. Mellado Garcia[33f], F. Meloni[46], A. Melzer[24], E.D. Mendes Gouveia[138a,138e], A.M. Mendes Jacques Da Costa[21], H.Y. Meng[165], L. Meng[36], S. Menke[114], E. Meoni[41b,41a], S.A.M. Merkt[137], C. Merlassino[133], P. Mermod[54], L. Merola[69a,69b], C. Meroni[68a], G. Merz[105], O. Meshkov[112,110], J.K.R. Meshreki[150], J. Metcalfe[6], A.S. Mete[6], C. Meyer[65], J-P. Meyer[143], M. Michetti[19], R.P. Middleton[142], L. Mijović[50], G. Mikenberg[178], M. Mikestikova[139], M. Mikuž[91], H. Mildner[148], A. Milic[165], C.D. Milke[42], D.W. Miller[37], L.S. Miller[34], A. Milov[178], D.A. Milstead[45a,45b], A.A. Minaenko[122], I.A. Minashvili[158b], L. Mince[57], A.I. Mincer[124], B. Mindur[83a], M. Mineev[79], Y. Minegishi[162], Y. Mino[85], L.M. Mir[14], M. Miralles Lopez[172], M. Mironova[133], T. Mitani[177], V.A. Mitsou[172], M. Mittal[60c], O. Miu[165], P.S. Miyagawa[92], Y. Miyazaki[87], A. Mizukami[81], J.U. Mjörnmark[96], T. Mkrtchyan[61a], M. Mlynarikova[120], T. Moa[45a,45b], S. Mobius[53], K. Mochizuki[109], P. Moder[46], P. Mogg[113], S. Mohapatra[39], G. Mokgatitswane[33f], B. Mondal[150], S. Mondal[140], K. Mönig[46], E. Monnier[101], A. Montalbano[151], J. Montejo Berlingen[36], M. Montella[94], F. Monticelli[88], N. Morange[64], A.L. Moreira De Carvalho[138a], M. Moreno Llácer[172], C. Moreno Martinez[14], P. Morettini[55b], M. Morgenstern[159], S. Morgenstern[176], D. Mori[151], M. Morii[59], M. Morinaga[177], V. Morisbak[132], A.K. Morley[36], A.P. Morris[94], L. Morvaj[36], P. Moschovakos[36], B. Moser[119], M. Mosidze[158b], T. Moskalets[52], P. Moskvitina[118], J. Moss[31,o], E.J.W. Moyse[102], S. Muanza[101], J. Mueller[137],

D. Muenstermann[89], G.A. Mullier[96], J.J. Mullin[135], D.P. Mungo[68a,68b], J.L. Munoz Martinez[14], F.J. Munoz Sanchez[100], M. Murin[100], P. Murin[28b], W.J. Murray[176,142], A. Murrone[68a,68b], J.M. Muse[127], M. Muškinja[18], C. Mwewa[29], A.G. Myagkov[122,af], A.A. Myers[137], G. Myers[65], J. Myers[130], M. Myska[140], B.P. Nachman[18], O. Nackenhorst[47], A.Nag Nag[48], K. Nagai[133], K. Nagano[81], J.L. Nagle[29], E. Nagy[101], A.M. Nairz[36], Y. Nakahama[116], K. Nakamura[81], H. Nanjo[131], F. Napolitano[61a], R.F. Naranjo Garcia[46], R. Narayan[42], I. Naryshkin[136], M. Naseri[34], T. Naumann[46], G. Navarro[22a], J. Navarro-Gonzalez[172], P.Y. Nechaeva[110], F. Nechansky[46], T.J. Neep[21], A. Negri[70a,70b], M. Negrini[23b], C. Nellist[118], C. Nelson[103], K. Nelson[105], M.E. Nelson[45a,45b], S. Nemecek[139], M. Nessi[36,g], M.S. Neubauer[171], F. Neuhaus[99], M. Neumann[180], R. Newhouse[173], P.R. Newman[21], C.W. Ng[137], Y.S. Ng[19], Y.W.Y. Ng[169], B. Ngair[35f], H.D.N. Nguyen[101], T. Nguyen Manh[109], E. Nibigira[38], R.B. Nickerson[133], R. Nicolaidou[143], D.S. Nielsen[40], J. Nielsen[144], M. Niemeyer[53], N. Nikiforou[11], V. Nikolaenko[122,af], I. Nikolic-Audit[134], K. Nikolopoulos[21], P. Nilsson[29], H.R. Nindhito[54], A. Nisati[72a], N. Nishu[3], R. Nisius[114], T. Nitta[177], T. Nobe[162], D.L. Noel[32], Y. Noguchi[85], I. Nomidis[134], M.A. Nomura[29], M.B. Norfolk[148], R.R.B. Norisam[94], J. Novak[91], T. Novak[46], O. Novgorodova[48], L. Novotny[140], R. Novotny[117], L. Nozka[129], K. Ntekas[169], E. Nurse[94], F.G. Oakham[34,ak], J. Ocariz[134], A. Ochi[82], I. Ochoa[138a], J.P. Ochoa-Ricoux[145a], K. O'Connor[26], S. Oda[87], S. Odaka[81], S. Oerdek[53], A. Ogrodnik[83a], A. Oh[100], C.C. Ohm[153], H. Oide[163], R. Oishi[162], M.L. Ojeda[165], Y. Okazaki[85], M.W. O'Keefe[90], Y. Okumura[162], A. Olariu[27b], L.F. Oleiro Seabra[138a], S.A. Olivares Pino[145c], D. Oliveira Damazio[29], D. Oliveira Goncalves[80a], J.L. Oliver[1], M.J.R. Olsson[169], A. Olszewski[84], J. Olszowska[84], Ö.O. Öncel[24], D.C. O'Neil[151], A.P. O'neill[133], A. Onofre[138a,138e], P.U.E. Onyisi[11], H. Oppen[132], R.G. Oreamuno Madriz[120], M.J. Oreglia[37], G.E. Orellana[88], D. Orestano[74a,74b], N. Orlando[14], R.S. Orr[165], V. O'Shea[57], R. Ospanov[60a], G. Otero y Garzon[30], H. Otono[87], P.S. Ott[61a], G.J. Ottino[18], M. Ouchrif[35e], J. Ouellette[29], F. Ould-Saada[132], A. Ouraou[143,*], Q. Ouyang[15a], M. Owen[57], R.E. Owen[142], V.E. Ozcan[12c], N. Ozturk[8], J. Pacalt[129], H.A. Pacey[32], K. Pachal[49], A. Pacheco Pages[14], C. Padilla Aranda[14], S. Pagan Griso[18], G. Palacino[65], S. Palazzo[50], S. Palestini[36], M. Palka[83b], P. Palni[83a], D.K. Panchal[11], C.E. Pandini[54], J.G. Panduro Vazquez[93], P. Pani[46], G. Panizzo[66a,66c], L. Paolozzi[54], C. Papadatos[109], S. Parajuli[42], A. Paramonov[6], C. Paraskevopoulos[10], D. Paredes Hernandez[62b], S.R. Paredes Saenz[133], B. Parida[178], T.H. Park[165], A.J. Parker[31], M.A. Parker[32], F. Parodi[55b,55a], E.W. Parrish[120], J.A. Parsons[39], U. Parzefall[52], L. Pascual Dominguez[134], V.R. Pascuzzi[18], J.M.P. Pasner[144], F. Pasquali[119], E. Pasqualucci[72a], S. Passaggio[55b], F. Pastore[93], P. Pasuwan[45a,45b], J.R. Pater[100], A. Pathak[179,k], J. Patton[90], T. Pauly[36], J. Pearkes[152], M. Pedersen[132], L. Pedraza Diaz[118], R. Pedro[138a], T. Peiffer[53], S.V. Peleganchuk[121b,121a], O. Penc[139], C. Peng[62b], H. Peng[60a], M. Penzin[164], B.S. Peralva[80a], M.M. Perego[64], A.P. Pereira Peixoto[138a], L. Pereira Sanchez[45a,45b], D.V. Perepelitsa[29], E. Perez Codina[166a], M. Perganti[10], L. Perini[68a,68b], H. Pernegger[36], S. Perrella[36], A. Perrevoort[119], K. Peters[46], R.F.Y. Peters[100], B.A. Petersen[36], T.C. Petersen[40], E. Petit[101], V. Petousis[140], C. Petridou[161], P. Petroff[64], F. Petrucci[74a,74b], M. Pettee[181], N.E. Pettersson[102], K. Petukhova[141], A. Peyaud[143], R. Pezoa[145d], L. Pezzotti[70a,70b], G. Pezzullo[181], T. Pham[104], P.W. Phillips[142], M.W. Phipps[171], G. Piacquadio[154], E. Pianori[18], F. Piazza[68a,68b], A. Picazio[102], R. Piegaia[30], D. Pietreanu[27b], J.E. Pilcher[37], A.D. Pilkington[100], M. Pinamonti[66a,66c], J.L. Pinfold[3], C. Pitman Donaldson[94], D.A. Pizzi[34], L. Pizzimento[73a,73b], A. Pizzini[119], M.-A. Pleier[29], V. Plesanovs[52], V. Pleskot[141], E. Plotnikova[79], P. Podberezko[121b,121a], R. Poettgen[96], R. Poggi[54], L. Poggioli[134], I. Pogrebnyak[106], D. Pohl[24], I. Pokharel[53], G. Polesello[70a], A. Poley[151,166a], A. Policicchio[72a,72b], R. Polifka[141], A. Polini[23b], C.S. Pollard[46], Z.B. Pollock[126], V. Polychronakos[29], D. Ponomarenko[111], L. Pontecorvo[36], S. Popa[27a], G.A. Popeneciu[27d], L. Portales[5], D.M. Portillo Quintero[58], S. Pospisil[140], P. Postolache[27c], K. Potamianos[133], I.N. Potrap[79], C.J. Potter[32], H. Potti[11], T. Poulsen[46], J. Poveda[172], T.D. Powell[148], G. Pownall[46], M.E. Pozo Astigarraga[36], A. Prades Ibanez[172], P. Pralavorio[101], M.M. Prapa[44], S. Prell[78], D. Price[100], M. Primavera[67a], M.A. Principe Martin[98], M.L. Proffitt[147], N. Proklova[111], K. Prokofiev[62c], F. Prokoshin[79],

S. Protopopescu[29], J. Proudfoot[6], M. Przybycien[83a], D. Pudzha[136], P. Puzo[64], D. Pyatiizbyantseva[111], J. Qian[105], Y. Qin[100], A. Quadt[53], M. Queitsch-Maitland[36], G. Rabanal Bolanos[59], F. Ragusa[68a,68b], G. Rahal[97], J.A. Raine[54], S. Rajagopalan[29], K. Ran[15a,15d], D.F. Rassloff[61a], D.M. Rauch[46], S. Rave[99], B. Ravina[57], I. Ravinovich[178], M. Raymond[36], A.L. Read[132], N.P. Readioff[148], M. Reale[67a,67b], D.M. Rebuzzi[70a,70b], G. Redlinger[29], K. Reeves[43], D. Reikher[160], A. Reiss[99], A. Rej[150], C. Rembser[36], A. Renardi[46], M. Renda[27b], M.B. Rendel[114], A.G. Rennie[57], S. Resconi[68a], E.D. Resseguie[18], S. Rettie[94], B. Reynolds[126], E. Reynolds[21], M. Rezaei Estabragh[180], O.L. Rezanova[121b,121a], P. Reznicek[141], E. Ricci[75a,75b], R. Richter[114], S. Richter[46], E. Richter-Was[83b], M. Ridel[134], P. Rieck[114], O. Rifki[46], M. Rijssenbeek[154], A. Rimoldi[70a,70b], M. Rimoldi[46], L. Rinaldi[23b], T.T. Rinn[171], M.P. Rinnagel[113], G. Ripellino[153], I. Riu[14], P. Rivadeneira[46], J.C. Rivera Vergara[174], F. Rizatdinova[128], E. Rizvi[92], C. Rizzi[54], S.H. Robertson[103,aa], M. Robin[46], D. Robinson[32], C.M. Robles Gajardo[145d], M. Robles Manzano[99], A. Robson[57], A. Rocchi[73a,73b], C. Roda[71a,71b], S. Rodriguez Bosca[172], A. Rodriguez Rodriguez[52], A.M. Rodríguez Vera[166b], S. Roe[36], J. Roggel[180], O. Røhne[132], R.A. Rojas[145d], B. Roland[52], C.P.A. Roland[65], J. Roloff[29], A. Romaniouk[111], M. Romano[23b,23a], N. Rompotis[90], M. Ronzani[124], L. Roos[134], S. Rosati[72a], G. Rosin[102], B.J. Rosser[135], E. Rossi[165], E. Rossi[5], E. Rossi[69a,69b], L.P. Rossi[55b], L. Rossini[46], R. Rosten[126], M. Rotaru[27b], B. Rottler[52], D. Rousseau[64], D. Rousso[32], G. Rovelli[70a,70b], A. Roy[11], A. Rozanov[101], Y. Rozen[159], X. Ruan[33f], A.J. Ruby[90], T.A. Ruggeri[1], F. Rühr[52], A. Ruiz-Martinez[172], A. Rummler[36], Z. Rurikova[52], N.A. Rusakovich[79], H.L. Russell[36], L. Rustige[38], J.P. Rutherfoord[7], E.M. Rüttinger[148], M. Rybar[141], E.B. Rye[132], A. Ryzhov[122], J.A. Sabater Iglesias[46], P. Sabatini[172], L. Sabetta[72a,72b], H.F-W. Sadrozinski[144], R. Sadykov[79], F. Safai Tehrani[72a], B. Safarzadeh Samani[155], M. Safdari[152], P. Saha[120], S. Saha[103], M. Sahinsoy[114], A. Sahu[180], M. Saimpert[36], M. Saito[162], T. Saito[162], D. Salamani[54], G. Salamanna[74a,74b], A. Salnikov[152], J. Salt[172], A. Salvador Salas[14], D. Salvatore[41b,41a], F. Salvatore[155], A. Salzburger[36], D. Sammel[52], D. Sampsonidis[161], D. Sampsonidou[60d,60c], J. Sánchez[172], A. Sanchez Pineda[66a,36,66c], H. Sandaker[132], C.O. Sander[46], I.G. Sanderswood[89], M. Sandhoff[180], C. Sandoval[22b], D.P.C. Sankey[142], M. Sannino[55b,55a], Y. Sano[116], A. Sansoni[51], C. Santoni[38], H. Santos[138a,138b], S.N. Santpur[18], A. Santra[178], K.A. Saoucha[148], A. Sapronov[79], J.G. Saraiva[138a,138d], O. Sasaki[81], K. Sato[167], C. Sauer[61b], F. Sauerburger[52], E. Sauvan[5], P. Savard[165,ak], R. Sawada[162], C. Sawyer[142], L. Sawyer[95], I. Sayago Galvan[172], C. Sbarra[23b], A. Sbrizzi[66a,66c], T. Scanlon[94], J. Schaarschmidt[147], P. Schacht[114], D. Schaefer[37], L. Schaefer[135], U. Schäfer[99], A.C. Schaffer[64], D. Schaile[113], R.D. Schamberger[154], E. Schanet[113], C. Scharf[19], N. Scharmberg[100], V.A. Schegelsky[136], D. Scheirich[141], F. Schenck[19], M. Schernau[169], C. Schiavi[55b,55a], L.K. Schildgen[24], Z.M. Schillaci[26], E.J. Schioppa[67a,67b], M. Schioppa[41b,41a], B. Schlag[99], K.E. Schleicher[52], S. Schlenker[36], K. Schmieden[99], C. Schmitt[99], S. Schmitt[46], L. Schoeffel[143], A. Schoening[61b], P.G. Scholer[52], E. Schopf[133], M. Schott[99], J. Schovancova[36], S. Schramm[54], F. Schroeder[180], A. Schulte[99], H-C. Schultz-Coulon[61a], M. Schumacher[52], B.A. Schumm[144], Ph. Schune[143], A. Schwartzman[152], T.A. Schwarz[105], Ph. Schwemling[143], R. Schwienhorst[106], A. Sciandra[144], G. Sciolla[26], F. Scuri[71a], F. Scutti[104], C.D. Sebastiani[90], K. Sedlaczek[47], P. Seema[19], S.C. Seidel[117], A. Seiden[144], B.D. Seidlitz[29], T. Seiss[37], C. Seitz[46], J.M. Seixas[80b], G. Sekhniaidze[69a], S.J. Sekula[42], L.P. Selem[5], N. Semprini-Cesari[23b,23a], S. Sen[49], C. Serfon[29], L. Serin[64], L. Serkin[66a,66b], M. Sessa[60a], H. Severini[127], S. Sevova[152], F. Sforza[55b,55a], A. Sfyrla[54], E. Shabalina[53], J.D. Shahinian[135], N.W. Shaikh[45a,45b], D. Shaked Renous[178], L.Y. Shan[15a], M. Shapiro[18], A. Sharma[36], A.S. Sharma[1], S. Sharma[46], P.B. Shatalov[123], K. Shaw[155], S.M. Shaw[100], M. Shehade[178], Y. Shen[127], P. Sherwood[94], L. Shi[94], C.O. Shimmin[181], Y. Shimogama[177], M. Shimojima[115], J.D. Shinner[93], I.P.J. Shipsey[133], S. Shirabe[163], M. Shiyakova[79], J. Shlomi[178], M.J. Shochet[37], J. Shojaii[104], D.R. Shope[153], S. Shrestha[126], E.M. Shrif[33f], M.J. Shroff[174], E. Shulga[178], P. Sicho[139], A.M. Sickles[171], E. Sideras Haddad[33f], O. Sidiropoulou[36], A. Sidoti[23b,23a], F. Siegert[48], Dj. Sijacki[16], M.V. Silva Oliveira[36], S.B. Silverstein[45a], S. Simion[64], R. Simoniello[36], S. Simsek[12b], P. Sinervo[165], V. Sinetckii[112], S. Singh[151], S. Sinha[33f],

M. Sioli[23b,23a], I. Siral[130], S.Yu. Sivoklokov[112], J. Sjölin[45a,45b], A. Skaf[53], E. Skorda[96], P. Skubic[127], M. Slawinska[84], K. Sliwa[168], V. Smakhtin[178], B.H. Smart[142], J. Smiesko[141], S.Yu. Smirnov[111], Y. Smirnov[111], L.N. Smirnova[112,s], O. Smirnova[96], E.A. Smith[37], H.A. Smith[133], M. Smizanska[89], K. Smolek[140], A. Smykiewicz[84], A.A. Snesarev[110], H.L. Snoek[119], I.M. Snyder[130], S. Snyder[29], R. Sobie[174,aa], A. Soffer[160], A. Søgaard[50], F. Sohns[53], C.A. Solans Sanchez[36], E.Yu. Soldatov[111], U. Soldevila[172], A.A. Solodkov[122], S. Solomon[52], A. Soloshenko[79], O.V. Solovyanov[122], V. Solovyev[136], P. Sommer[148], H. Son[168], A. Sonay[14], W.Y. Song[166b], A. Sopczak[140], A.L. Sopio[94], F. Sopkova[28b], S. Sottocornola[70a,70b], R. Soualah[66a,66c], A.M. Soukharev[121b,121a], Z. Soumaimi[35f], D. South[46], S. Spagnolo[67a,67b], M. Spalla[114], M. Spangenberg[176], F. Spanò[93], D. Sperlich[52], T.M. Spieker[61a], G. Spigo[36], M. Spina[155], D.P. Spiteri[57], M. Spousta[141], A. Stabile[68a,68b], B.L. Stamas[120], R. Stamen[61a], M. Stamenkovic[119], A. Stampekis[21], E. Stanecka[84], B. Stanislaus[133], M.M. Stanitzki[46], M. Stankaityte[133], B. Stapf[46], E.A. Starchenko[122], G.H. Stark[144], J. Stark[101], D.M. Starko[166b], P. Staroba[139], P. Starovoitov[61a], S. Stärz[103], R. Staszewski[84], G. Stavropoulos[44], P. Steinberg[29], A.L. Steinhebel[130], B. Stelzer[151,166a], H.J. Stelzer[137], O. Stelzer-Chilton[166a], H. Stenzel[56], T.J. Stevenson[155], G.A. Stewart[36], M.C. Stockton[36], G. Stoicea[27b], M. Stolarski[138a], S. Stonjek[114], A. Straessner[48], J. Strandberg[153], S. Strandberg[45a,45b], M. Strauss[127], T. Strebler[101], P. Strizenec[28b], R. Ströhmer[175], D.M. Strom[130], L.R. Strom[46], R. Stroynowski[42], A. Strubig[45a,45b], S.A. Stucci[29], B. Stugu[17], J. Stupak[127], N.A. Styles[46], D. Su[152], S. Su[60a], W. Su[60d,147,60c], X. Su[60a], N.B. Suarez[137], K. Sugizaki[162], V.V. Sulin[110], M.J. Sullivan[90], D.M.S. Sultan[54], S. Sultansoy[4c], T. Sumida[85], S. Sun[105], S. Sun[179], X. Sun[100], C.J.E. Suster[156], M.R. Sutton[155], M. Svatos[139], M. Swiatlowski[166a], S.P. Swift[2], T. Swirski[175], A. Sydorenko[99], I. Sykora[28a], M. Sykora[141], T. Sykora[141], D. Ta[99], K. Tackmann[46,y], A. Taffard[169], R. Tafirout[166a], E. Tagiev[122], R.H.M. Taibah[134], R. Takashima[86], K. Takeda[82], T. Takeshita[149], E.P. Takeva[50], Y. Takubo[81], M. Talby[101], A.A. Talyshev[121b,121a], K.C. Tam[62b], N.M. Tamir[160], J. Tanaka[162], R. Tanaka[64], S. Tapia Araya[171], S. Tapprogge[99], A. Tarek Abouelfadl Mohamed[106], S. Tarem[159], K. Tariq[60b], G. Tarna[27b,f], G.F. Tartarelli[68a], P. Tas[141], M. Tasevsky[139], E. Tassi[41b,41a], G. Tateno[162], Y. Tayalati[35f], G.N. Taylor[104], W. Taylor[166b], H. Teagle[90], A.S. Tee[89], R. Teixeira De Lima[152], P. Teixeira-Dias[93], H. Ten Kate[36], J.J. Teoh[119], K. Terashi[162], J. Terron[98], S. Terzo[14], M. Testa[51], R.J. Teuscher[165,aa], N. Themistokleous[50], T. Theveneaux-Pelzer[19], D.W. Thomas[93], J.P. Thomas[21], E.A. Thompson[46], P.D. Thompson[21], E. Thomson[135], E.J. Thorpe[92], Y. Tian[53], V.O. Tikhomirov[110,ag], Yu.A. Tikhonov[121b,121a], S. Timoshenko[111], P. Tipton[181], S. Tisserant[101], S.H. Tlou[33f], A. Tnourji[38], K. Todome[23b,23a], S. Todorova-Nova[141], S. Todt[48], M. Togawa[81], J. Tojo[87], S. Tokár[28a], K. Tokushuku[81], E. Tolley[126], R. Tombs[32], M. Tomoto[81,116], L. Tompkins[152], P. Tornambe[102], E. Torrence[130], H. Torres[48], E. Torró Pastor[172], M. Toscani[30], C. Tosciri[37], J. Toth[101,z], D.R. Tovey[148], A. Traeet[17], C.J. Treado[124], T. Trefzger[175], A. Tricoli[29], I.M. Trigger[166a], S. Trincaz-Duvoid[134], D.A. Trischuk[173], W. Trischuk[165], B. Trocmé[58], A. Trofymov[64], C. Troncon[68a], F. Trovato[155], L. Truong[33c], M. Trzebinski[84], A. Trzupek[84], F. Tsai[154], A. Tsiamis[161], P.V. Tsiareshka[107,ae], A. Tsirigotis[161,w], V. Tsiskaridze[154], E.G. Tskhadadze[158a], M. Tsopoulou[161], I.I. Tsukerman[123], V. Tsulaia[18], S. Tsuno[81], O. Tsur[159], D. Tsybychev[154], Y. Tu[62b], A. Tudorache[27b], V. Tudorache[27b], A.N. Tuna[36], S. Turchikhin[79], D. Turgeman[178], I. Turk Cakir[4b,u], R.J. Turner[21], R. Turra[68a], P.M. Tuts[39], S. Tzamarias[161], P. Tzanis[10], E. Tzovara[99], K. Uchida[162], F. Ukegawa[167], G. Unal[36], M. Unal[11], A. Undrus[29], G. Unel[169], F.C. Ungaro[104], K. Uno[162], J. Urban[28b], P. Urquijo[104], G. Usai[8], R. Ushioda[163], Z. Uysal[12d], V. Vacek[140], B. Vachon[103], K.O.H. Vadla[132], T. Vafeiadis[36], C. Valderanis[113], E. Valdes Santurio[45a,45b], M. Valente[166a], S. Valentinetti[23b,23a], A. Valero[172], L. Valéry[46], R.A. Vallance[21], A. Vallier[36], J.A. Valls Ferrer[172], T.R. Van Daalen[14], P. Van Gemmeren[6], S. Van Stroud[94], I. Van Vulpen[119], M. Vanadia[73a,73b], W. Vandelli[36], M. Vandenbroucke[143], E.R. Vandewall[128], D. Vannicola[72a,72b], L. Vannoli[55b,55a], R. Vari[72a], E.W. Varnes[7], C. Varni[55b,55a], T. Varol[157], D. Varouchas[64], K.E. Varvell[156], M.E. Vasile[27b], L. Vaslin[38], G.A. Vasquez[174], F. Vazeille[38], D. Vazquez Furelos[14], T. Vazquez Schroeder[36], J. Veatch[53], V. Vecchio[100], M.J. Veen[119],

L.M. Veloce[165], F. Veloso[138a,138c], S. Veneziano[72a], A. Ventura[67a,67b], A. Verbytskyi[114], M. Verducci[71a,71b], C. Vergis[24], M. Verissimo De Araujo[80b], W. Verkerke[119], A.T. Vermeulen[119], J.C. Vermeulen[119], C. Vernieri[152], P.J. Verschuuren[93], M.L. Vesterbacka[124], M.C. Vetterli[151,ak], N. Viaux Maira[145d], T. Vickey[148], O.E. Vickey Boeriu[148], G.H.A. Viehhauser[133], L. Vigani[61b], M. Villa[23b,23a], M. Villaplana Perez[172], E.M. Villhauer[50], E. Vilucchi[51], M.G. Vincter[34], G.S. Virdee[21], A. Vishwakarma[50], C. Vittori[23b,23a], I. Vivarelli[155], V. Vladimirov[176], M. Vogel[180], P. Vokac[140], J. Von Ahnen[46], S.E. von Buddenbrock[33f], E. Von Toerne[24], V. Vorobel[141], K. Vorobev[111], M. Vos[172], J.H. Vossebeld[90], M. Vozak[100], N. Vranjes[16], M. Vranjes Milosavljevic[16], V. Vrba[140,*], M. Vreeswijk[119], N.K. Vu[101], R. Vuillermet[36], I. Vukotic[37], S. Wada[167], C. Wagner[102], P. Wagner[24], W. Wagner[180], S. Wahdan[180], H. Wahlberg[88], R. Wakasa[167], M. Wakida[116], V.M. Walbrecht[114], J. Walder[142], R. Walker[113], S.D. Walker[93], W. Walkowiak[150], V. Wallangen[45a,45b], A.M. Wang[59], A.Z. Wang[179], C. Wang[60a], C. Wang[60c], H. Wang[18], J. Wang[62a], P. Wang[42], R.-J. Wang[99], R. Wang[59], R. Wang[120], S.M. Wang[157], S. Wang[60b], T. Wang[60a], W.T. Wang[60a], W.X. Wang[60a], X. Wang[171], Y. Wang[60a], Z. Wang[105], C. Wanotayaroj[36], A. Warburton[103], C.P. Ward[32], R.J. Ward[21], N. Warrack[57], A.T. Watson[21], M.F. Watson[21], G. Watts[147], B.M. Waugh[94], A.F. Webb[11], C. Weber[29], M.S. Weber[20], S.A. Weber[34], S.M. Weber[61a], C. Wei[60a], Y. Wei[133], A.R. Weidberg[133], J. Weingarten[47], M. Weirich[99], C. Weiser[52], P.S. Wells[36], T. Wenaus[29], B. Wendland[47], T. Wengler[36], S. Wenig[36], N. Wermes[24], M. Wessels[61a], T.D. Weston[20], K. Whalen[130], A.M. Wharton[89], A.S. White[59], A. White[8], M.J. White[1], D. Whiteson[169], W. Wiedenmann[179], C. Wiel[48], M. Wielers[142], N. Wieseotte[99], C. Wiglesworth[40], L.A.M. Wiik-Fuchs[52], H.G. Wilkens[36], L.J. Wilkins[93], D.M. Williams[39], H.H. Williams[135], S. Williams[32], S. Willocq[102], P.J. Windischhofer[133], I. Wingerter-Seez[5], F. Winklmeier[130], B.T. Winter[52], M. Wittgen[152], M. Wobisch[95], A. Wolf[99], R. Wölker[133], J. Wollrath[52], M.W. Wolter[84], H. Wolters[138a,138c], V.W.S. Wong[173], A.F. Wongel[46], N.L. Woods[144], S.D. Worm[46], B.K. Wosiek[84], K.W. Woźniak[84], K. Wraight[57], J. Wu[15a,15d], S.L. Wu[179], X. Wu[54], Y. Wu[60a], Z. Wu[143], J. Wuerzinger[133], T.R. Wyatt[100], B.M. Wynne[50], S. Xella[40], J. Xiang[62c], X. Xiao[105], X. Xie[60a], I. Xiotidis[155], D. Xu[15a], H. Xu[60a], H. Xu[60a], L. Xu[60a], R. Xu[135], W. Xu[105], Y. Xu[15b], Z. Xu[60b], Z. Xu[152], B. Yabsley[156], S. Yacoob[33a], D.P. Yallup[94], N. Yamaguchi[87], Y. Yamaguchi[163], M. Yamatani[162], H. Yamauchi[167], T. Yamazaki[18], Y. Yamazaki[82], J. Yan[60c], Z. Yan[25], H.J. Yang[60c,60d], H.T. Yang[18], S. Yang[60a], T. Yang[62c], X. Yang[60a], X. Yang[15a], Y. Yang[162], Z. Yang[105,60a], W-M. Yao[18], Y.C. Yap[46], H. Ye[15c], J. Ye[42], S. Ye[29], I. Yeletskikh[79], M.R. Yexley[89], P. Yin[39], K. Yorita[177], K. Yoshihara[78], C.J.S. Young[36], C. Young[152], R. Yuan[60b,j], X. Yue[61a], M. Zaazoua[35f], B. Zabinski[84], G. Zacharis[10], E. Zaffaroni[54], J. Zahreddine[101], A.M. Zaitsev[122,af], T. Zakareishvili[158b], N. Zakharchuk[34], S. Zambito[36], D. Zanzi[52], S.V. Zeißner[47], C. Zeitnitz[180], G. Zemaityte[133], J.C. Zeng[171], O. Zenin[122], T. Ženiš[28a], S. Zenz[92], S. Zerradi[35a], D. Zerwas[64], M. Zgubič[133], B. Zhang[15c], D.F. Zhang[15b], G. Zhang[15b], J. Zhang[6], K. Zhang[15a], L. Zhang[15c], M. Zhang[171], R. Zhang[179], S. Zhang[105], X. Zhang[60c], X. Zhang[60b], Z. Zhang[64], P. Zhao[49], Y. Zhao[144], Z. Zhao[60a], A. Zhemchugov[79], Z. Zheng[105], D. Zhong[171], B. Zhou[105], C. Zhou[179], H. Zhou[7], M. Zhou[154], N. Zhou[60c], Y. Zhou[7], C.G. Zhu[60b], C. Zhu[15a,15d], H.L. Zhu[60a], H. Zhu[15a], J. Zhu[105], Y. Zhu[60a], X. Zhuang[15a], K. Zhukov[110], V. Zhulanov[121b,121a], D. Zieminska[65], N.I. Zimine[79], S. Zimmermann[52,*], Z. Zinonos[114], M. Ziolkowski[150], L. Živković[16], A. Zoccoli[23b,23a], K. Zoch[53], T.G. Zorbas[148], R. Zou[37], W. Zou[39], L. Zwalinski[36].

[1]Department of Physics, University of Adelaide, Adelaide; Australia.
[2]Physics Department, SUNY Albany, Albany NY; United States of America.
[3]Department of Physics, University of Alberta, Edmonton AB; Canada.
[4(a)]Department of Physics, Ankara University, Ankara;[(b)]Istanbul Aydin University, Application and Research Center for Advanced Studies, Istanbul;[(c)]Division of Physics, TOBB University of Economics and Technology, Ankara; Turkey.
[5]LAPP, Univ. Savoie Mont Blanc, CNRS/IN2P3, Annecy ; France.

[6]High Energy Physics Division, Argonne National Laboratory, Argonne IL; United States of America.
[7]Department of Physics, University of Arizona, Tucson AZ; United States of America.
[8]Department of Physics, University of Texas at Arlington, Arlington TX; United States of America.
[9]Physics Department, National and Kapodistrian University of Athens, Athens; Greece.
[10]Physics Department, National Technical University of Athens, Zografou; Greece.
[11]Department of Physics, University of Texas at Austin, Austin TX; United States of America.
[12(a)]Bahcesehir University, Faculty of Engineering and Natural Sciences, Istanbul;[(b)]Istanbul Bilgi University, Faculty of Engineering and Natural Sciences, Istanbul;[(c)]Department of Physics, Bogazici University, Istanbul;[(d)]Department of Physics Engineering, Gaziantep University, Gaziantep; Turkey.
[13]Institute of Physics, Azerbaijan Academy of Sciences, Baku; Azerbaijan.
[14]Institut de Física d'Altes Energies (IFAE), Barcelona Institute of Science and Technology, Barcelona; Spain.
[15(a)]Institute of High Energy Physics, Chinese Academy of Sciences, Beijing;[(b)]Physics Department, Tsinghua University, Beijing;[(c)]Department of Physics, Nanjing University, Nanjing;[(d)]University of Chinese Academy of Science (UCAS), Beijing; China.
[16]Institute of Physics, University of Belgrade, Belgrade; Serbia.
[17]Department for Physics and Technology, University of Bergen, Bergen; Norway.
[18]Physics Division, Lawrence Berkeley National Laboratory and University of California, Berkeley CA; United States of America.
[19]Institut für Physik, Humboldt Universität zu Berlin, Berlin; Germany.
[20]Albert Einstein Center for Fundamental Physics and Laboratory for High Energy Physics, University of Bern, Bern; Switzerland.
[21]School of Physics and Astronomy, University of Birmingham, Birmingham; United Kingdom.
[22(a)]Facultad de Ciencias y Centro de Investigaciónes, Universidad Antonio Nariño, Bogotá;[(b)]Departamento de Física, Universidad Nacional de Colombia, Bogotá, Colombia; Colombia.
[23(a)]INFN Bologna and Universita' di Bologna, Dipartimento di Fisica;[(b)]INFN Sezione di Bologna; Italy.
[24]Physikalisches Institut, Universität Bonn, Bonn; Germany.
[25]Department of Physics, Boston University, Boston MA; United States of America.
[26]Department of Physics, Brandeis University, Waltham MA; United States of America.
[27(a)]Transilvania University of Brasov, Brasov;[(b)]Horia Hulubei National Institute of Physics and Nuclear Engineering, Bucharest;[(c)]Department of Physics, Alexandru Ioan Cuza University of Iasi, Iasi;[(d)]National Institute for Research and Development of Isotopic and Molecular Technologies, Physics Department, Cluj-Napoca;[(e)]University Politehnica Bucharest, Bucharest;[(f)]West University in Timisoara, Timisoara; Romania.
[28(a)]Faculty of Mathematics, Physics and Informatics, Comenius University, Bratislava;[(b)]Department of Subnuclear Physics, Institute of Experimental Physics of the Slovak Academy of Sciences, Kosice; Slovak Republic.
[29]Physics Department, Brookhaven National Laboratory, Upton NY; United States of America.
[30]Departamento de Física, Universidad de Buenos Aires, Buenos Aires; Argentina.
[31]California State University, CA; United States of America.
[32]Cavendish Laboratory, University of Cambridge, Cambridge; United Kingdom.
[33(a)]Department of Physics, University of Cape Town, Cape Town;[(b)]iThemba Labs, Western Cape;[(c)]Department of Mechanical Engineering Science, University of Johannesburg, Johannesburg;[(d)]National Institute of Physics, University of the Philippines Diliman;[(e)]University of South Africa, Department of Physics, Pretoria;[(f)]School of Physics, University of the Witwatersrand, Johannesburg; South Africa.
[34]Department of Physics, Carleton University, Ottawa ON; Canada.

[35](a)Faculté des Sciences Ain Chock, Réseau Universitaire de Physique des Hautes Energies - Université Hassan II, Casablanca;(b)Faculté des Sciences, Université Ibn-Tofail, Kénitra;(c)Faculté des Sciences Semlalia, Université Cadi Ayyad, LPHEA-Marrakech;(d)Moroccan Foundation for Advanced Science Innovation and Research (MAScIR), Rabat;(e)LPMR, Faculté des Sciences, Université Mohamed Premier, Oujda;(f)Faculté des sciences, Université Mohammed V, Rabat; Morocco.
[36]CERN, Geneva; Switzerland.
[37]Enrico Fermi Institute, University of Chicago, Chicago IL; United States of America.
[38]LPC, Université Clermont Auvergne, CNRS/IN2P3, Clermont-Ferrand; France.
[39]Nevis Laboratory, Columbia University, Irvington NY; United States of America.
[40]Niels Bohr Institute, University of Copenhagen, Copenhagen; Denmark.
[41](a)Dipartimento di Fisica, Università della Calabria, Rende;(b)INFN Gruppo Collegato di Cosenza, Laboratori Nazionali di Frascati; Italy.
[42]Physics Department, Southern Methodist University, Dallas TX; United States of America.
[43]Physics Department, University of Texas at Dallas, Richardson TX; United States of America.
[44]National Centre for Scientific Research "Demokritos", Agia Paraskevi; Greece.
[45](a)Department of Physics, Stockholm University;(b)Oskar Klein Centre, Stockholm; Sweden.
[46]Deutsches Elektronen-Synchrotron DESY, Hamburg and Zeuthen; Germany.
[47]Lehrstuhl für Experimentelle Physik IV, Technische Universität Dortmund, Dortmund; Germany.
[48]Institut für Kern- und Teilchenphysik, Technische Universität Dresden, Dresden; Germany.
[49]Department of Physics, Duke University, Durham NC; United States of America.
[50]SUPA - School of Physics and Astronomy, University of Edinburgh, Edinburgh; United Kingdom.
[51]INFN e Laboratori Nazionali di Frascati, Frascati; Italy.
[52]Physikalisches Institut, Albert-Ludwigs-Universität Freiburg, Freiburg; Germany.
[53]II. Physikalisches Institut, Georg-August-Universität Göttingen, Göttingen; Germany.
[54]Département de Physique Nucléaire et Corpusculaire, Université de Genève, Genève; Switzerland.
[55](a)Dipartimento di Fisica, Università di Genova, Genova;(b)INFN Sezione di Genova; Italy.
[56]II. Physikalisches Institut, Justus-Liebig-Universität Giessen, Giessen; Germany.
[57]SUPA - School of Physics and Astronomy, University of Glasgow, Glasgow; United Kingdom.
[58]LPSC, Université Grenoble Alpes, CNRS/IN2P3, Grenoble INP, Grenoble; France.
[59]Laboratory for Particle Physics and Cosmology, Harvard University, Cambridge MA; United States of America.
[60](a)Department of Modern Physics and State Key Laboratory of Particle Detection and Electronics, University of Science and Technology of China, Hefei;(b)Institute of Frontier and Interdisciplinary Science and Key Laboratory of Particle Physics and Particle Irradiation (MOE), Shandong University, Qingdao;(c)School of Physics and Astronomy, Shanghai Jiao Tong University, Key Laboratory for Particle Astrophysics and Cosmology (MOE), SKLPPC, Shanghai;(d)Tsung-Dao Lee Institute, Shanghai; China.
[61](a)Kirchhoff-Institut für Physik, Ruprecht-Karls-Universität Heidelberg, Heidelberg;(b)Physikalisches Institut, Ruprecht-Karls-Universität Heidelberg, Heidelberg; Germany.
[62](a)Department of Physics, Chinese University of Hong Kong, Shatin, N.T., Hong Kong;(b)Department of Physics, University of Hong Kong, Hong Kong;(c)Department of Physics and Institute for Advanced Study, Hong Kong University of Science and Technology, Clear Water Bay, Kowloon, Hong Kong; China.
[63]Department of Physics, National Tsing Hua University, Hsinchu; Taiwan.
[64]IJCLab, Université Paris-Saclay, CNRS/IN2P3, 91405, Orsay; France.
[65]Department of Physics, Indiana University, Bloomington IN; United States of America.
[66](a)INFN Gruppo Collegato di Udine, Sezione di Trieste, Udine;(b)ICTP, Trieste;(c)Dipartimento Politecnico di Ingegneria e Architettura, Università di Udine, Udine; Italy.
[67](a)INFN Sezione di Lecce;(b)Dipartimento di Matematica e Fisica, Università del Salento, Lecce; Italy.

[68](a)INFN Sezione di Milano;(b)Dipartimento di Fisica, Università di Milano, Milano; Italy.
[69](a)INFN Sezione di Napoli;(b)Dipartimento di Fisica, Università di Napoli, Napoli; Italy.
[70](a)INFN Sezione di Pavia;(b)Dipartimento di Fisica, Università di Pavia, Pavia; Italy.
[71](a)INFN Sezione di Pisa;(b)Dipartimento di Fisica E. Fermi, Università di Pisa, Pisa; Italy.
[72](a)INFN Sezione di Roma;(b)Dipartimento di Fisica, Sapienza Università di Roma, Roma; Italy.
[73](a)INFN Sezione di Roma Tor Vergata;(b)Dipartimento di Fisica, Università di Roma Tor Vergata, Roma; Italy.
[74](a)INFN Sezione di Roma Tre;(b)Dipartimento di Matematica e Fisica, Università Roma Tre, Roma; Italy.
[75](a)INFN-TIFPA;(b)Università degli Studi di Trento, Trento; Italy.
[76]Institut für Astro- und Teilchenphysik, Leopold-Franzens-Universität, Innsbruck; Austria.
[77]University of Iowa, Iowa City IA; United States of America.
[78]Department of Physics and Astronomy, Iowa State University, Ames IA; United States of America.
[79]Joint Institute for Nuclear Research, Dubna; Russia.
[80](a)Departamento de Engenharia Elétrica, Universidade Federal de Juiz de Fora (UFJF), Juiz de Fora;(b)Universidade Federal do Rio De Janeiro COPPE/EE/IF, Rio de Janeiro;(c)Instituto de Física, Universidade de São Paulo, São Paulo; Brazil.
[81]KEK, High Energy Accelerator Research Organization, Tsukuba; Japan.
[82]Graduate School of Science, Kobe University, Kobe; Japan.
[83](a)AGH University of Science and Technology, Faculty of Physics and Applied Computer Science, Krakow;(b)Marian Smoluchowski Institute of Physics, Jagiellonian University, Krakow; Poland.
[84]Institute of Nuclear Physics Polish Academy of Sciences, Krakow; Poland.
[85]Faculty of Science, Kyoto University, Kyoto; Japan.
[86]Kyoto University of Education, Kyoto; Japan.
[87]Research Center for Advanced Particle Physics and Department of Physics, Kyushu University, Fukuoka ; Japan.
[88]Instituto de Física La Plata, Universidad Nacional de La Plata and CONICET, La Plata; Argentina.
[89]Physics Department, Lancaster University, Lancaster; United Kingdom.
[90]Oliver Lodge Laboratory, University of Liverpool, Liverpool; United Kingdom.
[91]Department of Experimental Particle Physics, Jožef Stefan Institute and Department of Physics, University of Ljubljana, Ljubljana; Slovenia.
[92]School of Physics and Astronomy, Queen Mary University of London, London; United Kingdom.
[93]Department of Physics, Royal Holloway University of London, Egham; United Kingdom.
[94]Department of Physics and Astronomy, University College London, London; United Kingdom.
[95]Louisiana Tech University, Ruston LA; United States of America.
[96]Fysiska institutionen, Lunds universitet, Lund; Sweden.
[97]Centre de Calcul de l'Institut National de Physique Nucléaire et de Physique des Particules (IN2P3), Villeurbanne; France.
[98]Departamento de Física Teorica C-15 and CIAFF, Universidad Autónoma de Madrid, Madrid; Spain.
[99]Institut für Physik, Universität Mainz, Mainz; Germany.
[100]School of Physics and Astronomy, University of Manchester, Manchester; United Kingdom.
[101]CPPM, Aix-Marseille Université, CNRS/IN2P3, Marseille; France.
[102]Department of Physics, University of Massachusetts, Amherst MA; United States of America.
[103]Department of Physics, McGill University, Montreal QC; Canada.
[104]School of Physics, University of Melbourne, Victoria; Australia.
[105]Department of Physics, University of Michigan, Ann Arbor MI; United States of America.
[106]Department of Physics and Astronomy, Michigan State University, East Lansing MI; United States of

America.
[107]B.I. Stepanov Institute of Physics, National Academy of Sciences of Belarus, Minsk; Belarus.
[108]Research Institute for Nuclear Problems of Byelorussian State University, Minsk; Belarus.
[109]Group of Particle Physics, University of Montreal, Montreal QC; Canada.
[110]P.N. Lebedev Physical Institute of the Russian Academy of Sciences, Moscow; Russia.
[111]National Research Nuclear University MEPhI, Moscow; Russia.
[112]D.V. Skobeltsyn Institute of Nuclear Physics, M.V. Lomonosov Moscow State University, Moscow; Russia.
[113]Fakultät für Physik, Ludwig-Maximilians-Universität München, München; Germany.
[114]Max-Planck-Institut für Physik (Werner-Heisenberg-Institut), München; Germany.
[115]Nagasaki Institute of Applied Science, Nagasaki; Japan.
[116]Graduate School of Science and Kobayashi-Maskawa Institute, Nagoya University, Nagoya; Japan.
[117]Department of Physics and Astronomy, University of New Mexico, Albuquerque NM; United States of America.
[118]Institute for Mathematics, Astrophysics and Particle Physics, Radboud University/Nikhef, Nijmegen; Netherlands.
[119]Nikhef National Institute for Subatomic Physics and University of Amsterdam, Amsterdam; Netherlands.
[120]Department of Physics, Northern Illinois University, DeKalb IL; United States of America.
[121 (a)]Budker Institute of Nuclear Physics and NSU, SB RAS, Novosibirsk;[(b)]Novosibirsk State University Novosibirsk; Russia.
[122]Institute for High Energy Physics of the National Research Centre Kurchatov Institute, Protvino; Russia.
[123]Institute for Theoretical and Experimental Physics named by A.I. Alikhanov of National Research Centre "Kurchatov Institute", Moscow; Russia.
[124]Department of Physics, New York University, New York NY; United States of America.
[125]Ochanomizu University, Otsuka, Bunkyo-ku, Tokyo; Japan.
[126]Ohio State University, Columbus OH; United States of America.
[127]Homer L. Dodge Department of Physics and Astronomy, University of Oklahoma, Norman OK; United States of America.
[128]Department of Physics, Oklahoma State University, Stillwater OK; United States of America.
[129]Palacký University, RCPTM, Joint Laboratory of Optics, Olomouc; Czech Republic.
[130]Institute for Fundamental Science, University of Oregon, Eugene, OR; United States of America.
[131]Graduate School of Science, Osaka University, Osaka; Japan.
[132]Department of Physics, University of Oslo, Oslo; Norway.
[133]Department of Physics, Oxford University, Oxford; United Kingdom.
[134]LPNHE, Sorbonne Université, Université de Paris, CNRS/IN2P3, Paris; France.
[135]Department of Physics, University of Pennsylvania, Philadelphia PA; United States of America.
[136]Konstantinov Nuclear Physics Institute of National Research Centre "Kurchatov Institute", PNPI, St. Petersburg; Russia.
[137]Department of Physics and Astronomy, University of Pittsburgh, Pittsburgh PA; United States of America.
[138 (a)]Laboratório de Instrumentação e Física Experimental de Partículas - LIP, Lisboa;[(b)]Departamento de Física, Faculdade de Ciências, Universidade de Lisboa, Lisboa;[(c)]Departamento de Física, Universidade de Coimbra, Coimbra;[(d)]Centro de Física Nuclear da Universidade de Lisboa, Lisboa;[(e)]Departamento de Física, Universidade do Minho, Braga;[(f)]Departamento de Física Teórica y del Cosmos, Universidad de Granada, Granada (Spain);[(g)]Dep Física and CEFITEC of Faculdade de Ciências e Tecnologia, Universidade Nova de Lisboa, Caparica;[(h)]Instituto Superior Técnico, Universidade de Lisboa, Lisboa;

Portugal.
[139]Institute of Physics of the Czech Academy of Sciences, Prague; Czech Republic.
[140]Czech Technical University in Prague, Prague; Czech Republic.
[141]Charles University, Faculty of Mathematics and Physics, Prague; Czech Republic.
[142]Particle Physics Department, Rutherford Appleton Laboratory, Didcot; United Kingdom.
[143]IRFU, CEA, Université Paris-Saclay, Gif-sur-Yvette; France.
[144]Santa Cruz Institute for Particle Physics, University of California Santa Cruz, Santa Cruz CA; United States of America.
[145(a)]Departamento de Física, Pontificia Universidad Católica de Chile, Santiago;[(b)]Universidad Andres Bello, Department of Physics, Santiago;[(c)]Instituto de Alta Investigación, Universidad de Tarapacá;[(d)]Departamento de Física, Universidad Técnica Federico Santa María, Valparaíso; Chile.
[146]Universidade Federal de São João del Rei (UFSJ), São João del Rei; Brazil.
[147]Department of Physics, University of Washington, Seattle WA; United States of America.
[148]Department of Physics and Astronomy, University of Sheffield, Sheffield; United Kingdom.
[149]Department of Physics, Shinshu University, Nagano; Japan.
[150]Department Physik, Universität Siegen, Siegen; Germany.
[151]Department of Physics, Simon Fraser University, Burnaby BC; Canada.
[152]SLAC National Accelerator Laboratory, Stanford CA; United States of America.
[153]Physics Department, Royal Institute of Technology, Stockholm; Sweden.
[154]Departments of Physics and Astronomy, Stony Brook University, Stony Brook NY; United States of America.
[155]Department of Physics and Astronomy, University of Sussex, Brighton; United Kingdom.
[156]School of Physics, University of Sydney, Sydney; Australia.
[157]Institute of Physics, Academia Sinica, Taipei; Taiwan.
[158(a)]E. Andronikashvili Institute of Physics, Iv. Javakhishvili Tbilisi State University, Tbilisi;[(b)]High Energy Physics Institute, Tbilisi State University, Tbilisi; Georgia.
[159]Department of Physics, Technion, Israel Institute of Technology, Haifa; Israel.
[160]Raymond and Beverly Sackler School of Physics and Astronomy, Tel Aviv University, Tel Aviv; Israel.
[161]Department of Physics, Aristotle University of Thessaloniki, Thessaloniki; Greece.
[162]International Center for Elementary Particle Physics and Department of Physics, University of Tokyo, Tokyo; Japan.
[163]Department of Physics, Tokyo Institute of Technology, Tokyo; Japan.
[164]Tomsk State University, Tomsk; Russia.
[165]Department of Physics, University of Toronto, Toronto ON; Canada.
[166(a)]TRIUMF, Vancouver BC;[(b)]Department of Physics and Astronomy, York University, Toronto ON; Canada.
[167]Division of Physics and Tomonaga Center for the History of the Universe, Faculty of Pure and Applied Sciences, University of Tsukuba, Tsukuba; Japan.
[168]Department of Physics and Astronomy, Tufts University, Medford MA; United States of America.
[169]Department of Physics and Astronomy, University of California Irvine, Irvine CA; United States of America.
[170]Department of Physics and Astronomy, University of Uppsala, Uppsala; Sweden.
[171]Department of Physics, University of Illinois, Urbana IL; United States of America.
[172]Instituto de Física Corpuscular (IFIC), Centro Mixto Universidad de Valencia - CSIC, Valencia; Spain.
[173]Department of Physics, University of British Columbia, Vancouver BC; Canada.
[174]Department of Physics and Astronomy, University of Victoria, Victoria BC; Canada.
[175]Fakultät für Physik und Astronomie, Julius-Maximilians-Universität Würzburg, Würzburg; Germany.

[176]Department of Physics, University of Warwick, Coventry; United Kingdom.
[177]Waseda University, Tokyo; Japan.
[178]Department of Particle Physics and Astrophysics, Weizmann Institute of Science, Rehovot; Israel.
[179]Department of Physics, University of Wisconsin, Madison WI; United States of America.
[180]Fakultät für Mathematik und Naturwissenschaften, Fachgruppe Physik, Bergische Universität Wuppertal, Wuppertal; Germany.
[181]Department of Physics, Yale University, New Haven CT; United States of America.
[a] Also at Borough of Manhattan Community College, City University of New York, New York NY; United States of America.
[b] Also at Bruno Kessler Foundation, Trento; Italy.
[c] Also at Center for High Energy Physics, Peking University; China.
[d] Also at Centro Studi e Ricerche Enrico Fermi; Italy.
[e] Also at CERN, Geneva; Switzerland.
[f] Also at CPPM, Aix-Marseille Université, CNRS/IN2P3, Marseille; France.
[g] Also at Département de Physique Nucléaire et Corpusculaire, Université de Genève, Genève; Switzerland.
[h] Also at Departament de Fisica de la Universitat Autonoma de Barcelona, Barcelona; Spain.
[i] Also at Department of Financial and Management Engineering, University of the Aegean, Chios; Greece.
[j] Also at Department of Physics and Astronomy, Michigan State University, East Lansing MI; United States of America.
[k] Also at Department of Physics and Astronomy, University of Louisville, Louisville, KY; United States of America.
[l] Also at Department of Physics, Ben Gurion University of the Negev, Beer Sheva; Israel.
[m] Also at Department of Physics, California State University, East Bay; United States of America.
[n] Also at Department of Physics, California State University, Fresno; United States of America.
[o] Also at Department of Physics, California State University, Sacramento; United States of America.
[p] Also at Department of Physics, King's College London, London; United Kingdom.
[q] Also at Department of Physics, St. Petersburg State Polytechnical University, St. Petersburg; Russia.
[r] Also at Department of Physics, University of Fribourg, Fribourg; Switzerland.
[s] Also at Faculty of Physics, M.V. Lomonosov Moscow State University, Moscow; Russia.
[t] Also at Faculty of Physics, Sofia University, 'St. Kliment Ohridski', Sofia; Bulgaria.
[u] Also at Giresun University, Faculty of Engineering, Giresun; Turkey.
[v] Also at Graduate School of Science, Osaka University, Osaka; Japan.
[w] Also at Hellenic Open University, Patras; Greece.
[x] Also at Institucio Catalana de Recerca i Estudis Avancats, ICREA, Barcelona; Spain.
[y] Also at Institut für Experimentalphysik, Universität Hamburg, Hamburg; Germany.
[z] Also at Institute for Particle and Nuclear Physics, Wigner Research Centre for Physics, Budapest; Hungary.
[aa] Also at Institute of Particle Physics (IPP); Canada.
[ab] Also at Institute of Physics, Azerbaijan Academy of Sciences, Baku; Azerbaijan.
[ac] Also at Instituto de Fisica Teorica, IFT-UAM/CSIC, Madrid; Spain.
[ad] Also at Istanbul University, Dept. of Physics, Istanbul; Turkey.
[ae] Also at Joint Institute for Nuclear Research, Dubna; Russia.
[af] Also at Moscow Institute of Physics and Technology State University, Dolgoprudny; Russia.
[ag] Also at National Research Nuclear University MEPhI, Moscow; Russia.
[ah] Also at Physics Department, An-Najah National University, Nablus; Palestine.
[ai] Also at Physikalisches Institut, Albert-Ludwigs-Universität Freiburg, Freiburg; Germany.

[aj] Also at The City College of New York, New York NY; United States of America.
[ak] Also at TRIUMF, Vancouver BC; Canada.
[al] Also at Universita di Napoli Parthenope, Napoli; Italy.
[am] Also at University of Chinese Academy of Sciences (UCAS), Beijing; China.
[*] Deceased